

Aus dem Universitätsklinikum Münster  
Department für Kardiologie und Angiologie  
Labor für Experimentelle und molekulare Kardiologie  
Direktor (bis 2018): Univ.-Prof. Dr. med. Johannes Waltenberger

---

Functional evaluation of the PTPase DEP-1 as a novel regulator of  
monocytes and macrophages in diabetes and inflammation

---

INAUGURAL-DISSERTATION  
zur  
Erlangung des doctor medicinae  
der Medizinischen Fakultät  
der Westfälischen Wilhelms-Universität Münster

vorgelegt von Obergassel, Julius  
aus Paderborn  
im Jahr 2022

Gedruckt mit Genehmigung der Medizinischen Fakultät der Westfälischen Wilhelms-  
Universität Münster

**Dekan:** Univ.-Prof. Dr. med. Frank Ulrich Müller

**1. Berichtstatter:** Univ.-Prof. Dr. med. Johannes Waltenberger

**2. Berichtstatter:** Univ.-Prof. Dr. med. Heymut Omran

Tag der mündlichen Prüfung: 07. Februar 2022

Aus dem Universitätsklinikum Münster  
Department für Kardiologie und Angiologie  
Labor für Experimentelle und molekulare Kardiologie  
- Univ.-Prof. Dr. med. Johannes Waltenberger –  
Referent: Univ.-Prof. Dr. med. Johannes Waltenberger  
Koreferent: Univ.-Prof. Dr. med. Heymut Omran

### ZUSAMMENFASSUNG

#### **Functional evaluation of the PTPase DEP-1 as a novel regulator of monocytes and macrophages in diabetes and inflammation**

Obergassel, Julius

**Einleitung** Diabetes mellitus (DM) ist eine Erkrankung mit hoher Morbidität und Mortalität. Die Inzidenz ist steigend. Monozyten und Makrophagen spielen eine aktive Rolle in der Pathogenese der Atherosklerose, der relevantesten Komplikation von DM. Density-enhanced phosphatase 1 (DEP-1), für die bereits relevante Funktionen in der Regulation von Tumor- und Endothelzellen gezeigt wurden, ist insbesondere in Makrophagen vergleichsweise stark exprimiert, ohne dass die funktionelle Relevanz in diesem Zelltyp hinreichend untersucht wurde.

**Methoden** DEP-1 mRNA-Expression wurde via rt-qPCR in isolierten, primären CD14<sup>++</sup>CD16<sup>-</sup> Monozyten hospitalisierter Patienten gemessen und zwischen einer an DM erkrankten und einer nicht an DM erkrankten Gruppe verglichen. Der Einfluss inflammatorischer und metabolischer Stimuli auf die Expression wurde *in-vitro* untersucht. Ein *in-vitro* DM-Modell humaner Makrophagen mit DEP-1 Knock-down (KD) via RNA-Interferenz wurde etabliert um mittels MTT-Tests, Migrationsversuchen und Expressions-tests die funktionelle Relevanz von DEP-1 in DM-assoziiierter Atherosklerose in Monozyten und Makrophagen zu untersuchen.

**Ergebnisse** DEP-1 mRNA war in der T2DM-Gruppe heraufreguliert (40%,  $p < 0.05$ ). Im Vergleich zu nicht stimulierten Monozyten war DEP-1 in TNF- $\alpha$  (260%,  $p < 0.001$ ) und unter hyperglykämischen Bedingungen kultivierten Monozyten heraufreguliert (466%, ns). Die DEP-1-Aktivität zeigte sich im Vergleich zwischen nicht-, M1- und M2-aktivierten Makrophagen in M1-Makrophagen am höchsten. DEP-1 KD führte zu reduzierter Makrophagen-Migration im Wundheilungsversuch. p65-Expression und -Phosphorylierung, sowie TNF- $\alpha$ -Expression zeigten sich unter DEP-1 KD erhöht, die Zellvitalität, gemessen im MTT-Test, war unbeeinflusst.

**Diskussion** Diese Arbeit untersucht und diskutiert die funktionelle Relevanz von DEP-1 in CD14<sup>++</sup>CD16<sup>-</sup> Monozyten, u. a. in Monozyten an DM erkrankter Patienten und in einem *in-vitro* Inflammations- und Hyperglykämie-Modell, sowie in *in-vitro* differenzierten Makrophagen. Es wird gezeigt und diskutiert, dass inflammatorische Signalwege, die NF- $\kappa$ B involvieren, von DEP-1 reguliert werden und umgekehrt auch DEP-1 regulieren. Mögliche Signalwege, die die Makrophagen-Migration sowie den NF- $\kappa$ B-Signalweg DEP-1-abhängig regulieren könnten, werden diskutiert.

Tag der mündlichen Prüfung: 07. Februar 2022

## **Eidesstattliche Erklärung**

---

Hiermit erkläre ich, dass ich die Dissertation mit dem Titel

**Functional evaluation of the PTPase DEP-1 as a novel regulator of monocytes and macrophages in diabetes and inflammation**

im Labor für Experimentelle und Molekulare Kardiologie des Departments für Kardiologie und Angiologie am Universitätsklinikum Münster

unter der Anleitung von: Univ.-Prof. Dr. med. Johannes Waltenberger

1. selbstständig angefertigt,
2. nur unter Benutzung der im Literaturverzeichnis angegebenen Arbeiten angefertigt und sonst kein anderes gedrucktes oder ungedrucktes Material verwendet,
3. keine unerlaubte fremde Hilfe in Anspruch genommen,
4. sie weder in der gegenwärtigen noch in einer anderen Fassung einer in- oder ausländischen Fakultät als Dissertation, Semesterarbeit, Prüfungsarbeit, oder zur Erlangung eines akademischen Grades, vorgelegt habe.

Hamburg, den 19.03.2021

Julius Obergassel

# Contents

1	INTRODUCTION	4
1.1	Atherosclerosis is a major complication of diabetes mellitus	4
1.2	Monocytes, macrophages and their role in health and disease	5
1.2.1	Monocytes: Ontogenesis, subsets, and function	5
1.2.2	Monocyte to macrophage differentiation	8
1.2.3	Macrophage function and activation	8
1.2.4	Monocytes and macrophages in atherosclerosis	10
1.2.5	Macrophage migration	12
1.2.6	NF- $\kappa$ B signaling in macrophages	13
1.3	Protein tyrosine phosphatases (PTPs)	13
1.4	Density-enhanced phosphatase 1 (DEP-1)	14
1.4.1	DEP-1 as a regulator in cancer, metastasis, autoimmunity, and insulin resistance	14
1.4.2	Upstream regulation and downstream targets of DEP-1	15
1.4.3	DEP-1 regulates proliferation, adhesion, cell cycle and has impact on tumor metastasis, invasion and angiogenesis in cancer	16
1.4.4	Yet known aspects about DEP-1 's role in immunity and inflammation	17
2	RESEARCH AIM AND QUESTIONS	18
3	MATERIALS AND METHODS	19
3.1	Materials	19
3.1.1	Chemicals	19
3.1.2	Solutions	20
3.1.3	Antibodies for Western Blot	20
3.1.4	Kits and transfection reagents	21
3.1.5	Consumables	21
3.1.6	Laboratory equipment	22
3.1.7	Software	22
3.2	Isolation of peripheral blood mononuclear cells (PBMCs)	23
3.2.1	Isolation of PBMCs from thrombocyte reduction filters	23
3.2.2	Patient recruitment	23
3.2.3	Isolation of PBMCs from whole blood	24
3.3	Isolation of primary human monocytes, CD14+CD16- from PBMCs	24
3.4	Cell culture of monocytes and macrophages	25
3.4.1	Cryo-preservation and thawing of freshly isolated monocytes	25

3.4.2	Differentiation, activation, and culturing of primary monocytes to monocyte-derived macrophages	26
3.4.3	Cell counting for experiments	26
3.5	Transfection of primary monocyte-derived macrophages with small-interfering RNA (siRNA)	27
3.5.1	Transfection protocol for Lipofectamine® RNAiMAX	28
3.5.2	Transfection protocol for Viromer® Blue	29
3.6	RNA biochemical methods and polymerase chain-reaction assays	30
3.6.1	RNA lysis and extraction	30
3.6.2	cDNA synthesis	31
3.6.3	Principles of real-time PCR with SYBR green	32
3.6.4	Implementation of rt-qPCR	33
3.6.5	rt-qPCR data analysis	35
3.7	Protein biochemical methods, SDS-PAGE and Western Blot	36
3.7.1	Protein lysis and protein determination assay	37
3.7.2	Preparation of polyacrylamide gels	38
3.7.3	Sample preparation	38
3.7.4	SDS-PAGE	39
3.7.5	Western Blot	39
3.8	Macrophage cell proliferation and viability assay	41
3.9	Immunoprecipitation and phosphatase activity assay	42
3.10	Scratch migration assay	42
3.11	Data collection and statistical analysis	43
4	RESULTS	45
4.1	DEP-1 is upregulated in monocytes from patients suffering from type 2 diabetes mellitus	45
4.2	Hyperglycemia and methylglyoxal treatment potentially lead to upregulation of DEP-1 in primary monocytes <i>in-vitro</i>	46
4.3	TNF- $\alpha$ induced pro-inflammatory signaling stimulates DEP-1 expression in primary monocytes	48
4.4	Inflammatory M1-macrophages show highest expression and activity of DEP-1 among non-activated and activated macrophage subpopulations	49
4.5	DEP-1 knockdown inflammatory <i>in-vitro</i> macrophage model	52
4.5.1	Knockdown efficiency	54
4.5.2	Knockdown toxicity	55
4.6	DEP-1 knockdown negatively influences macrophage migration	56

4.7	DEP-1 knockdown did not reveal significant differences in macrophage proliferation nor viability	60
4.8	DEP-1 knockdown mediates NF- $\kappa$ B transcription factor upregulation in inflammatory macrophages	62
5	DISCUSSION	65
5.1	DEP-1 protein expression can be efficiently reduced by siRNA-mediated knockdown in a time-efficient, reproducible and easily performable approach	65
5.2	DEP-1 expression is a target of metabolic stress and pro-inflammatory stimulation in type 2 diabetes mellitus	68
5.2.1	DEP-1 is elevated in the hyperglycemic diabetic disease	68
5.2.2	Inflammation and related pathways are potential mediators of elevated DEP-1 expression in diabetic individuals	70
5.2.3	TNF- $\alpha$ stimulation showed strongest capabilities of DEP-1 induction in monocytes <i>in-vitro</i> and the NF- $\kappa$ B pathway is a potential mediator in between	72
5.3	DEP-1 depletion impairs macrophage migration, possibly by dephosphorylating and activating SFKs	74
5.4	DEP-1 depletion enhances NF- $\kappa$ B expression and activation possibly as a feedback regulation	78
5.5	DEP-1's role in atherosclerosis	82
6	CONCLUSIONS	83
7	REFERENCES	84
8	FIGURE DIRECTORY	102
8.1	Figure references	102
9	TABLE DIRECTORY	103
10	ABBREVIATIONS	104
11	ETHICAL APPROVALS	106
12	ACKNOWLEDGEMENT	110
13	CURRICULUM VITAE	111



# 1 Introduction

## 1.1 Atherosclerosis is a major complication of diabetes mellitus

Diabetes mellitus (DM) is one of the most emerging diseases regarding prevalence, mortality and health care expenses. The International Diabetes Federation (IDF) estimates the world-age adjusted prevalence of diabetes in Europe in adults between 20 and 79 years 6.3 % with an 16 % increase to 7.3 % until 2030. The IDF suggests a proportion of 32.9 % of all deaths in Europe before the age of 60 years to be due to diabetes (99). This data is concordant with 2020 data from the Centers for Disease Control and Prevention (28). A recent prospective trial performed on five continents could show that just a high-glycemic-index diet is associated with an increased rate of major cardiovascular events, independent of pre-existing cardiovascular disease or diabetes (103).

Along the autoimmune type 1 diabetes mellitus (T1DM), gestational diabetes and other specific secondary subtypes, such as genetic forms, endocrinopathies, DM following total pancreatectomy or pharmaceutically induced diabetes, type 2 diabetes mellitus (T2DM) is the leading subtype with a prevalence of 87 to 91% (99). This metabolic disease evolves roughly from long term elevated levels of blood glucose leading to increased stimulation of  $\beta$ -cells in the pancreatic islands to produce insulin. This phenomenon is typical for obesity (15) and leads by time to peripheral insulin resistance, requiring absolutely more insulin to keep the blood glucose levels in a normal range (109). At some point, the  $\beta$ -cells' capability to produce sufficient insulin decreases and  $\beta$ -cells become dysfunctional. This is when the blood glucose levels begin to rise and impaired glucose tolerance develops to a manifest T2DM (264). Today, the disease's pathophysiology is much more elucidated, including knowledge about genetic predisposition, regulatory mechanisms in the nervous system, remodeling of adipose tissue and concepts of systemic and local inflammation, for example within the  $\beta$ -cell islands, which all contribute to the feedback loops between insulin resistance,  $\beta$ -cell dysfunction and rising blood glucose levels (108).

The burden of patients suffering from T2DM, in contrast to T1DM, is usually not the diabetes itself, because typical acute complications like non-controlled blood glucose with hypo- and hyperglycemic episodes and symptoms such as nycturia and exsiccosis, unwanted weight loss, urinary tract infections or lassitude are much rarer in this subtype. However, T2DM disease burden, mortality, decreased quality of life, increased hospital

admissions and associated health care costs, etc. are caused by the development of chronic complications from the disease (247), classified as chronic macrovascular (e. g. coronary artery disease, peripheral artery disease) and microvascular (e. g. diabetic nephropathy, diabetic retinopathy) complications (35, 250).

Atherosclerosis is the main pathology causing the chronic vascular complications of DM which are ischemic stroke and coronary as well as peripheral artery disease (178). Atherosclerosis is the accumulation of aggregated lipoproteins together with fibrous material in the subintimal layer, as well as proliferation of vascular smooth muscle cells and calcification within the walls of the macro- and microvasculature which leads to a chronic obstruction of the vessel lumen and ischemia of the tissue served. Tissue ischemia has functional implications (e. g. neurological deficits, decreased cardiac function and output, etc.) and causes clinical symptoms such as aphasia, paresis or angina pectoris. Most known from coronary artery disease, an atherosclerotic plaque can ultimately rupture (18) which exposes the thrombotic core to the bloodstream, leading to acute thrombosis of the respective vessel (47). In the heart, this pathology called type 1 myocardial infarction causes severe ischemia up to necrosis of the served tissue and acute and chronic life-threatening conditions. Chronic ischemic heart disease, acute myocardial infarction and heart failure account for nearly a quarter of all cases of death in Germany in 2015 (232), diseases of the cardiovascular system (ICD I00-I99) accounted for 375274 out of 957874 deaths (40.2 %) in Germany in 2018 (231). Well established risk factors for atherosclerosis and ischemic heart disease are dyslipidemia (elevated low-density lipoprotein (LDL), reduced levels of high-density lipoprotein (HDL)), diabetes (110), hypertension, smoking, overweight and obesity, and age, as well as a genetic predisposition for premature cardiovascular disease as non-modifiable cardiovascular risk factors (65, 153). Other established biomarkers for risk assessment are elevated lipoprotein(a) (Lp(a)) (177), homocysteine (34), other forms of dyslipidemia (7) or elevated high-sensitivity C-reactive protein (CRP) (200, 201).

## 1.2 Monocytes, macrophages and their role in health and disease

### 1.2.1 Monocytes: Ontogenesis, subsets, and function

Monocytes account for 5 % of the leucocytes (257). Together with macrophages and antigen-presenting dendritic cells, monocytes and their hematopoietic progenitors constitute

the mononuclear phagocyte system (MPS). The MPS is mainly responsible for the innate immune response but also involved in the adaptive immune response (98). Besides that but as important is the function of the above-mentioned cells, especially tissue-resident macrophages, in homeostasis, tissue repair and regeneration (272) or elimination of dead cells (92) and many other housekeeping tasks.

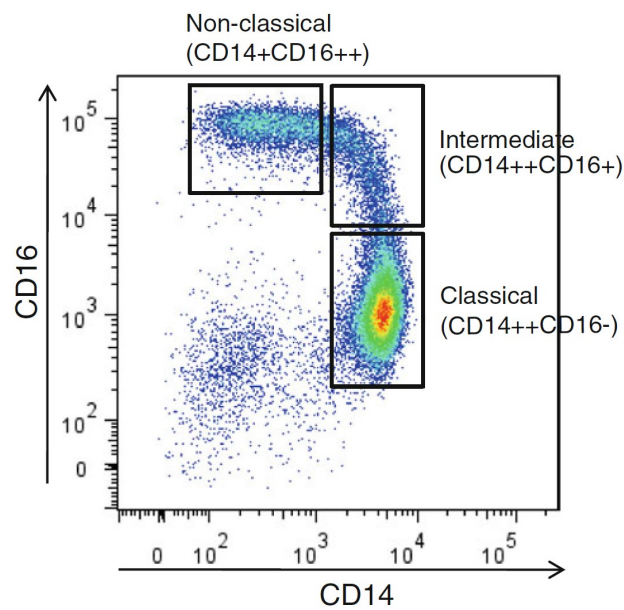


**Figure 1: Monocyte subpopulations in fluorescence assisted cell sorting.** Monocytes and peripheral blood of humans can be divided into three different subsets based on their expression of the surface proteins CD14 and CD16. While classical monocytes express high CD14 and no CD16 (CD14<sup>++</sup>CD16<sup>-</sup>), non-classical monocytes and intermediate monocytes express both surface proteins and can be distinguished by the CD14/CD16 ratio (non-classical: low CD14, intermediate: high CD14, both: high CD16). The figure displays a gating strategy for CD14 and CD16 stained mononuclear cells in fluorescence assisted cell sorting. (271)

After leaving the bone marrow, monocytes remain in the circulation for one to seven days, depending on their state of activation before they either migrate into tissues and become macrophages or die through apoptosis (186, 265). In humans, monocytes were roughly divided into three subsets depending on surface protein expression, especially cluster of

differentiation protein 14 (CD14) and CD16, which is associated with different roles in physiological and pathophysiological conditions (286) (**Figure 1**).

Classical monocytes express CD14 at high levels and do not express CD16 (CD14<sup>++</sup>CD16<sup>-</sup>). They are mainly involved in phagocytosis and inflammatory processes. Classical monocytes express several surface markers such as C-C motif receptor 2 (CCR2, also known as monocyte chemoattractant protein 1 (MCP-1) receptor or CD62L (also known as L-selectin), which are among other receptors crucial for recruitment of monocytes to sites of inflammation or atherosclerosis (271). Classical monocytes in humans correspond to the Ly6C<sup>hi</sup>-subset in mice.

Intermediate CD 14<sup>++</sup>CD16<sup>+</sup> monocytes are equally involved in pro-inflammatory processes producing high amounts of pro-inflammatory cytokines upon stimulation through bacterial products (88). Besides, intermediate monocytes express the surface markers endoglin, angiopoietin receptor and vascular endothelial growth factor receptor 2 (VEGFR2) which are associated to angiogenesis (280). Intermediate monocytes express the highest amount of major histocompatibility complex class II (MHC class II) and further genes crucial for antigen presentation (270). Classical and intermediate monocytes where shown to be involved in cardiovascular atherosclerosis (128).

Non-classical monocytes (CD14<sup>+</sup>CD16<sup>+</sup>) are currently known for their patrolling behavior along the luminal endothelium (9, 38). In opposite to classical monocytes, this subset does not express MCP-1 receptor CCR2 nor L-selectin. CD14<sup>+</sup>CD16<sup>+</sup> express CX<sub>3</sub>CR1, the only known receptor for fractalkine (CX<sub>3</sub>CL1), at high amounts which was shown to be crucial for monocyte homeostasis and survival, as well as for migration (70, 134). CCR2, CCR5 and CX<sub>3</sub>CR1 seem to be important for migration of monocytes into atherosclerotic plaques (184, 240). Non-classical monocytes correspond to the Ly6C<sup>low</sup>-subset in mice. Interestingly, clinical studies have shown expansion of the CD14<sup>+</sup>CD16<sup>+</sup> subset in blood during sepsis and hemolytic uremic syndrome (58, 60).

Of note, there is a continuum of differentiation between all monocyte subsets and phenotype is mainly defined by the differentiation state at emigration from their origin, mainly the bone marrow, into the circulation, as well as upon immigration into the tissue (88, 238). Monocytes can be differentiated into macrophages *in-vitro* by exposing them to macrophage colony-stimulating factor (M-CSF) for 5-7 days (283).

### 1.2.2 Monocyte to macrophage differentiation

Macrophages are known and named for their morphology as comparably large cells and phagocytotic activity, first discovered more than a hundred years ago. Macrophages mainly derive from circulating monocytes (253), originating from hematopoietic stem cells (HSC) in the bone marrow, or – as so called tissue-resident macrophages – from primitive embryonic macrophages (187).

Circulating monocytes were found to emigrate through the endothelial barrier into the subendothelial tissue upon certain stimuli where they further differentiate into macrophages (98, 253, 254). These macrophages with certain roles and function depending on the tissue and the local conditions defined by the cytokines present, were originally believed to be maintained only by recruitment and differentiation of monocytes from the peripheral blood (56, 82, 214). M-CSF is crucial for this monocyte to macrophage differentiation (42, 173) and is the main ligand of the M-CSF receptor, better known as colony stimulating factor 1 receptor (CSF-1R).

More recent research has shown that tissue macrophages originating from circulating monocytes coexist with those originating from tissue-resident primitive embryonic progenitor macrophages. The latter were shown to be genetically different to those originating from HSCs, which again originate from erythro-myeloid precursors in the embryonic yolk sac (75, 76, 213). These so-called tissue-resident macrophages have been found to be self-renewal and independent from monocyte recruitment during adult life (3, 104).

Development of macrophages from their progenitors is mediated by lineage determining cytokines, especially M-CSF and granulocyte-macrophage colony-stimulating factor (GM-CSF) (25, 229, 283). These factors are also used in *in-vivo* studies to differentiate primary human monocytes into monocyte-derived macrophages (171).

### 1.2.3 Macrophage function and activation

Macrophages exist in nearly all tissues of a human adult and represent one of the most heterogenous and plastic cell types (81). None the less, main functions of macrophages reside host defense (79, 98), tissue repair and homeostasis (272), including clearing debris (92). Besides, macrophages fulfill tasks in embryonic development (96) or certain metabolic tasks as tissue resident macrophages. The phenotype of macrophages mainly defines

their functional specializations in their tissue of residence, such as Langerhans cells in the epidermis, osteoclasts, microglia, cardiac macrophages or alveolar macrophages (82).

Monocyte-derived macrophages are subdivided by their so-called activation or polarization states (17, 159). Classically-activated macrophages (M1 macrophages) were first described by Mackaness in 1962 finding an "immunological activation" of macrophages by *Listeria monocytogenes* (154). Meanwhile it is known, that classical activation of macrophages happens through interferon-gamma (IFN- $\gamma$ ), as produced by T<sub>H</sub>1-lymphocytes during an acute inflammatory reaction in combination with a following stimulation of toll-like receptors (TLR) by microbial antigens, such as lipopolysaccharides (LPS) (236). M1-macrophages are the proinflammatory, microbicidal phagocytes in an acute immune reaction following an infection. Besides, nitric oxide production through the inducible nitric oxide synthetase is enhanced in this phenotype (164). Typical markers are CD68, CD80, TLR 2 and TLR4 and secretion of pro-inflammatory cytokines, such as IL-1 $\beta$ , tumor necrosis factor  $\alpha$  (TNF- $\alpha$ ) and IL-12 (30, 43, 159), is characteristic.

Alternatively activated macrophages (M2-macrophages) are defined by expressional and functional changes following stimulation with interleukin 4 (IL-4) and interleukin 13 (IL-13) (164). M2-macrophages express the mannose receptor (MRC1 or CD206) and MHC class II, although at slighter lower levels and with lower immunological response than M1-macrophages (43, 139). The production of pro-inflammatory cytokines is lower in M2-macrophages (165). There as, they produce regulatory cytokines such as IL-10 or growth factors, such as transforming growth-factor  $\beta$  (TGF- $\beta$ ). M2-macrophages mainly regulate and contribute to wound healing, repair and regeneration during chronic infections and homeostasis, allergies and asthma, parasite infections and as immune regulators (80, 157, 159).

More recently, macrophage activation was suggested to be a continuum between M1 and M2 macrophages, as there are other cytokines and stimulants that also regulate macrophage function and their gene expression and more different phenotypes were recently found. Macrophages are now more seen in response to different microenvironmental conditions, being more plastic about their phenotype (68, 157, 159, 169, 196, 219). This newer view on macrophage activation was well reviewed by Wang et al. including

involved molecular pathways and their reciprocal interference upon stimulation with different factors (219, 258).

Nevertheless, the concept of classical inflammatory activation through IFN- $\gamma$  and a TLR-stimulant like LPS versus alternative activation through IL-4 and IL-13 is used in this work to discriminate between two opposite activation states *in-vitro*, knowing that these represent the different *in-vivo* phenotypes only partwise which is still a common practice in basic research (171).

#### 1.2.4 Monocytes and macrophages in atherosclerosis

Research about atherosclerosis reaches back multiple centuries. A recent definition of plaque histology was established in 1995 by the Committee on Vascular Lesions of the Council on Arteriosclerosis of the American Heart Association (230). Among several historical hypothesis about the pathogenesis of atherosclerosis (e. g. proliferative disease, resorption of thrombi) the leading hypothesis today is based on the response-to-injury model, originally postulated by Ross *et al.* in 1977 (208). It is known that atherosclerosis is a result of lipid, mainly LDL, accumulation in the vascular wall, leading to recruitment of immune cells, a corresponding maladaptive immune response and chronic inflammation with a disturbed homeostasis and clearance. Especially during leukocyte recruitment, endothelial dysfunction plays an important role, as the endothelium gets activated, expresses leukocyte adhesion molecules, and increases its permeability. In consequence, the core of the atherosclerotic lesion grows through further extensive recruitment of monocytes becoming macrophages and LDL-uptake. A fibrous collagen-rich cap is formed especially through smooth muscle cells which get recruited from the media into the intima (143).

Monocytes and macrophages are crucial for the development and further establishment of atherosclerotic plaques in all stages of the disease: Early stages of atherosclerosis involve monocyte recruitment through the endothelium, associated signaling processes, foam cell, and the balance between pro- and anti-inflammatory pathways that contribute to atherosclerotic inflammation (64, 167, 207). More recent research focused on discovering mechanisms behind macrophage emigration from the plaque – either back to the vessel lumen or out of the vessel towards the adventitia – which can decrease velocity of plaque progression (74). One potential mechanism described is the upregulation of

macrophage inhibitory factor (MIF) during progression of atherosclerosis (24) which is in line with the very early made observation that macrophage emigration from the atherosclerotic lesions decreases with plaque progression (74).

LDL and modified forms of LDL such as oxidized LDL (oxLDL) are hallmarks in the early development of atherosclerotic lesions and therapeutic lowering of circulating LDL was shown to be crucial in cardiovascular risk reduction during primary and secondary prevention (67, 221, 233, 244, 276). OxLDL is generated enzymatically or through non-enzymatic oxidation, e.g. via reactive oxygen-species (ROS) (87, 277). Although researchers agree that LDL oxidation mainly takes place in the subendothelial space, plasma levels of oxLDL are elevated in diabetic metabolic conditions (94). OxLDL binds to class A (SR-AI and SR-AII), class B (SR-B1 and CD36), and class E (lectin-like oxidized low-density lipoprotein receptor-1 (LOX-1)) scavenger receptors (SR) expressed in many vascular cells but also in monocytes and macrophages (22, 141). Class B SR do not bind normal LDL protein to the same extent as class A and class E SR (175). Besides oxLDL and other forms of normal LDL protein, also conjugates with other pro-inflammatory were found to be taken up by macrophages and contribute to foam cell formation, e. g. a CRP-opsonized native LDL (287). The process of lipid uptake via phagocytosis, pinocytosis and SRs, the intracellular lysosomal and enzymatic degradation, the balance between free cholesterol efflux and lipid accumulation and related signaling cascades is complex, not yet fully understood and remains elusive (167). Also, the role of the different macrophage-expressed scavenger receptors is not dichotomic pro- or anti-atherosclerotic (166): For example, modern studies in *Msr<sup>-/-</sup>*-mice (SR-AI null and SR-AII null) found increased lesion size (11, 146), while two studies on overexpression of *Msr* in the most used atherosclerosis mice models (*Ldlr<sup>-/-</sup>* and *Apoe<sup>-/-</sup>*) did not find an increased plaque progression (90, 252). It is currently a common dogma, that lipid uptake may be handled to a certain amount by macrophages and is therefore rather anti-atherosclerotic because LDL and its modified forms do not accumulate as free particles in the vessel wall. However, if the lipid supply exceeds macrophages' capabilities of clearing which leads to trapping of mostly modified LDL particles within macrophages (160). This process is called foam cell formation (141, 167). Indirectly, oxLDL stimulates monocytes and macrophages contribution to atherosclerosis by modifying the endothelium and therefore increasing leukocyte infiltration, e.g. by upregulation of adhesion molecule VCAM-1 via



NF- $\kappa$ B activation (278) or by increasing endothelial permeability (191). LOX-1 was shown to activate NF- $\kappa$ B in endothelial cells (36).

Besides direct contribution to lipid metabolism, scavenger receptors interact with several macrophage intracellular signaling pathways in a complex manner which was well reviewed (170, 195). Reduced NF- $\kappa$ B activation and cytokine release was observed in macrophages obtained from CD36-deficient patients (274). This was explained by the observation that CD36 together with heterodimer of TLR4 and TLR6 activates NF- $\kappa$ B upon binding of oxLDL (235). Besides oxLDL binding to CD36 seems to inhibit macrophage motility (185). Aside from receptor-initiated signaling cascades, free cholesterol within the cell membrane, organized in lipid rafts, seems to enhance TLR-initiated intracellular pro-inflammatory NF- $\kappa$ B signaling (279, 285).

Therefore, LDL and modified LDL-forms are not only passive components of foam cells and the atherosclerotic lesions. In fact, they are among other cytokines and cell-cell-interaction important mediators and regulators of the atherosclerotic inflammation, especially through SR and TLR and more downstream through NF- $\kappa$ B signaling.

#### 1.2.5 Macrophage migration

Macrophage migration is crucial for their function in many physiological contexts such as wound healing and in innate immunity when they need to be recruited to sites of damage or infection. Among monocyte functions such as adhesion (184), or other macrophage functions such as proliferation (205), inhibited macrophage migration contributes to the monocyte-macrophage-axis of atherogenesis and atherosclerotic plaque progression, as macrophages are retained within a plaque and reverse migration back to the vessel lumen or through the adventitia out of the vessel wall is weakened (167). The process of reverse migration in resolving inflammation is also discussed for neutrophils as another cell type in innate immunity (206). Migration is a complex process of building and releasing focal adhesions, cell protrusion and retraction. Many signaling molecules are involved in this process, such as tyrosine kinases, Rho GTPases, integrins and the cytoskeleton itself (106, 192). Src-family kinases (SFKs) were shown in various studies to be important proximal regulators of macrophage migration (27, 148).

### 1.2.6 NF- $\kappa$ B signaling in macrophages

The signaling pathway of the transcription factor nuclear factor 'kappa-light-chain-enhancer' of activated B-cells (NF- $\kappa$ B) is considered mainly a pro-inflammatory signaling pathway in many cell types, especially leukocytes, although also regulating and inflammation resolving functions of NF- $\kappa$ B signaling have been identified. It is associated with many chronic inflammatory diseases. It plays a major and complex regulatory role in atherosclerosis (268), for example when monocytes are getting activated and recruited to the sub-endothelium (220) or when macrophages produce pro-inflammatory cytokines through prior NF- $\kappa$ B activation (78). In diabetes insulin signaling impairment is partly mediated by NF- $\kappa$ B activation (150). NF- $\kappa$ B mediates acute activation in inflammatory contexts through pattern recognition receptors such as Toll-like receptors which sense microbial products. It is also activated by cytokine receptors from the TNF-receptor family or the IL-1-receptor family. Besides, NF- $\kappa$ B can be activated alternatively through LT $\beta$ , CD40L, BAFF and RANKL with altered, non-canonical, downstream signaling (237). The canonical signaling pathway includes formation and activation of the IKK complex, phosphorylation of I $\kappa$ B subunit of NF- $\kappa$ B which gets degraded while the two other subunits p50 and p65 get translocated into the nucleus where they act directly as a transcription factor (136). TGF- $\beta$  is a chemoattractant and activator as well as an inhibitor of monocytes and macrophages and functions highly context-dependent. It has been shown that TGF- $\beta$  might be a potential inhibitor of NF- $\kappa$ B (223).

### 1.3 Protein tyrosine phosphatases (PTPs)

Signal transduction at a cellular level is crucial to regulate and control cell function. Signal transduction takes place intra- and extracellularly. Protein phosphorylation by protein kinases is a key component of intracellular signaling and signal transduction from extracellular stimuli to intracellular functions. Phosphorylation of proteins occurs at tyrosine, serin or threonine amino acids. An important aspect of extracellular to intracellular signal transduction involves receptor tyrosine kinases (RTKs) and protein tyrosine phosphatases (PTP) as their natural opponents, both controlling the tyrosine phosphorylation states of signaling proteins (181).

PTPs are therefore important mediators and modifiers of intracellular signaling downstream of growth factors, cytokines, and hormones being involved in regulation of cell

cycle, metabolism and function (248). Together, RTKs and PTPs maintain a balance in phosphorylation stages while a disbalance can result in various cell abnormalities which can again lead to severe diseases. For example, the protein tyrosine phosphatase non-receptor type 11 (PTPN11, also known as SHP-2) is known to mutate during disease progression of primary myelodysplastic syndrome (32), to be associated with a worse prognosis in certain subgroups of acute myeloid leukemia (97) and in its mutated form to be the cause of more than 50 % of the cases of the autosomal-dominant disorder Noonan syndrome (243). Protein tyrosine phosphatases can be split in multiple groups, typically in the transmembrane receptor-like PTPs and the intracellular non-transmembrane PTPs. DEP-1 is in opposition to SHP-2 a member of the receptor-like PTPs.

Among many PTPs, Density-enhanced phosphatase 1 (DEP-1; also known as PTPRJ, hPTP- $\eta$ , ) is one, expressed at highest levels in human and murine macrophages compared to other cell types and tissues (129, 145, 180).

#### 1.4 Density-enhanced phosphatase 1 (DEP-1)

DEP-1 belongs to the family of PTPs, those protein phosphatases which are highly selective to tyrosine dephosphorylation (5), and is a 180-220 kD product of the PTPRJ gene (21) present in the plasma membranes of many cell types, including all hematopoietic lineages (especially in macrophages and B-lymphocytes), endothelial cells, epithelial cells, fibroblasts and further cell types (21, 69, 95, 182). Compared to other tissues and cell types, DEP-1 expression is high in human and murine macrophages (234). Other relevant PTPs in myeloid cells, especially macrophages and macrophage activation are PTP $\phi$ , SHP1, SHP2 and PTP1B, PTPN22, DUSP1 (123, 194). The human PTPRJ gene was located at chromosome 11p11.2 (95). Besides its single cytoplasmatic catalytic domain and a single transmembrane domain, DEP-1 has an extracellular domain with eight to twelve fibronectin type III repeats (182). Regulatory roles for DEP-1 have been identified in many physiological and pathophysiological contexts: It is especially known as a tumor suppressor (210), and more lately in autoimmunity (10, 46).

##### 1.4.1 DEP-1 as a regulator in cancer, metastasis, autoimmunity, and insulin resistance

As relations to diseases are reported for several PTPs (248), Ruivenkamp *et al.* found that DEP-1 is a candidate for the mouse susceptibility to colon cancer 1 gene (Scc1) as well

as a frequent deletion of the PTPRJ gene in human colon, lung and breast cancer, and suggested DEP-1 as a tumor suppressor (210). An association of DEP-1 to leukemogenesis of acute myeloid leukemia by being involved in the cell transforming process through FLT-IT3 has been suggested by Godfrey, Arora *et al.* in 2012 (77). More lately, DEP-1 has been related to diseases aside from cancer: Dave *et al.* showed an upregulation of DEP-1 in experimental arthritis in mice, as well as in human rheumatoid arthritis (46). Earlier, an association of DEP-1 with Cogan's syndrome (151) and Crohn's disease (10), two other autoimmune diseases, was mentioned. A yet unknown autosomal-recessive variant of familial inherited thrombocytopenia with a biallelic loss-of-function mutation in the PTPRJ gene was described by Marconi *et al.* (158). Also more recently, two studies have shown that DEP-1 activity is increased in high-fat diet-induced obesity (126, 218) and dephosphorylates and therefore negative regulates the insulin receptor (125). Reducing DEP-1 activity by antisense oligonucleotides led to significant reduction of body weight, basal glucose levels, serum insulin and leptin, and an improvement in insulin sensitivity, possibly by hyperphosphorylation in the insulin signaling cascade, in these obese mice (126).

#### 1.4.2 Upstream regulation and downstream targets of DEP-1

Besides regulation of DEP-1 expression and activity in pathological contexts as stated above, there are not many upstream regulators of DEP-1 in a cellular context identified yet. However, there is strong *in-vitro* evidence that DEP-1 is downregulated by M-CSF in its basal and stimulated expression. Furthermore it has been shown that LPS is a positive regulator of DEP-1 messenger ribonucleic acid (mRNA) expression (44, 180). This data, gained from human and mouse macrophages, suggests a potential role in regulating inflammation, as well. Additionally, there is evidence that there is a 13 amino acid long sequence in the 5'-end of the PTPRJ-mRNA which is attenuating the transcription of the mRNA in a possibly self-limiting matter (112).

In opposite to the narrow amount of knowledge about upstream regulation of DEP-1, several downstream targets and intracellular functions have yet been identified in various cell types. Nevertheless, the overall role of DEP-1 in intracellular signaling is not understood yet. Identified direct targets of DEP-1 include tyrosine kinases from the Src family (SFks) (234) – to be exact Lck, Fyn and Src – the platelet-derived growth factor receptor

(PDGF-R) (122), the vascular endothelial growth factor receptor 2 (VEGF-R2) (133), the hepatocyte growth factor receptor (183), the regulatory p85 subunit of phosphatidylinositol-4,5-bisphosphate 3-kinase (PI3K) (249) and janus kinase 2 (218). Shalev et al. identified a direct dephosphorylation of CSF-1R and CBL, a protein involved especially in ubiquitination, by DEP-1 (217). Besides an interaction between p120-catenin (93) was suggested. While DEP-1 – as a phosphatase – acts as a negative regulator, reducing a signaling pathway's activity, in most of the above-mentioned cases, it is a positive regulator of the Src kinase activity by dephosphorylating it specifically at its inhibitory sites Y528 and Y530 (62, 227, 234).

#### 1.4.3 DEP-1 regulates proliferation, adhesion, cell cycle and has impact on tumor metastasis, invasion and angiogenesis in cancer

Research groups have discovered functional roles of DEP-1 in multiple contexts while focus has been set on its role in cancer as a tumor suppressor and more lately on its DEP-1-regulated proliferation and permeability in endothelial cells and therefore angiogenesis, especially tumor angiogenesis.

With regard to cancer, an important and intensively studied pathway in which DEP-1 is involved is contact inhibition: Expression of DEP-1 increases with cell density in fibroblasts (182) which – in another study in epithelial colon cancer cells – was reported to inhibit pathways involved in cell cycle progression and proliferation (12). DEP-1's negative regulatory effect on proliferation through contact inhibition was also described for endothelial cells with a vascular endothelial growth factor (VEGF) stimulus for proliferation and following angiogenesis (83, 241). In these studies, angiogenesis, capillary formation, vascular permeability and therefore tumor growth and metastasis were inhibited through DEP-1. There against, Fournier *et al.* recently showed experiments which suggested that DEP-1 may be a positive regulator of angiogenesis and vascular permeability and therefore tumor progression (62). The authors suggested DEP-1's strong positive regulatory effect on Src-family kinases, overwhelming negative regulatory effects on other pathways, as the potential mechanism behind this observation. Similar observations regarding permeability were made in human umbilical vein endothelial cells (HUVEC) by Spring *et al.* with the additional finding that overexpression of DEP-1 at very high levels lead to negative regulation Src signaling and therefore contrary downstream effects (226).

The same group showed later, that DEP-1 silencing in breast cancer cell lines impaired invasion and metastasis but not cell proliferation (227).

#### 1.4.4 Yet known aspects about DEP-1 's role in immunity and inflammation

Other research focused on DEP-1's role in immune cells and inflammatory processes. One important study from Zhu *et al.* was conducted on B-cells and bone marrow derived macrophages (BMDM) from DEP-1 and CD45 single-knockout (KO), as well as in double-knockout (DKO) mice. They showed that mitogen activated protein kinase's (MAPK) downstream pathway is attenuated in B-cells from DKO mice with reduced levels of phosphorylated extracellular signal-regulated kinase (ERK). Also, B-cell-receptor mediated intracellular signaling was reduced. Since phosphorylation was reduced at many sites within the DKO b-cells, the authors suggested and experimentally found Src-family kinases as possible proximal mediators. These effects were mild in DEP-1-KO-, higher in CD45-KO- and highest in B-cells from DKO-mice. This conclusively suggests possible redundant functions of DEP-1 and CD45 in B lymphocytes.

Looking at the myeloid lineage, phagocytosis and TNF- $\alpha$  production were impaired, as well as Src-signaling, with strongest effects in DKO BMDMs, although reduction of TNF- $\alpha$  production was similar between both single KO and the DKO cells (284). Dave, Hume *et al.* treated BMDMs with anti-DEP-1-antibodies and observed a reduction in M-CSF induced cell spreading and membrane ruffling, as well as migration towards an M-CSF gradient while no differences were observed in proliferation and total tyrosine phosphorylation. The same group discovered an upregulation of DEP-1 in infiltrating T-cells and inflammatory macrophages in human rheumatoid arthritis later. This was shown in joint tissues from mice with collagen-induced arthritis as well (46).

## 2 Research aim and questions

As demonstrated in the previous chapter, DM and atherosclerosis as its important complication confront not only the western world with a high disease burden and mortality (**chapter 1.1**). Medicine yet lacks sufficient molecular, targeted treatment options (114). Monocytes and macrophages are important mediators of atherogenesis and DEP-1 is a PTP which is highly expressed in the myeloid lineage (**chapter 1.4**), while its functional and regulatory role in these cells, in inflammation itself, in hyperglycemia and diabetes and with regard to atherosclerosis is not yet conclusively investigated and remains unclear (**chapter 1.4.4**). However, a relevant pathophysiological role in these contexts seems presumable and would be in line with findings for the PTPs SHP-2 (52) and PTP1B (2, 50, 282) in diabetes, as well as with its already shown involvement in insulin signaling and relevance in obesity (125).

This work aims to further elucidate whether DEP-1's functional relevance in monocytes and macrophages with focus on DM as a pathophysiological context. The following research questions tailor this broader aim:

1. Does monocytic DEP-1 expression differ between diabetic patients and healthy controls? This question elucidates a general “pathophysiological relevance” of DEP-1 in DM.
2. Are metabolic stress – as present in DM – and inflammatory cytokines upstream regulators of DEP-1? Which upstream pathways are involved and to which extent?
3. Which are the most important functional effectors of DEP-1 in macrophages?
  - 3.1. As regulatory roles for DEP-1 in cell cycle and proliferation signaling processes but also in macrophage migration were suggested (**chapters 1.4.3 and 1.4.4**), effects of DEP-1 on macrophage viability and migration will be investigated.
  - 3.2. As macrophages' core function is residing in host defense and since NF- $\kappa$ B is at least among, if not the most important inflammatory signaling pathway(s), DEP-1's impact on NF- $\kappa$ B activation and its effectors will be investigated to further clear the PTP's role in inflammation.

## 3 Materials and Methods

### 3.1 Materials

#### 3.1.1 Chemicals

**Table 1: Chemicals.**

<b>Chemical</b>	<b>Manufacturer</b>
Ammonium persulfate (APS)	AppliChem GmbH, Germany
Bovine serum albumin (BSA)	Merck KGaA, Germany
Dimethyl sulfoxide (DMSO)	CalBiochem (Merck KGaA), Germany
Ethanol absolute	AppliChem GmbH, Germany
Ethylenediaminetetraacetic acid (EDTA)	AppliChem GmbH, Germany
Ethylenglycol-bis(2-aminoethylether)-N,N,N',N'-tetraacetic acid (EGTA)	Carl Roth GmbH + Co. KG, Germany
Fetal bovine serum (FBS)	Sigma-Aldrich (Merck KGaA), Germany
Gelatin	Merck KGaA, Germany
ECL substrate	Bio-Rad Laboratories Inc., USA
D-(+)-Glucose solution for cell culture	Sigma-Aldrich (Merck KGaA), Germany
Glycine	AppliChem GmbH, Germany
HCl (37%)	AppliChem GmbH, Germany
Histopaque®-1077	Sigma-Aldrich (Merck KGaA), Germany
Interferon gamma (IFN- $\gamma$ )	PeproTech GmbH, Germany
Interleukin 10 (IL-10)	PeproTech GmbH, Germany
Interleukin 13 (IL-13)	PeproTech GmbH, Germany
Interleukin 4 (IL-4)	PeproTech GmbH, Germany
Macrophage colony-stimulating factor (M-CSF)	PeproTech GmbH, Germany
Pam3Cys-SK4	EMC microcollections GmbH, Germany
Methanol	VWR International GmbH, Germany
NaCl	AppliChem GmbH, Germany
PageRuler™ Prestained Protein Ladder	Thermo Fisher Scientific, USA
PBS (phosphate buffered saline)	Invitrogen, Thermo Fisher Scientific, USA
Penicillin-Streptomycin (100X)	gibco™, Thermo Fisher Scientific, USA
Recombinant Human Platelet-derived growth factor BB (PDGF)	PeproTech GmbH, Germany
Halt™ Phosphatase Inhibitor Cocktail	Thermo Fisher Scientific, USA
Ponceau Xylidine	Thermo Fisher Scientific, USA
Halt™ Protease Inhibitor Cocktail	Thermo Fisher Scientific, USA
Opti-MEM™ I Reduced Serum Medium	gibco™, Thermo Fisher Scientific, USA
RPMI-1640 medium without glucose	gibco™, Thermo Fisher Scientific, USA
Skim milk powder	Sigma-Aldrich (Merck KGaA), Germany
Sodium dodecyl sulfate (SDS)	AppliChem GmbH, Germany
Synth-a-Freeze™, 50 ml	gibco™, Thermo Fisher Scientific, USA
Tetramethylethylenediamine (TEMED)	AppliChem GmbH, Germany
Human TNF- $\alpha$ (recombinant)	Reliatech GmbH, Germany
Tris(hydroxymethyl)aminomethane (Tris)	AppliChem GmbH, Germany
Tween 20	AppliChem GmbH, Germany
$\beta$ -Mercaptoethanol	AppliChem GmbH, Germany
CASYton	OLS OMNI Life Science GmbH, Switzerland
Calbiochem InSolution™ NF- $\kappa$ B Activation Inhibitor	Merck KGaA, Germany
GF 109203X (PKC inhibitor)	Enzo Life Sciences, Inc., USA



### 3.1.2 Solutions

**Table 2: Recipes for solutions.**

NET-G solution (10X) <i>(washing) buffer for PVDF membranes</i>	1.5 mM NaCl 50 mM EDTA 100 mM Tris pH 8.0 0.5 % Tween 20 1 % gelatin
RIPA buffer <i>cell lysis buffer for protein extraction</i>	20 mM Tris-HCl (pH 7.5) 150 mM NaCl 1 mM EDTA 1 mM EGTA 1 % NP-40 1 % sodium deoxycholate 2.5 mM sodium pyrophosphate 1 mM beta-glycerophosphate  Stable in refrigerator for 1 month. For long term storage, store at -20 °C freezer in 10ml aliquots.
SDS-PAGE running buffer (5X)	1.92 M Tris 0.25 M Glycine  For use: Dilute 1:5 with H <sub>2</sub> O and add 1/200 vol% 20% SDS Mix well.
SDS-PAGE protein-sample loading-buffer (6X)	3 ml 20% SDS 3 ml β-Mercaptoethanol 4 ml Glycerol + few grains of bromophenol blue
SDS-PAGE separation gel buffer	2 M Tris-HCl pH 8.8
SDS-PAGE stacking gel buffer	0.5 M Tris-HCl pH 6.8
Western Blot transfer buffer (Tris-Glycine-Mix)	24 mM Tris 192 mM Glycine  For use: Dilute 1:15 with H <sub>2</sub> O and add 20% Methanol 0.05 % SDS

### 3.1.3 Antibodies for Western Blot

**Table 3: Primary antibodies used in Western Blot analyses.**

Protein target	Dilution	Type	Species	Manufacturer	Cat. no°
DEP-1	1:1000	monoclonal	mouse	Santa Cruz Biotechnology, Inc., USA	sc-21761
NF-κB phospho-p65 subunit	1:1000	monoclonal	rabbit	Cell Signaling Technology®, USA	3033S
NF-κB p65 subunit	1:1000	polyclonal	rabbit	Santa Cruz Biotechnology, Inc., USA	sc-372
α-Vinculin	1:1000	polyclonal	rabbit	Santa Cruz Biotechnology, Inc., USA	sc-5573

**Table 4: Secondary antibodies.**

Antibody	Dilution	Manufacturer	Cat. no°
goat-anti-mouse	1:10000	Santa Cruz Biotechnology, Inc., USA	sc-2005
goat-anti-rabbit	1:10000	Santa Cruz Biotechnology, Inc., USA	sc-2004

### 3.1.4 Kits and transfection reagents

**Table 5: Kits and transfection reagents.**

<b>Kit</b>	<b>Manufacturer</b>	<b>Cat. no°</b>
Classical Monocyte Isolation Kit	Miltenyi Biotec GmbH, Germany	130-117-337
Maxima SYBR Green/ROX qPCR Master Mix	Thermo Fisher Scientific, USA	K0221
NucleoSpin® RNA	Macherey-Nagel GmbH & Co. KG, Germany	740955.250
RC DC Protein Assay	Bio-Rad Laboratories Inc., USA	500-0119
RevertAid H Minus First Strand cDNA Synthesis Kit	Thermo Fisher Scientific, USA	K1632
RQ1 RNase-Free DNase	Promega GmbH, Germany	M6101
CellTiter 96® AQueous Non-Radioactive Cell Proliferation Assay (MTS)	Promega GmbH, Germany	G5430
Tyrosine Phosphatase Assay System	Promega GmbH, Germany	V2471
Viomer® Blue	Lipocalyx GmbH, Germany	VB-01LB-01
Viomer® Green	Lipocalyx GmbH, Germany	VG-01LB-01
Lipofectamine® RNAiMAX	Thermo Fisher Scientific, USA	13778075
INTERFERin®	Polyplus transfection®, France	409-50
jetPRIME®	Polyplus transfection®, France	114-01

### 3.1.5 Consumables

**Table 6: Plasticware consumables.**

<b>Consumable</b>	<b>Manufacturer</b>
ybond P 0.2 PVDF membrane	GE Healthcare Life Sciences, USA
CASYcups	OLS OMNI Life Science GmbH, Switzerland
CELLSTAR® multiwell culture/suspension plate (12-well)	Greiner Bio-One GmbH, Germany
CELLSTAR® multiwell culture/suspension plate (24-well)	Greiner Bio-One GmbH, Germany
CELLSTAR® multiwell culture/suspension plate (6-well)	Greiner Bio-One GmbH, Germany
CELLSTAR® culture flasks	Greiner Bio-One GmbH, Germany
Reaction tubes 500 µl / 1.5 ml	SARSTEDT AG & Co. KG, Germany
Falcon® 15 ml	Corning Inc., USA
Falcon® 50 ml	Corning Inc., USA
Freezing tubes 2 ml	SARSTEDT AG & Co. KG, Germany
Hard-Shell® 96-Well PCR Plates	Bio-Rad Laboratories Inc., USA
Leucosep™ tubes 50 ml	Greiner Bio-One GmbH, Germany
Microseal® 'B' PCR Plate Sealing Film	Bio-Rad Laboratories Inc., USA
Stripette® 2/5/10/25 ml	Corning Inc., USA

### 3.1.6 Laboratory equipment

**Table 7: Laboratory equipment**

<b>Equipment</b>	<b>Purpose</b>	<b>Manufacturer</b>
Amersham™ Imager 600	Western Blot imaging system	GE Healthcare Life Sciences, USA
Amersham™ TE 77 PWR Semi-Dry Transfer Unit	SDS-PAGE/PVDF semi-dry transfer unit	GE Healthcare Life Sciences, USA
Axio Observer 7	Inverse microscope	Carl Zeiss Microscopy GmbH
Axioskop 2 Plus Fluorescence	Fluorescence microscope	Carl Zeiss Microscopy GmbH
Biofuge fresco 4°C	Desk centrifuge with cooling unit	Heraeus, Germany
Biofuge pico	Desk centrifuge	Heraeus, Germany
CASY	Automatic cell counting system	OLS OMNI Life Science GmbH, Switzerland
CFX Connect™ PCR Detection-System	rt-qPCR thermal cycler and readout system	Bio-Rad Laboratories Inc., USA
Eppendorf® PCR Cooler	96-well plate cooling block	Merck KGaA, Germany
Eppendorf® Thermomixer Compact	Heatable tube mixer	Merck KGaA, Germany
GFL 1083 Waterbath	Waterbath	GFL Gesellschaft für Labortechnik mbH, Germany
Guava easyCyte 12	Flow cytometer	Merck KGaA, Germany
Hera Safe KS	Class II aseptic work bench	Heraeus, Germany
Heracell™ 150	CO <sub>2</sub> -incubator	Heraeus, Germany
Heracell™ 150i	CO <sub>2</sub> -incubator	Thermo Fisher Scientific, USA
Heraeus LaminAir HA 2448 GS	Aseptic work bench	Thermo Fisher Scientific, USA
Megafuge 1.0 R	Centrifuge (17,860g; minimum temperature 0-4°C)	Heraeus, Germany
Mini-PROTEAN® Tetra System	Vertical gel-electrophoreses system (gel casting stands, running tank with lid and electrodes)	Bio-Rad Laboratories Inc., USA
Mr. Frosty™ Freezing Container	Isopropanol-containing box for slow sample cooling to -80°C	Thermo Fisher Scientific, USA
MS2 Minishaker	Desk shaker	IKA®-Werke GmbH & CO. KG, Germany
NanoDrop ND1000	Spectrophotometer 220-750nm	Thermo Fisher Scientific, USA
Perfect Spin Plate Centrifuge	PCR plate centrifuge	PEQLAB Biotechnologie GmbH, Germany
PowerPac™ HC	Gel-electrophoreses power unit	Bio-Rad Laboratories Inc., USA
T-Gradient Thermocycler	Thermal cycler	Biometra GmbH, Germany
Tube Roller	Tube roller	STARLAB GmbH, Germany
Victor <sup>3</sup>	Multilabel plate reader	PerkinElmer Inc., USA
Vortex IR	Desk vortexer	STARLAB GmbH, Germany

### 3.1.7 Software

**Table 8: Software**

<b>Software</b>	<b>Manufacturer</b>
CFX Manager 3.1	Bio-Rad Laboratories Inc., USA
HeidiSQL 9.5	Ansgar Becker, Germany
ImageJ2 (Fiji)	National Institutes of Health, USA
MariaDB Server 10	MariaDB Corporation, USA
Office Professional Plus 2016	Microsoft Corporation, USA
Prism 9	GraphPad Software Inc., USA
Illustrator CC 2020	Adobe Systems Inc., USA
SPSS Statistics 26	IBM Corporation, USA

## 3.2 Isolation of peripheral blood mononuclear cells (PBMCs)

### 3.2.1 Isolation of PBMCs from thrombocyte reduction filters

For *in-vitro* experiments, primary human monocytes were isolated from thrombocyte reduction filters, a side product during thrombocyte donation from healthy donors, obtained as a gift from the institute for transfusion medicine and cell therapy, Priv.-Doz. Dr. med. Georg Geißler, University Hospital Münster, Germany.

Primary human monocytes were isolated from peripheral blood mononuclear cells (PBMC). Therefore, leucosep tubes were filled with 15 ml of fridge-cold Histopaque®-1077 (Sigma-Aldrich, Thermo Scientific, USA, density: 1.077 g/ml) and span for one minute to get the Histopaque® below the separation foam. Then, 7.5 ml concentrated blood from thrombocyte reduction filters were diluted with 22.5 ml PBS and transferred into the prepared Leucosep™ tubes to a total volume of 45 ml. Now, PBMCs were separated by density gradient centrifugation at 2200 rpm without break for 20 minutes at room temperature. The buffy-coats were taken out of the Leucosep™ tubes by pipetting and washed multiple times in PBS with centrifugation at 1800 rpm for thrombocyte reduction. Washing<sup>1</sup> until particles of thrombocyte-size counted less than 80.000 particles/ml. This was verified through cell counting by particle size (CASY cell counter, OLS GmbH).

### 3.2.2 Patient recruitment

Monocytes from type 2 DM patients and non-DM controls were isolated from peripheral whole blood. All participating individuals were recruited from the University Hospitals Jena (Prof. Dr. Frank-D. Böhrer) and Münster (Univ.-Prof. Dr. Johannes Waltenberger). Inclusion criteria for the T2DM group was - besides the diagnosis of T2DM - an elevated level of glycated hemoglobin (HbA<sub>1c</sub>) above 7.5 %. Exclusion criteria for the control group was an HbA<sub>1c</sub> above 6.5 %. Active smoking within the past 6 months, active infections or current anti-inflammatory therapy were exclusion criteria for both groups. All patients provided written informed consent to participate in the study. It was approved by the local ethics committee of Münster University Hospital, Germany (license no° 2011-

---

<sup>1</sup> Washing in this context is spinning the cell suspension at 1200 rpm for 10 minutes at room temperature, discarding the supernatant and resuspending the cell pellet in the same amount of PBS.

612-f-S) and Jena University Hospital, Germany (license no° 4125-06/14). The study conforms to the declaration of Helsinki.

### 3.2.3 Isolation of PBMCs from whole blood

Approximately 50 ml of whole blood were used to isolate PBMCs with the intention to isolate primary monocytes subsequently for sufficient yields. Whole blood was diluted with PBS in a ratio of 1:1 and blood-PBS-mix was laid on top of Histopaque®-1077 (Sigma-Aldrich, Thermo Scientific, USA, density: 1.077 g/ml) in a 2:1 ratio in regular 50 ml tubes. When using 50 ml of whole blood, this would mean splitting up the volume into 4 times 12.5 ml whole blood, diluting every portion with 12.5 ml PBS and laying these on top of 12.5 ml Histopaque®-1077 in regular 50 ml tubes (total volume: 4 x 37.5 ml). Final gradient preparations were centrifuged at 2200 rpm without break for 20 minutes at room temperature. Buffy-coats were pipetted into new tubes and washed multiple times in PBS as exemplified for isolation from thrombocyte reduction filters (**chapter 3.2.1**).

### 3.3 Isolation of primary human monocytes, CD14<sup>+</sup>CD16<sup>-</sup> from PBMCs

From thrombocyte-reduced PBMCs, primary human monocytes were isolated using Miltenyi Classical Monocyte Isolation Kit for negative selection of CD14-positive and CD16-negative monocytes via magnetic-activated cell sorting (MACS). An antibody cocktail against other cell types such as lymphocytes, dendritic cells, natural killer cells or basophils removes non-monocytes and microbeads against resulting in a verified suspension of CD14-positive untouched non-activated monocytes.

Thrombocyte-reduced PBMCs are counted expecting an average yield of 15%, depending on the number of monocytes needed. After spinning at 1200 rpm for 10 minutes at room temperature they are getting resuspended in a PBS solution with 0.5 % bovine serum albumin (BSA). Following incubation with an Fc-receptor blocking reagent together with the above-mentioned biotin-antibody cocktail for 10 minutes at 4 °C, the suspension was incubated with anti-biotin-microbeads for 15 minutes at 4 °C. Now the whole suspension was washed with PBS 0.5 % BSA and added onto the magnetic columns. The column was washed three times, each time with 3 ml PBS 0.5 % BSA. The resulting cell suspension collected from the column-output contains enriched CD14-positive monocytes and was counted again by CASY cell counter (OLS OMNI Life Science GmbH). The cells were seeded directly after isolation or at least spun down and resuspended in glucose

containing medium to limit the starvation time which starts with the isolation and was usually around six hours.

### 3.4 Cell culture of monocytes and macrophages

Cells were cultured in CO<sub>2</sub>-incubators (Heraeus, Thermo Fisher Scientific) at a constant temperature of 37 °C and constant CO<sub>2</sub> concentration of 5 % in 24-, 12-, and 6-well cell suspension plates (Greiner Bio-One GmbH, Germany).

Monocytes were seeded depending on the intended usage. For protein and RNA work, monocytes were seeded at a density of approximately 2.5 million cells / ml in 2 ml medium in a 6-well cell suspension plate. For macrophage differentiation, monocytes were usually seeded at a density of 0.2 million cells / ml in 1 ml M-CSF-supplemented-medium (50 ng/μl recombinant human-M-CSF) in a 12-well cell suspension plate.

Primary human monocytes and macrophages were generally cultured in RPMI-1640 medium (gibco™ by Life Technologies, Thermo Fisher Scientific) manufactured without glucose but with L-Glutamine. The medium, hereafter culturing medium was supplemented with 10% FBS (gibco™), 100 U/ml Penicillin (gibco™), 100 μg/ml Streptomycin (gibco™). Glucose (Sigma-Aldrich Co. LLC) was generally adjusted to a concentration of 5 mM (equates 90 mg/dl) which is described as normoglycemia (NG). In experiments which required an *in-vitro* model of diabetes, glucose was adjusted to 30 mM (541 mg/dl), referenced to as hyperglycemia (HG).

#### 3.4.1 Cryo-preservation and thawing of freshly isolated monocytes

When freshly isolated monocytes were not needed immediately, more cells than needed were isolated or for reproduction purposes, cells from many donors were cryo-preserved. Therefore, primary monocytes were washed right after isolation and resuspended in freezing medium (Synth-a-Freeze®, gibco™) at a concentration of approximately up to 10 million cells per 1 ml freezing medium. The suspension was then transferred into freezing vials (SARSTEDT AG & Co. KG). The tubes were cooled down slowly (approximately -1 °C/min) in Mr. Frosty™ freezing container to -80 °C and transferred to the liquid nitrogen storage after minimally 2 hours and maximally 12 hours.

Thawing of cells coming from liquid nitrogen was performed as quick as possible in a 37 °C waterbath. As soon as the medium was thawed, cells were centrifuged at 1200 rpm for

10 minutes at room temperature, the supernatant containing the freezing medium was removed and cells were resuspended in cell culture medium at the concentration desired for the planned experiment.

#### 3.4.2 Differentiation, activation, and culturing of primary monocytes to monocyte-derived macrophages

Primary monocytes were differentiated into primary M $\phi$ -macrophages by culturing them for 7-10 days in medium supplemented with 50 ng/ $\mu$ l recombinant human-M-CSF right after isolation.

Cells already start to adhere and spread-out after 3 to 4 days which can be observed visually by microscopy. Nevertheless, for comparable and reliable experimental conditions, a complete 80-90% dense monolayer of macrophages is required which can be assessed visually by microscopy, as well. As soon as this state is reached, medium can be changed to regular macrophage culture medium, which is RPMI-1640 medium, supplemented with 20% FBS (Gibco™), 100 U/ml Penicillin (Gibco™), 100  $\mu$ g/ml Streptomycin (Gibco™) and 5 mM glucose.

Macrophages were activated for 18 hours with 50 ng/ml IFN- $\gamma$  and 20 ng/ml LPS to M1-macrophages respectively with 25 ng/ml IL-4 and 25 ng/ml IL-13 to M2-macrophages after reaching a confluent growth state. Success of activation was checked for each experiment by examining the expression of macrophage activation markers CD80 and CD206 via real-time quantitative polymerase chain-reaction (rt-qPCR). An upregulation of CD80 for M1-macrophages without upregulation of CD206 and oppositely upregulation of CD206 without a significant change in CD80 expression, respectively, was required (30). Untypical pattern changes in surface marker expression led to exclusion of the experiment.

#### 3.4.3 Cell counting for experiments

To perform experiments reliably and comparably, accurate cell counting and seeding in pre-defined concentrations is indispensable. Cells were usually counted by pipetting 10  $\mu$ l of the cell suspension into a Neubauer counting chamber and counting all living cells in  $n$  squares using light microscopy. When cells were visible on cross lines, only those cells which presented on the upper or left cross line were counted.

The concentration of the cell suspension could then be calculated according to the following formula:

$$\text{concentration} = \frac{\sum_{i=0}^n \text{cells in square } i}{n} \cdot 10^4 \cdot \frac{1}{\text{ml}}$$

During monocyte isolation, cells and particles were counted by size using CASY cell counter (OLS OMNI Life Science GmbH). Right after isolation, the final number of isolated monocytes was also verified by manual counting as described above.

### 3.5 Transfection of primary monocyte-derived macrophages with small-interfering RNA (siRNA)

RNA interference is gene silencing via siRNA which binds to transcribed mRNA and inhibits translation (57). Monocytes were seeded in 12- or 24-well cell suspension plates right after isolation at a density of 0.2 million cells / ml in 1 ml respectively 500  $\mu$ l culturing medium supplemented with 50 ng/ml M-CSF and differentiated respectively activated into monocyte derived macrophages. Medium was changed after differentiation for activation and after M1- respectively M2-activation for transfection.

Transfections for functional experiments were performed chemically using either Lipofectamine<sup>®</sup> RNAiMAX (Thermo Fisher Scientific), in the following RNAiMAX, or Viromer<sup>®</sup> Blue (Lipocalyx GmbH). Further reagents were assessed for efficiency and toxicity (**chapter 4.5**).

The DEP-1 siRNA was customly synthesized from Sigma-Aldrich according to the following sequences (6):

5'-UACUGUGUCUUGGAAUCUAdGdC-3' (sense)

5'-UAGAUUCCAAGACACAGUAdGdG-3' (antisense)

A non-targeting control siRNA was purchased from Sigma-Aldrich:

5'-UAAGGCUAUGAAGAGAUACdGdC-3' (sense)

5'-GUAUCUCUUCAUAGCCUUAdGdG-3' (antisense)

Both siRNA main stocks were resolved to a concentration of 50  $\mu$ M.



The following protocols are the outcome of several assessments with differing concentrations of siRNA, knockdown reagent, supplementary ingredients, cells, and plate sizes. Best results were achieved with a final 25 nM siRNA concentration per well. Transfection succeeded in 12-, 24- and 96-well-plates. As finding this methodology was part of this project, further assessments of knockdown efficiency and toxicity are described in the results (**chapter 4.5**). Besides evaluation of knockdown efficiency and toxicity, basic quality criteria for continuation and inclusion of experiments where a stable cell morphology as observed in light microscopy, a confluent cell layer at all parts of the well without major cell detachment during the whole time of the experiment and continuous incubation at 37 °C and 5% CO<sub>2</sub>-concentration with only short interruptions for experimental bench work, kept as short as possible.

### 3.5.1 Transfection protocol for Lipofectamine® RNAiMAX

Depending on experiment or readout, transfection with RNAiMAX was performed in 12-well-, 24-well- or 96-well plates. Macrophages were transfected under starvation conditions (0 % FBS in the medium) for 4 hours. Starvation was afterwards interrupted by addition of 60 % FBS medium to make the resulting FBS-concentration 20 % for the remaining transfection time.

The following amounts are calculated for transfection of a single well and were upscaled according to the number of wells to transfect with 10 % extra.

For transfections in 24-well-plates, 50 µl transfection mix were added to 283.3 µl transfection medium (RPMI-1640, 0% FBS, 1xP/S, 5mM glucose).

The transfection mix was prepared in 1.5 ml reaction tubes named “tube A” and “tube B”:

- in tube A, 0.25 µl 50 µM siRNA were added evenly into 25 µl Opti-MEM
- in tube B, 1.5 µl RNAiMAX were added into 25 µl Opti-MEM.

Solutions from both tubes were combined (approximately 50 µl) and mixed well, before the resulting final transfection mix was incubated for 15 minutes at room temperature for complexation. It was then added to the previously prepared 283 µl transfection medium. After 4 hours, 167 µl 60 % FBS medium were added, resulting in a 20 % FBS medium.

**Table 9** summarizes amounts of compounds used for transfections in a 12-well- and 96-well-plate, respectively.

**Table 9: Reagents and amounts for transfections with Lipofectamine® RNAiMAX.**

	12-well-plate	24-well-plate	96-well-plate
<b>tube A</b>			
<b>Opti-MEM</b>	50 µl	25 µl	5 µl
<b>50 µM siRNA</b>	0.5 µl	0.25 µl	0.05 µl
<b>tube B</b>			
<b>Opti-MEM</b>	50 µl	25 µl	5 µl
<b>Lipofectamine® RNAiMAX</b>	3 µl	1.5 µl	0.3 µl
<b>Total transfection mix</b>	100 µl	50 µl	10 µl
<b>0 % FBS medium</b>	567 µl	283 µl	57 µl
<b>60 % FBS medium</b>	333 µl	167 µl	33 µl

### 3.5.2 Transfection protocol for Viromer® Blue

Transfection with Viromer® Blue was usually performed in 12-well plates. Starvation conditions were not needed since the transfection efficiencies were high enough without.

For transfecting one well of a 12-well-plate with 1 ml medium, 100 µl transfection mix were prepared and added onto the medium, resulting in totally 1.1 ml medium. The transfection mix was prepared as described:

- In tube A, 0.55 µl 50 µM siRNA were added into 10 µl of Viromer® buffer and mixed.
- In tube B, a 1 µl droplet of Viromer® was added to the wall and 90 µl Viromer® buffer were added on top of that. Immediately after, the tube was vortexed for 5 seconds.

Both tubes were combined ( $\approx$  100 µl), incubated for 15 minutes at room temperature for complexation and then added dropwise onto the cells. There was no need to change the medium later, unless necessary for the experiment, because of very low toxicity.

**Table 10** summarizes amounts of compounds, used for transfections in a 24-well- respectively in a 96-well-plate.

**Table 10: Reagents and amounts for transfections with Viromer® Blue.**

	12-well-plate	24-well-plate	96-well-plate
<b>tube A</b>			
- <b>Viromer® buffer</b>	10 µl	5 µl	1 µl
- <b>50 µM siRNA</b>	0.55 µl	0.275 µl	0.055 µl
<b>tube B</b>			
- <b>Viromer® Blue droplet</b>	1 µl	0.5 µl	0.1 µl
- <b>Viromer® buffer</b>	90 µl	45 µl	9 µl

### 3.6 RNA biochemical methods and polymerase chain-reaction assays

Determining gene expression by measuring transcribed mRNA qualitatively and quantitatively by polymerase chain-reaction is a very well-known and ubiquitously established molecular biology technique. The basic principle is to amplify a pre-defined sequence of a desoxy ribonucleic acid(DNA) template exponentially in multiple replication steps.

#### 3.6.1 RNA lysis and extraction

For assessing the status of gene expression in a cell association at a certain timepoint, intracellular RNA needs to be extracted from the cell sample. In this work, RNA lysis and extraction were performed by a silica-membrane based kit called NucleoSpin® RNA (Macherey-Nagel GmbH & Co. KG). The manufacturer's protocol was used as is and not adjusted.

In short, 3.5 µl β-mercaptoethanol for irreversible denaturation of RNAses were added to 350 µl of the kit's RA1 buffer per sample. Right before planned lysis, cell suspensions were taken into 15 ml tubes, centrifuged at 1200 rpm for 10 minutes at room temperature, resuspended in PBS and centrifuged again. The supernatant was removed, and the cell pellet resuspended in 350 µl RNA lysis buffer, prepared as described.

Adherent cells, such as primary monocyte-derived macrophages were washed once with PBS in-plate, before 350 µl of prepared RNA lysis buffer were added directly onto the cells in the wells.

Lysis completes immediately so that the samples could either be processed directly for RNA extraction or frozen in the plate or vial at -80 °C and taken out for later extraction.

For RNA extraction, samples were used directly after lysis or frozen, stored samples were quick-thawed (e. g. in a CO<sub>2</sub>-incubator). Samples were transferred into the NucleoSpin® filter tubes, centrifuged and thereby filtered for one minute at 11000 rpm. Then, 350 µl of 70% ethanol were added into each tube and mixed by pipetting up and down at least five times until the viscous cords within the fluid disappear. The sample was then transferred into the NucleoSpin® RNA column and centrifuged at 11000 rpm for 30 seconds. The nucleic acids are now on the silica-membrane of the column. For desalting, which makes RNA digestion more efficient, 350 µl membrane desalting buffer were added onto each membrane, followed by centrifugation at 11000 rpm for 30 seconds. Afterwards,

remaining DNA was digested by adding 95  $\mu\text{l}$  (1:10 dilution) rDNase in a specific reaction buffer onto the membrane and allowing 15 minutes incubation at room temperature for reaction. DNA digestion was followed by three washing steps (step 1: 200  $\mu\text{l}$  RAW2, step 2: 600  $\mu\text{l}$  RA3, step 3: 250  $\mu\text{l}$  RA3), each one followed by centrifugation at 11000 rpm for 30 seconds and 120 seconds after the last washing step, respectively. Finally, the purified RNA was eluted by 20-60  $\mu\text{l}^2$  RNase-free water and centrifugation at 11000 rpm for 60 seconds.

Afterwards, RNA concentration and purity was measured using the NanoDrop micro-volume spectral-photometer (Thermo Fisher Scientific, USA). Ideally, the purified RNA had only a single absorption maximum at 260 nm (260:280 ratio  $\leq 1$ , 260:230  $> 1.9$ ) and concentration exceeds at least 15 ng/ $\mu\text{l}$  for accurate synthesis of complimentary DNA (cDNA)). Samples, not meeting these quality standards, were not used for further analysis. RNA was stored at  $-80\text{ }^\circ\text{C}$  or used immediately for cDNA synthesis.

### 3.6.2 cDNA synthesis

Extracted RNA can be used to synthesize cDNA directly, if quality exceeds requirements, or after DNase treatment. cDNA can then be analyzed and quantified by rt-qPCR.

DNase treatment becomes necessary when there is evidence for genomic DNA contamination of the RNA samples. Since genomic DNA might be copied and amplified in a later polymerase chain reaction (PCR) or interfere with the reaction itself, it is important to have very clean RNA samples.

For DNase treatment, RQ1 RNase-Free DNase from Promega GmbH, Germany, was used. 10  $\mu\text{g}$  of extracted RNA, 3  $\mu\text{l}$  of reaction buffer, 10  $\mu\text{l}$  of DNase were pipetted into a reaction tube and supplemented with  $\text{H}_2\text{O}$  until a total reaction volume of 30  $\mu\text{l}$ . Samples were incubated for 30 minutes at  $37\text{ }^\circ\text{C}$ . Afterwards, 1  $\mu\text{l}$  of STOP-buffer was added and the samples were incubated for another 10 minutes at  $65\text{ }^\circ\text{C}$  for DNase inactivation.

After DNase treatment or – if DNase treatment was not necessary – directly after RNA extraction, the resulting highly purified RNA can be used for cDNA synthesis.

---

<sup>2</sup> The amount of water during the elution step was chosen by experience and desired final RNA concentration, concerning the expected amount of RNA on the column which is again dependent on number of previously seeded cells, well size, culturing conditions and cell viability.

In cDNA synthesis the single-stranded RNA which comes from the cellular mRNA and represents the expression state of cell at the time of lysis is being transcribed into complementary double-stranded DNA (cDNA) which can be used in a PCR later on. This transcription is done by the enzyme reverse transcriptase, known from retroviruses which uses the reverse transcriptase to copy their RNA-genome into genomic DNA which can be read by the enzymes of their host cells (13, 163). The reverse transcriptase reads the RNA and adds a complementary RNA-DNA-hybrid-strand through its RNA-dependant-DNA-polymerase. Next, the same enzyme digests the remaining RNA strand with its RNA-DNA-heteroduplex-recognizing RNase-H and completes the single DNA-strand to a double-stranded final cDNA by its DNA-dependent-DNA-polymerase.

The RevertAid H Minus First Strand cDNA Synthesis Kit (Thermo Fisher Scientific, USA) was used to transcribe RNA into cDNA. In a first step, equal RNA amounts (dependent on measured concentration) per sample were added into a reaction tube. Minimum amounts between 100 and 200 ng RNA per sample are required, 500-1000 ng are recommended. Together with the RNA, 1  $\mu$ l of oligo dT primers was added and the tube was filled up to a total reaction volume of 12  $\mu$ l with nuclease-free H<sub>2</sub>O. For primer annealing, the RNA-primer-mix was incubated for 5 minutes at 65 °C. Afterwards, 8  $\mu$ l of a pre-prepared mastermix, consisting of 4  $\mu$ l 5X reaction buffer, 2  $\mu$ l 10 mM dNTPs, 1  $\mu$ l “RiboLOCK” and 1 $\mu$ l reverse transcriptase, were added. cDNA synthesis reacted at a temperature of 65 °C for 60 minutes, ideally in a rapidly heating and cooling thermocycler. After synthesis, the components were inactivated at 70 °C for 5 minutes and transcribed cDNA was diluted with nuclease free (routinely 60 – 100  $\mu$ l). cDNA could be used directly for PCR applications, while temporarily storing it on ice, or long-term stored at -80 °C.

### 3.6.3 Principles of real-time PCR with SYBR green

The template double-stranded DNA (dsDNA) is denaturized, and the enzymes are activated by exposing the samples to 95 °C for 10 minutes. Next, DNA is amplified in multiple cycles. One cycle consists of an annealing step in which the forward and reverse primers anneal to the now single-stranded DNA (ssDNA) templates, framing the sequence desired for amplification. The second amplification step is the elongation step, which is temperature-optimized for the thermostable Taq-DNA-polymerase. In this step,

the DNA polymerase synthesizes a complimentary DNA strand on the template, beginning at the position of the forward or backward primer. By repeating these cycles, the sequence of interest, framed by the primer pair, gets amplified exponentially. Therefore, quantification of the resulting amount of DNA by the fluorochrome SYBR green, which complexes mainly with DNA and – with less intense fluorescence – with ssDNA and RNA, can be correlated with the initial amount of mRNA from which the samples were prepared. In a basic PCR application, the thermocycler is the machine in which the samples are incubated at different temperatures for the specified durations. It can heat up and cool down rapidly and is programmed according to the desired PCR protocol. In rt-qPCR, the thermocycler can also measure the fluorescence intensity of the samples at given trigger point, e. g. after each cycle. Therefore, the amplification of the nucleic acids can be monitored in real-time. Since SYBR green is not specific for the product of interest, the experimenter verified that only the desired sequence, framed by the primers, was amplified by melting curve analysis (203): The melting curve is the SYBR green fluorescence intensity plotted against temperature. Different DNR products have different melting temperatures depending on their GC/AT ratio. Therefore, the number of melting curve drops correlates with the number of amplified products. If only one product was amplified, only one melting point should be measurable. Unspecific products which may exist due to unspecificity of the primer, primer dimers or contamination, would melt at other, usually lower (e. g. primer dimers) temperatures, than the desired product.

#### 3.6.4 Implementation of rt-qPCR

In this project, rt-qPCR was performed with the CFX Connect™ Real-Time PCR Detection System from Bio-Rad, the included software CFX Manager 3.1 and the Maxima SYBR Green/ROX qPCR Master Mix from Thermo Fisher Scientific.

**Table 11: Used primers against human target genes.**

Target gene	Primer sequences
YWHAZ	Forward: ACTTTTGGTACATTGTGGCTTCAA Reverse: CCGCCAGGACAAACCAGTAT
DEP-1	Forward: AGCAGGCTCAGGACTATGGA Reverse: AACGAGGTACCGGAAGTTGA
p65	Forward: ATGGCTTCTATGAGGCTGAG Reverse: CACAGCATTTCAGGTCGTAGT
TNF- $\alpha$	Forward: CCCAGGCAGTCAGATCATCTTC Reverse: AGCTGCCCCTCAGCTTGA
rPL0	Forward: CGCTGGCTCCCACTTTGT Reverse: AATCTCCAGGGGCACCATT
uPAR	Forward: GAGAAGAGCTGGAGCTGGTG Reverse: CTTCGGAATAGGTGACAGC
PDGFR	Forward: CAGCAAGGACACCATGCGGCT Reverse: GGGGCTCCTGGGACATCCGT
CD80	Forward: CTGCCTGACCTACTGCTTTG Reverse: GGCGTACACTTTCCCTTCTC
CD206 (MRC1)	Forward: TGGTTTCCATTGAAAGTGCTGC Reverse: TTCCTGGGCTTGACTGACTGTTA
Bax	Forward: GGACGAACTGGACAGTAACATGG Reverse: GCAAAGTAGAAAAGGGCGACAAC
Bcl-2	Forward: CTGCACCTGACGCCCTTACC Reverse: CACATGACCCCACCGAACTCAAAGA

Primers were ordered from Sigma-Aldrich. Each primer sequence's specificity was evaluated by melting curve analysis.

First, PCR master mixes with forward- and backward-primers for each target gene and the housekeeping gene were created individually (**Table 11**). In this work, YWHAZ was used as a housekeeping gene in all qPCR experiments (85, 101).

Per sample, the PCR master mix contained 5  $\mu$ l SYBR green (Thermo Fisher Scientific, USA), 0.3  $\mu$ l 10 mM forward-primer dilution, 0.3  $\mu$ l 10 mM backward-primer dilution

and 2.4  $\mu$ l nuclease free H<sub>2</sub>O and amounts were upscaled depending on the number of samples and target genes.

Samples and master mix were then added to the PCR plate (Bio-Rad Laboratories Inc., USA). Each target-sample-combination was added at least in duplicates. Each well contained 2  $\mu$ l cDNA sample (equal dilution per experiment) and 8  $\mu$ l mastermix which was prepared as described above. Pipetting was performed on ice or on a -20 °C cooling block holding the PCR plate (Eppendorf<sup>®</sup>, Merck, Germany), respectively. The plate was finally sealed with plate-specific seal-films (Bio-Rad Laboratories Inc., USA), centrifuged at 2500 rpm for 10 seconds and placed in the thermocycler.

The PCR started with a 10-minutes initial dsDNA-denaturation step at 95 °C, followed by 40 replication cycles, each one containing a 10 second long step at 95 °C for dsDNA-denaturation, followed by 60 seconds at 60 °C for primer annealing, extension and fluorescence read-out. The replication cycles were followed by a 30 second long final extension step at 95 °C and melting curve acquisition. **Table 12** visualizes the employed PCR program.

**Table 12: Tabular visualization of the applied PCR program**

Cy- cles	Duration (min:sec)	Temperature	
1x	10:00	95 °C	Initial denaturation
40x	0:10	95 °C	Denaturation
	1:00	60 °C	Primmer annealing, elongation, fluorescence read-out
1x	0:30	95 °C	Final denaturation
70x	0:10	60-95 °C + 0.5 °C / 10 sec.	Melting curve acquisition
1x	unlimited	4 °C	Hold / Storage

### 3.6.5 rt-qPCR data analysis

rt-qPCR was usually used to compare the expression of one certain gene between multiple, differently treated samples. For this, relative expression values, comparing the target gene expression in all tested samples to a non-treated, scrambled-siRNA-treated etc. control sample, needed to be calculated. The data output of a rt-qPCR experiment contains – besides many other data – the Cq or Ct value. This is the non-distinct number of cycles, after which the relative fluorescence units (RFU) of a sample passes a certain threshold RFU which is automatically (by the software) or manually set above the background fluorescence signals but also low enough to be in the beginning of the exponential replication



phase. A low Cq value indicates a higher amount of detected nucleic acids whereas a high Cq value stands for low amounts of nucleic acids.

To make multiple qPCR experiments comparable to each other, normalize different substrate amounts per sample, different primer- and PCR-efficiencies, varying annealing and elongation times, Pfaffl 2001 introduced the  $\Delta\Delta Cq$ -method which makes relative quantification accurate and easy (189).

In this work, usually duplicates or triplicates for each sample were run. The difference of the mean  $Cq_{SAMPLE}$ -value and the mean  $Cq_{HOUSEKEEPING}$ -value is the  $\Delta Cq$  value:

$$\Delta Cq = \overline{Cq_{SAMPLE}} - \overline{Cq_{HOUSEKEEPING}}$$

The relative expression could then be calculated by the following potency formula:

$$\text{relative expression} = 2^{-\Delta Cq} = 2^{\overline{Cq_{HOUSEKEEPING}} - \overline{Cq_{SAMPLE}}}$$

This way of calculation assumes, that the amount of cDNA is doubled in each cycle (100% PCR-efficiency) and equal for the reference housekeeping gene and the target gene. Although these assumptions are usually not completely reached, the method was positively validated by its developer and is the most common used principle of dealing with qPCR data.

Finally, the relative expression values can be normalized to a control sample as described above by applying the following formula which introduces the  $\Delta\Delta Cq$  value:

$$\text{normalized relative expression} = 2^{-\Delta\Delta Cq} = 2^{-(\Delta Cq_{SAMPLE} - \Delta Cq_{CONTROL})} = \frac{2^{\Delta Cq_{CONTROL}}}{2^{\Delta Cq_{SAMPLE}}}$$

### 3.7 Protein biochemical methods, SDS-PAGE and Western Blot

Sodium dodecyl sulfate polyacrylamide gel electrophoresis (SDS-PAGE) and western blotting are commonly biochemical techniques for protein analysis. In SDS-PAGE proteins are complexed with SDS to create an equal charge-mass-ratios among all containing proteins of a lysate. The proteins in the pre-processed samples can be separated by mass when running the samples in a polyacrylamide gel on which voltage is applied. The separated protein samples can then be transferred onto a blotting membrane, again by applying voltage, this time perpendicularly. On the blotting membrane, specific proteins can be detected by hybridization with specific antibodies.

In this work, the protein workflow and recipes are adapted and partly modified from Laemmli (130).

### 3.7.1 Protein lysis and protein determination assay

Since protein expression and activity is also influenced by many other mechanisms such as splicing, silencing, interference, protein degradation or its phosphorylation states, there is a need to analyze the proteome of a cell as well.

#### 3.7.1.1 Protein lysis

Protein lysates were acquired after washing cells once or twice with ice-cold PBS. Afterwards, the plates respectively the Falcon tubes, when lysing cell suspensions, were immediately transferred on ice to protect the proteome from degradation through proteases. The medium and PBS should be removed completely before lysing the cells with 150  $\mu$ l (up to 12-well-plate) respectively 200  $\mu$ l (6-well-plate) complete lysis buffer for 15 minutes on ice. Lysis buffer was added dropwise onto plates or the cell pellet after centrifugation (after discarding the supernatant) was resuspended in lysis buffer, respectively. The lysis buffer was pipetted into 1.5 ml tubes after lysis which were centrifuged at 13.000 rpm in a pre-cooled centrifuge at 4 °C for 30 minutes. After centrifugation, the supernatant contained the proteome and could be stored at -20 °C or processed immediately. Complete lysis buffer for one sample consisted of 147  $\mu$ l RIPA buffer, supplemented with 1.5  $\mu$ l each of a 100x-concentrated commercially available protease inhibitor and phosphatase inhibitor cocktail (according to manufacturer's instructions, Thermo Fisher Scientific, USA). Lysis buffer was prepared freshly for all samples before lysis and upscaled according to the number of samples.

#### 3.7.1.2 Protein concentration measurement

For protein concentration measurement an assay kit (Bio-Rad Laboratories Inc., USA) which is based on the Lowry (149) method but modified for compatibility with reducing agents and detergents was used. Basically, proteins are quantified by a colorimetric assay. The Folin-Ciocalteu-Reagent becomes colorimetrically at 750 nm detectable Molybdenum blue in presence of Cu(I) ions which were reduced by the protein itself before. For each assay, a standard curve is created by diluting and measuring BSA protein standards (0.2 mg/ml to 3.0 mg/ml; increment 0.2 mg/ml until 1.0 mg/ml, then 0.5 mg/ml). The sample's protein concentration can then be determined employing the Beer-Lambert law:

$$E = \log_{10} \left( \frac{I_0}{I} \right) = \epsilon_{\lambda} \cdot c \cdot d$$

In this formula,  $E$  is the measured extinction which can be calculated from the intensity of the incident light ( $I_0$ ) and the intensity of the transmitted light ( $I$ ). There is a linear correlation between the protein concentration ( $c$ ) and product of the specific molar attenuation coefficient ( $\epsilon$ ) at the wave length  $\lambda$  and the thickness of the cuvette ( $d$ ) which can be used to determine the protein concentration from the standard curve.

### 3.7.2 Preparation of polyacrylamide gels

Gels for SDS-PAGE were usually prepared one day before planned electrophoresis to allow sufficient drying time. Components for the stacking and resolving gel (**chapter 3.1.2, Table 13**) were scaled up to the number of needed gels and prepared separately. APS and TEMED were added only directly before gel casting since polymerization starts immediately after adding these substances. Separating gel dried for 45-60 minutes before pre-prepared separating gel buffer was supplemented with APS and TEMED and added onto the polymerized separating gel. Stacking gel with inserted well-template combs dried for another 15 – 25 minutes. Usually, a comb leading to 10 wells, each of 66  $\mu$ l volume, was used. Dried gels were stored, wrapped in wet paper, at 4 °C for up to 4 to 5 days.

**Table 13: Components and amounts for casting 7.5% stacking and separating gels**

	Stacking gel	Separating gel
<b>H2O</b>	1550.0 $\mu$ l	5400.0 $\mu$ l
<b>30% Acrylamide</b>	350.0 $\mu$ l	2490.0 $\mu$ l
<b>Stacking gel buffer</b>	650.0 $\mu$ l	1900.0 $\mu$ l
<b>20% SDS</b>	12.5 $\mu$ l	50.0 $\mu$ l
<b>20% APS</b>	15.0 $\mu$ l	40.0 $\mu$ l
<b>TEMED</b>	2.0 $\mu$ l	8.0 $\mu$ l

### 3.7.3 Sample preparation

Protein lysates were diluted 1:6 by adding 10  $\mu$ l sample solution to 50  $\mu$ l lysate. If necessary, protein lysates can be adjusted to the same protein concentration by diluting high concentrated samples with complete lysis buffer (**chapter 3.7.1.1**). Sample solution contains SDS to charge all proteins with equalized negative charge-mass-ratio, needed for SDS-PAGE, as well as  $\beta$ -Mercaptoethanol for denaturation and reduction of disulfide bonds within the proteins and glycerol for increased density of the sample, so that it stays within the well and the different samples do not mix.

After adding sample buffer and mixing well, the samples are cooked at 95 °C for not more than 5 minutes. Afterwards, the samples can be used immediately for SDS-PAGE or can be frozen again at -20 °C.

#### 3.7.4 SDS-PAGE

For gel casting and SDS-PAGE, the Mini-PROTEAN<sup>®</sup> Tetra System (Bio-Rad Laboratories Inc., USA) was used. Handcasted gels were mounted to the system. The electrophoresis cell was filled with 1:5 diluted 5X running buffer to at least one fourth. The combs were finally carefully removed from the gels and protein samples were loaded into the wells. Injection of samples was performed very slowly, bubble- and contamination-free. After loading the wells, the cell was filled up to the indicated line with diluted running buffer and closed. The gels were run slowly at 80 V voltage until the blue dyeline was in the upper part of the stacking gel. Afterwards, voltage was increased up to 160 – 180 V, whereas a voltage of 120 V was optimal. After the dye ran out of the gel, voltage should be removed from the cell and gels should be taken out and carefully transferred into methanol- and SDS-supplemented transfer buffer. Stacking gels were chopped off.

#### 3.7.5 Western Blot

Western blotting is the staining of proteins with specific primary antibodies and detection of those by secondary antibodies which are technically detectable, e. g. by staining, colorimetry, fluorescence, or radioactivity.

Before proteins can be detected on the polyvinylidene fluoride (PVDF) membrane, they needed to be transferred from the gel onto it. Gels, as well as membranes and filter paper were adjusted to the same transfer buffer for approximately 10 minutes. Before, the membranes were activated in 100% methanol for 5 minutes in a shaker.

Now the transfer stacks are assembled:

- 3 filter papers (pre-soaked in transfer buffer)
- PVDF membrane (activated in methanol, adjusted to transfer buffer)
- SDS-PAGE gel (adjusted to transfer buffer)
- 3 filter papers (pre-soaked in transfer buffer)

Air bubbles were removed carefully by gently rolling over the stack once after adding each layer, to make the transfer stack equally conductive.

Transfer completed at a current of 500 mA for 1:10 hours in the Amersham™ TE 77 PWR semi-dry transfer unit (GE Healthcare Life Sciences, USA).

Afterwards, the stacks were disassembled and disposed while only the PVDF membrane was kept and stored in 1X NET-G solution. Success of the transfer was evaluated by staining the membrane with Ponceau red (Sigma-Aldrich Co. LLC) which required washing with NET-G three times after staining.

Membranes were blocked by incubating the membrane for one hour in 50 ml 1X NET-G supplemented with 2.5 g milk powder (Sigma-Aldrich Co. LLC). Through this blocking step, not used protein “slots” within the membrane were occupied with milk protein, so that the membrane could not be contaminated with other environment proteins.

After blocking, membranes were ready for incubation with the primary antibody which binds specifically to certain proteins of interest on the membrane. In this work, a dilution of 1:1000 was used for all primary antibodies. Primary antibodies were diluted with NET-G and membranes were incubated with the primary antibody in a 50 ml Falcon tube on a roller at 4 °C, usually overnight; approximately 18 to 36 hours are acceptable. Too long incubation increases unspecific binding of the antibody which should be avoided. Primary antibody incubation was finished by washing the membrane three times in NET-G solution.

The secondary antibodies (Santa Cruz Biotechnology, Inc., USA) were selected depending on the origin of the primary antibody and incubated with the washed membranes in a 1:10000 dilution for one hour in a 50 ml Falcon tube on a roller. After washing the membrane with NET-G solution again for three times to wash away non-bound secondary antibodies, the bound antibodies respectively the membrane can be developed by short incubation with ECL substrate (Bio-Rad Laboratories Inc., USA) according to manufacturer’s instructions and read out in the chemiluminescence imaging system (GE Healthcare Life Sciences, USA).

Acquired western blot images were densitometrically quantified using the machine’s internal software according to the manufacturer’s instructions. In all experiments,  $\alpha$ -Vinculin was stained, detected, and analyzed as a loading control as well. Therefore, protein

densities were normalized to  $\alpha$ -Vinculin density individually for each sample, before the samples were compared to each other.

### 3.8 Macrophage cell proliferation and viability assay

Directly after isolation, primary monocytes were seeded in technical duplicates and replicates depending on the number of measured time points (usually triplicates for 0 hours, 24 hours and 48 hours) in a 96-well cell suspension plate at a density of 0.1 million cells per ml in 100  $\mu$ l medium (10.000 cells). The medium was supplemented with 50 ng/ $\mu$ l M-CSF and monocytes were left for macrophage differentiation. After 7 to 10 days, depending on the microscopic morphological differentiation state, medium was removed and replaced with culturing medium respectively M1- and M2-macrophage-activation-medium as described above and left for another 18 hours. After macrophage activation, the cells were stimulated according to the protocol. Afterwards, the medium was replaced again with general culturing medium respectively stimulation medium and cells were transfected using Lipofectamine<sup>®</sup> RNAiMAX as described. After the knockdown, medium was changed to a proliferation medium equivalent to the previous culturing conditions and supplemented with 20 ng/ml recombinant human PDGF-BB.

Cell proliferation respectively viability was measured using the tetrazolium based CellTiter 96<sup>®</sup> AQueous Non-Radioactive Cell Proliferation Assay (Promega GmbH, Germany) according to the manufacturer's instructions. In this assay, cells are incubated with a certain tetrazolium compound ([3-(4,5-dimethylthiazol-2-yl)-5-(3-carboxymethoxyphenyl)-2-(4-sulfophenyl)-2H-tetrazolium], MTS) that is reduced to a product which's absorbance is measurable at 490 nm. The reduction is catalyzed by dehydrogenase-enzymes that are present in metabolically active cells.

The MTS compound together with the PMS-solution from the above-mentioned kit was added 24 hours after transfection after a medium change. Absorbance was then measured at defined timepoints after addition of MTS each time and with regular incubation under stimulation conditions in between. The amount of the detected reduced product correlates with the cells' metabolic activity.

### 3.9 Immunoprecipitation and phosphatase activity assay

Freshly isolated monocytes were seeded at a density of in a 12-well cell suspension plate at a density of 0.2 million cells per ml in 1 ml medium. The medium was supplemented with 50 ng/ $\mu$ l M-CSF for macrophage differentiation. As described, after successful visual signs of differentiation, medium was removed and replaced with culturing medium respectively M1- and M2-macrophage-activation-medium as described before and left for another 18 hours. After a medium change, the samples were lysed in an anoxic chamber. For pre-clearing, which is to reduce non-specific binding of the protein G beads to already existing antibodies in the medium and lysates, respectively, 20  $\mu$ l protein G sepharose beads (Santa Cruz Biotechnology) were added for one hour to the samples which were continuously mixed on a rotating wheel at 12 rpm and cooled to 4 °C. The supernatants were transferred into new 1.5 ml reaction tubes. Next, 5  $\mu$ l DEP-1 antibody (Santa Cruz Biotechnology) and 30  $\mu$ l protein G sepharose beads were added and the samples were again incubated for 2.5 hours in the earlier described mixing and cooling conditions. During this immunoprecipitation step, DEP-1 antibody binds to the DEP-1 protein. At the same time, the protein G coupled sepharose beads bind to the antibodies and the heavy bead-antibody-protein complexes precipitate at the bottom of the tube.

Next, the purified DEP-1 enzymes were used to measure their phosphatase activity employing the Tyrosine Phosphatase Assay System (Promega) according to the manufacturer's instructions. The system contains two different tyrosine-phosphorylated peptides, END(pY)INASIL and DADE(pY)LIPQQG, which are substrates for many PTPs including DEP-1. During an incubation time, DEP-1 dephosphorylates the phosphor-peptides and phosphate(V) ions are released. Phosphate(V) ions react with ammonium molybdate and produce a colored complex. The complex's absorbance was measured at 620 nm in a plate reader (Victor X3 Multilabel, Perkin Elmer). The amount of released phosphate can be determined by a standard curve which is measured using the same dye and buffers and differently diluted phosphate ion standard solutions. The amount of released phosphate ions correlates with the phosphatase activity of the enzyme.

### 3.10 Scratch migration assay

Macrophage migration was analyzed employing scratch or wound healing assays (89). The basic idea of a scratch assay is that after creating a scratch in a confluent cell layer,

the remaining cells will proliferate and migrate to close this scratch and make the cell layer confluent again. The time until the scratch is closed completely, or the remaining open area at a specific time point relative to the initial open area right after making the scratch are indicators for the migratory ability of the assayed cells (37).

Scratch assays were usually performed in 12-well suspension plates in which 0.2 million monocytes were seeded right after isolation in 1 ml M-CSF-supplemented medium for macrophage differentiation and grown until an 80-90 % confluent monolayer without larger visible cell gaps. Now, further experimental steps such as knockdown or stimulation were performed as described and according to the protocol.

The scratch itself was drawn straight and along a ruler into each well with a 1.0 ml or 200  $\mu$ l pipette tip, resulting in a scratch size of 0.5-1.0 mm. It is important to perform this step with moderate and not too much force to keep the well's bottom architecture and extracellular matrix intact. After making the scratch the medium was removed and the wells were washed at least twice with warm medium. The complete removal of all scratched floating cells was confirmed using light microscopy, otherwise the wells were washed again. Finally, the wells were filled with 1.0 ml medium again which was adjusted to the previous experimental conditions, such as NG, HG or PAM(3)-stimulation.

Phase-contrast images with focus on the well bottom were taken at at least two pre-defined positions per well right after scratching ( $t=0$ h) and after pre-defined time intervals, usually 24 and 48 hours using the Axio Observer (Carl Zeiss Microscopy GmbH, Germany) microscope. The open area of each scratch was measured for each timepoint using ImageJ. Fractional open areas (FOA) were calculated with respect to the initial open area at  $t=0$ h for each time series. Experiments in which major cell detachment or morphology changes – both being associated with cell death – were observed at the time of image analysis were excluded retrospectively from analysis.

### 3.11 Data collection and statistical analysis

Data was collected in native storage formats and homogenized in Microsoft Excel and a SQL-based database on MariaDB Server 10. Statistical analysis was performed with Prism 9 (GraphPad) as well as SPSS Statistics 25 (IBM). Statistical testing was performed using the whole spectrum of available tests depending on the data acquired, including non-parametric Mann-Whitney-U-Test (156, 267) respectively Kruskal-Wallis-Test



(127) for comparing more than two groups. Normally distributed variables were compared using the paired or unpaired Student's t-test, or the 1-way analysis of variance (ANOVA). Bonferroni's method was used for post-hoc testing both after ANOVA and Dunn's method for Kruskal-Wallis tests. The used test, as well as resulting p-values are indicated in the figure legends. Figures were created with Prism 9 (Graph Pad), Photoshop CC 21.1.2 and Illustrator CC 24.1.2 (Adobe). If not stated otherwise, data is plotted as mean values and error bars represent the standard error of the mean (SEM). Standard deviations (SD) and 95% confidence intervals (CI) are reported where indicated. Boxplots with minimum- to maximum-whiskers were used to present datasets containing at least 4 biological replicates.

## 4 Results

### 4.1 DEP-1 is upregulated in monocytes from patients suffering from type 2 diabetes mellitus

**Table 14** summarizes clinical and biomarker baseline characteristics of included 22 diabetic patients and 27 control individuals which were recruited from both recruiting sites as described after careful consideration of inclusion and exclusion criteria (**chapter 3.2.2**).

**Table 14: Clinical and biomarker patient characteristics.**

n		controls		T2DM	
		22		27	
<b>Diabetes mellitus, type 2</b>		0	0.0 %	27	100.0 %
<b>Coronary artery disease</b>		12	54.5 %	0	0.0 %
<b>Ex-Smoker</b>		2	9.1 %	1	3.7 %
<b>Gender</b>	<b>Female</b>	6	27.3 %	11	40.7 %
	<b>Male</b>	16	72.7 %	16	59.3 %
<b>Age (years)</b>		55.59	(14.61)	64.04	(7.41)
<b>Body mass index (kg/m<sup>2</sup>)</b>		27.34	(3.96)	35.84	(7.60)
<b>HbA<sub>1c</sub> (%)</b>		5.30	(0.38)	8.40	(0.72)
<b>Fasting glucose (mM)</b>		5.37	(0.92)	11.64	(4.32)

*Nominal variables (Diabetes mellitus yes/no, coronary artery disease yes/no, ex-smoker yes/no, gender female/male) are presented as absolute counts and relative column percentages of the included patients. Metric variables are presented as means with the standard deviation of the mean in brackets in the unit given behind the name of the variable.*

Besides the diagnosis of DM, both groups differed in the prevalence of coronary artery disease with 54.5 % in the control group versus none in the T2DM group. With active smoking within the past 6 months before inclusion being an exclusion criterion for both groups, the number of ex-smokers is low in both groups. The number of male patients was higher in the control group while T2DM patients were in average 10 years older than control patients. Body mass index was elevated according to WHO definition in both groups, although much higher in T2DM patients.

The differences in prevalence of cardiovascular disease, age and sex are explainable by the two recruiting sites: While diabetic patients were mainly recruited from an endocrinology department, non-diabetic controls were recruited from cardiology wards and are therefore in different medical conditions explaining their impatient stay there. This will be discussed.

Monocytes were isolated from 50 ml heparinized whole blood from all patients and lysed immediately. RNA was extracted and analyzed in an rt-qPCR regarding the monocytic

expression of different phosphatases. The mean relative expression of DEP-1 was  $0.10 \pm 0.009$  within the control group and  $0.14 \pm 0.014$  within the DM group. Among other phosphatases, DEP-1 expression was 1.34-fold upregulated in the group of diabetic hyperglycemic patients ( $p=0.0466$ , **Figure 2A**). Levels of DEP-1 expression were analyzed in a linear regression model in which a correlation to the corresponding HbA<sub>1C</sub> values could not be determined ( $r^2=0.057$ ) (**Figure 2B**).

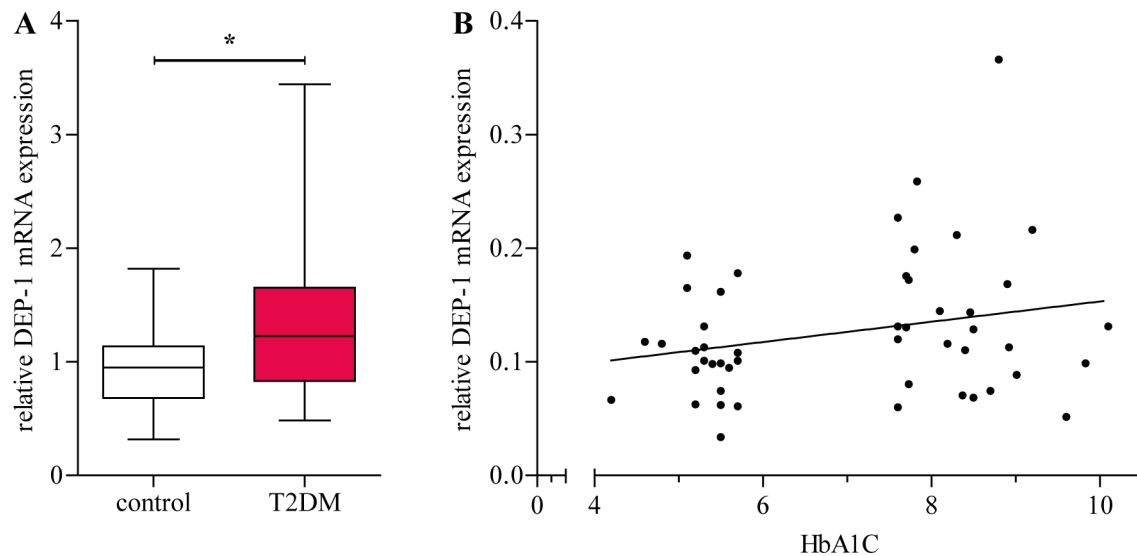


**Figure 2: DEP-1 expression in patients with T2DM.** Monocytes were isolated from whole blood of  $n=27$  patients suffering from T2DM and  $n=22$  controls. DEP-1 mRNA expression was analyzed employing rt-qPCR. **A:** DEP-1 expression was 1.34-fold upregulated in the hyperglycemic group ( $p=0.0466$ ) **B:** There was no linear correlation between HbA<sub>1C</sub> and level of DEP-1 expression ( $r^2=0.057$ ). Statistical analysis employed Mann-Whitney-U-test at a significance level of  $\alpha = 0.05$ . Plotted are boxplots with minimum-to maximum whiskers. \*  $p < 0.05$ .

#### 4.2 Hyperglycemia and methylglyoxal treatment potentially lead to upregulation of DEP-1 in primary monocytes *in-vitro*

Questioning the relevance of DEP-1 in diabetic monocytes and macrophages and knowing about its upregulation in monocytes from diabetic hyperglycemic patients, it is relevant to know whether glucose itself or other mechanisms such as glucose degradation and accumulation of toxic side metabolites trigger the upregulation of DEP-1 observed in monocytes of diabetic patients (**chapter 4.1**).

Primary, freshly isolated monocytes were stimulated in an established hyperglycemia model by culturing 0.5 million monocytes in 2 ml culture medium in a 6-well cell suspension plate for 48 hours in NG (5 mM glucose) or HG (30 mM glucose) (245). Additionally, cells were exposed to either methylglyoxal (MG, 100  $\mu$ M), a side metabolite of

glycolysis, or oxLDL (20  $\mu$ g/ml) during the second 24 hours of the experiments. The cells were then lysed, protein was extracted and analyzed in SDS-PAGE and by Western Blot.

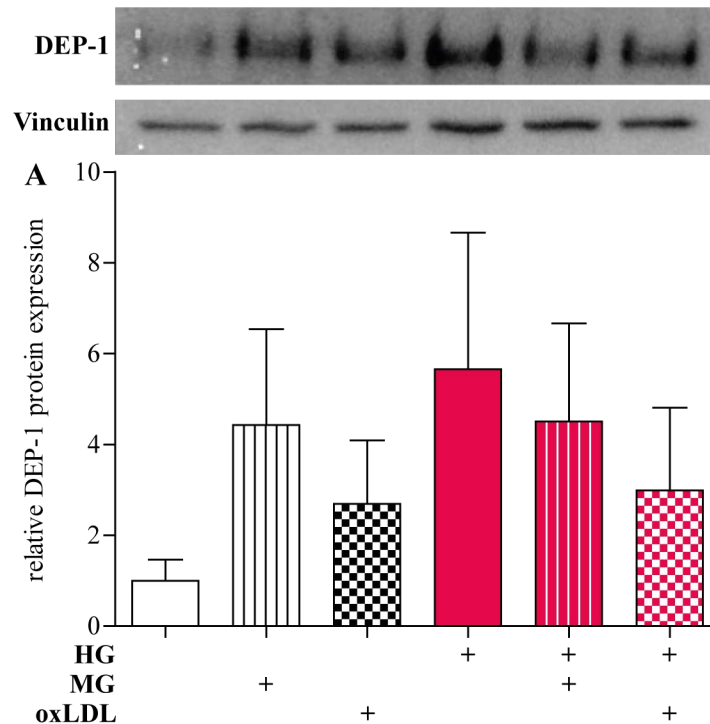


**Figure 3: DEP-1 expression in HG-cultured monocytes.** Primary human monocytes were isolated from healthy donors (n=3 biological replicates) and cultured for 48 hours in either NG (5 mM glucose) or HG (30 mM glucose). Effects of MG and oxidized oxLDL were evaluated by stimulating samples during the last 24 hours of the total 48 hour incubation with either 100 mM MG or 20  $\mu$ g/ml oxLDL, respectively. After 48 hours, cells were lysed, protein was collected, and samples were run in iso-volume SDS-PAGE and stained for DEP-1 and Vinculin. Density of DEP-1 bands were normalized to Vinculin. The graph shows a potential upregulation of DEP-1 through HG, MG and oxLDL, although additive effects of the three conditions were not observed. Plotted are means and SEM error bars. Kruskal-Wallis testing was not significant (p=0.6766). An exemplary western blot shows the induction of DEP-1 through HG, MG and oxLDL.

There was a trend of elevated DEP-1 protein expression in HG-cultured monocytes (fold change: 5.6, SD: 5.2). Methylglyoxal, a side-product of glucose metabolism and known mediator of diabetic complications, led to upregulation of DEP-1 in HG (fold change: 4.5, SD: 3.7) and also in NG (fold change: 4.4, SD: 3.7). Additive effects of HG and MG were not observed. oxLDL lead to an upregulation of DEP-1 (fold change: 2.7, SD: 2.4) in NG compared to the untreated control sample. However, regulation through oxLDL seemed less intense compared to HG and MG. Interestingly, oxLDL limited the upregulation of DEP-1 through HG (HG + oxLDL: 3.0x mean fold change versus 5.7x mean fold change in HG alone) (**Figure 3**). Kruskal-Wallis-testing of quantified Western Blot data was not significant (p=0.6766). However, these results justify further experiments

under improved conditions and more stable cells, e.g., from cell lines to further elucidate the effects of HG, hypercholesterolemia, and relevant side products of both metabolic conditions on monocytic DEP-1 expression *in-vitro*.

### 4.3 TNF- $\alpha$ induced pro-inflammatory signaling stimulates DEP-1 expression in primary monocytes

HG is a pro-inflammatory stimulus in DM, induces DEP-1 expression in primary monocytes *in-vitro* (**chapter 4.2**) and is therefore a possible mediator of DEP-1 upregulation in diabetic patients (**chapter 4.1**). Inflammation is considered to be one of the most important mediators linking DM to its cardiovascular complications and first anti-inflammatory treatments for DM itself and limitation of its complications are investigated in clinical trials (51). Since it was earlier reported that DEP-1 expression can be induced by TNF- $\alpha$  stimulation of T-lymphocytes (46) it seems rational to investigate the impact of this inflammatory pathway on DEP-1 expression in monocytes.

Primary human monocytes were stimulated with 10-25 ng/ml human recombinant TNF- $\alpha$  for 24 hours and then analyzed in a rt-qPCR experiment. To investigate the intracellular downstream signaling further, an inhibitor of NF- $\kappa$ B activation (InSolution™ NF- $\kappa$ B activation inhibitor, 1  $\mu$ M) and an inhibitor of protein kinase C (GF 109203X, 5  $\mu$ M) were applied simultaneously without preincubation time.

Stimulation with TNF- $\alpha$  led to a significant 3.6-fold (SD: 1.0, 95%-CI: 2.6-4.7,  $p=0.0002$  vs. control) upregulation of DEP-1 protein expression, which indicates that DEP-1 could be involved in inflammatory processes. NF- $\kappa$ B inhibition via InSolution™ NF- $\kappa$ B activation inhibitor limited this upregulation to 2.7-fold (- 24 %, SD: 0.99, 95%-CI: 1.7-3.8,  $p=0.0110$  vs. control,  $p=0.5316$  vs. TNF- $\alpha$ ) of the baseline expression. PKC inhibition via GF 109203X nearly bisected TNF- $\alpha$ -induced upregulation to only 1.9-fold (- 46 %, SD: 0.67, 95%-CI: 1.2-2.7,  $p=0.3787$  vs. control,  $p=0.0166$  vs. TNF- $\alpha$ ) of the baseline expression. Downregulation of DEP-1 expression via GF 109203X compared to TNF- $\alpha$  stimulation alone was therefore statistically significant, as well as the initial upregulation through TNF- $\alpha$  itself compared to the non-stimulated control (**Figure 4**).

This data suggests that TNF- $\alpha$  as one of the most potent pro-inflammatory cytokines has a significant positive regulatory impact on DEP-1 expression. This effect is most probably

signaled through downstream NF- $\kappa$ B activation because of the very likely limiting effect of the applied direct NF- $\kappa$ B-inhibitor and the significant limiting effect of the applied PKC-inhibitor.

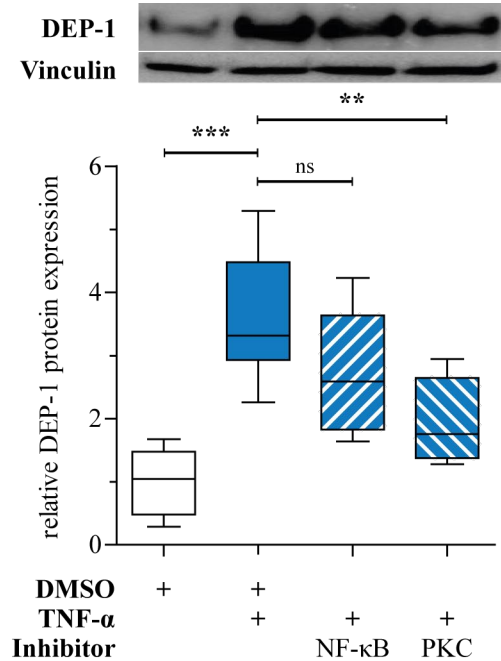


**Figure 4: TNF- $\alpha$  upregulates DEP-1 protein expression in monocytes.** Primary human monocytes isolated from healthy donors (n=6 biological replicates) were stimulated with 10-25 ng/ml TNF- $\alpha$  directly after isolation for 24 hours. Simultaneously, NF- $\kappa$ B activation inhibitor at a concentration of 1  $\mu$ M and a PKC-inhibitor at a concentration of 5  $\mu$ M were applied without preincubation. Protein was collected after 24-hour incubation. Proteins were run in iso-volume SDS-PAGE and stained overnight for DEP-1 and Vinculin, respectively. Density of DEP-1 bands were normalized to Vinculin. TNF- $\alpha$  stimulation led to a highly significant 3.6-fold (SD: 1.0, 95%-CI: 2.6-4.7, p=0.0002 vs. control) upregulation of DEP-1 expression which could be partly rescued by NF- $\kappa$ B inhibition via InSolution™ NF- $\kappa$ B activation inhibitor (- 24 %, SD: 0.99, 95%-CI: 1.7-3.8, p=0.0110 vs. control, p=0.5316 vs. TNF- $\alpha$ ) and PKC inhibition via GF 109203X (- 46 %, SD: 0.67, 95%-CI: 1.2-2.7, p=0.3787 vs. control, p=0.0166 vs. TNF- $\alpha$ ). An exemplary western blot shows the induction of DEP-1 through TNF- $\alpha$  stimulation, as well as the limiting effects of InSolution™ NF- $\kappa$ B activation inhibitor (NF- $\kappa$ B-i) and GF 109203X (PKC-i). Plotted are box plots with minimum- to maximum-whiskers. Data was analyzed employing Kruskal-Wallis with Bonferroni post-hoc testing at a significance level of  $\alpha=0.05$ . \*\* p<0.01, \*\*\* p<0.001, <sup>ns</sup> not significant.

#### 4.4 Inflammatory M1-macrophages show highest expression and activity of DEP-1 among non-activated and activated macrophage subpopulations

Primary monocytes can be differentiated into monocyte-derived macrophages *in-vitro* and activated into distinct functional phenotypes by cytokine combinations. These activation stages can also be observed *in-vivo* as a continuum between the two extremes of classical M1-activation and non-classical alternative M2-activation. However, functional experiments on these extremes *in-vitro* are commonly used in macrophage basic research.

This experiment intended to test whether DEP-1 is present in macrophages in the same way as in monocytes and whether a pro-inflammatory context modelled by *in-vitro* M1-activation of macrophages contributes to changes in expression or activity of the phosphatase.

For both, expression and activity assays, primary monocytes were isolated freshly from healthy donors and cultured in regular monocyte culture medium supplemented with 50 ng/ $\mu$ l recombinant human-M-CSF for differentiation into M $\phi$ -macrophages within 7 to 10 days. Final differentiation and activation were evaluated on an experiment-individual basis for most experiments by assessing macrophage activation markers, as well as by visual control under light microscopy considering typical morphology changes in each experiment. All wells were changed to regular macrophage culture medium while the medium in the wells for M1- and M2-activation was supplemented with either 50 ng/ml IFN- $\gamma$  and 20 ng/ml LPS (M1) or 25 ng/ml each of IL-4 and IL-13. After 18 hours, medium was again changed to regular macrophage culture medium without M-CSF nor activating cytokines. Macrophages in different activation stages were then cultured in either 5 mM glucose (NG) or 30 mM glucose (HG) for 48 hours, lysed and prepared for rt-qPCR analysis, or phosphatase activity assay was performed.

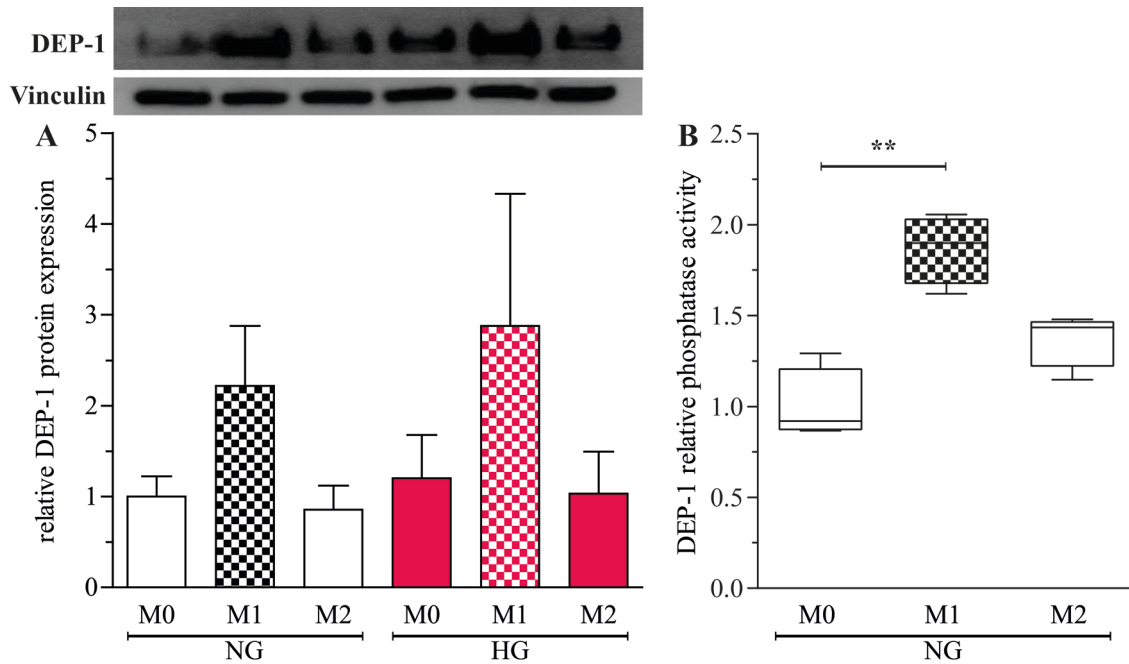


**Figure 5: DEP-1 expression and phosphatase activity in macrophage subpopulations.** Primary monocyte-derived macrophages from healthy donors (n=3 biological replicates for rt-qPCR and n=4 biological replicates for phosphatase activity) were activated to well established *in-vitro* phenotypes M1 (50 ng/ml IFN- $\gamma$  and 20 ng/ml LPS) and M2 (20 ng/ml IL-4 and 20 ng/ml IL-13). After activation, macrophages were cultured in normoglycemia (NG, 5 mM glucose) or hyperglycemia (HG, 30 mM glucose) for 24 hours. **A:** NG- and HG-stimulated, activated macrophages were lysed, DEP-1 mRNA expression was analyzed. DEP-1 upregulation in the M1-phenotype in NG was 2.2-fold (SD: 1.1) and to 2.9-fold accentuated in HG (SD: 2.5). Plotted are NG-M0-normalized means and SEM. Kruskal-Wallis-testing was not significant (p=0.8053) at a significance level of  $\alpha=0.05$ . **B:** Activated monocytes were lysed after activation without further stimulation and DEP-1-specific phosphatase activity was analyzed. DEP-1 phosphatase activity was increased in the M1-phenotype (1.9-fold, SD: 0.19, p=0.0071). Plotted are boxplots with Turkey-whiskers, normalized to M0. Kruskal-Wallis test was significant (p=0.0005) at a significance level of  $\alpha=0.05$ . Dunn's post-hoc testing results are indicated in the graph and figure legend. \*\* p<0.01.

Although Kruskal-Wallis-testing of the rt-qPCR results of DEP-1 expression in different macrophage phenotypes was not significant (p=0.8053), DEP-1 expression was markedly upregulated in the established *in-vitro* pro-inflammatory macrophage phenotype M1 compared to M0-macrophages in NG (2.2-fold, SD: 1.1) which was even accentuated in HG (2.9-fold, SD: 2.5). There against, HG alone showed no effects with a non-significant 1.2-fold expression change in the M0 phenotype compared to NG. Just as little, DEP-1 expression changed in the M2-phenotype compared to M0 in NG (0.8-fold, SD: 0.5) as well as HG (1.0-fold, SD 0.8) (**Figure 5A**).

Similar results were obtained regarding DEP-1's phosphatase activity which is functionally more relevant than its expression. Here, activity in the M1 subpopulation was 1.9-



fold increased (SD: 0.19,  $p=0.0071$ ) compared to M0, while activity only slightly increased in the M2-subpopulation (1.4-fold, SD: 0.15,  $p=0.2866$ ) (**Figure 5B**).

This data suggests a relevant upregulation of DEP-1 expression and activity during activation of macrophages which follows cytokine stimulation *in-vitro* as well as *in-vivo*. The rt-qPCR data also shows a trend of a positive regulatory effect of HG on DEP-1 expression, which is consistent with the data obtained in monocytes, the natural macrophage precursors (**chapter 4.2**).

#### 4.5 DEP-1 knockdown inflammatory *in-vitro* macrophage model

For further analysis of the above-described findings regarding DEP-1's behavior within diabetic patients, hyperglycemia and inflammatory stimulation, a reliable system with knockdown capabilities and a model for DM and inflammation was required.

A suitable *in-vitro* model which starts out with primary monocytes being differentiated into monocyte-derived macrophages in which knockdown experiments can be stably performed under varying glycemie as well as inflammatory conditions was established (**Figure 6**). The model was assessed for functionality and stability on an experiment-individual basis by analysis of surface markers as described (**chapter 3.4.2**).

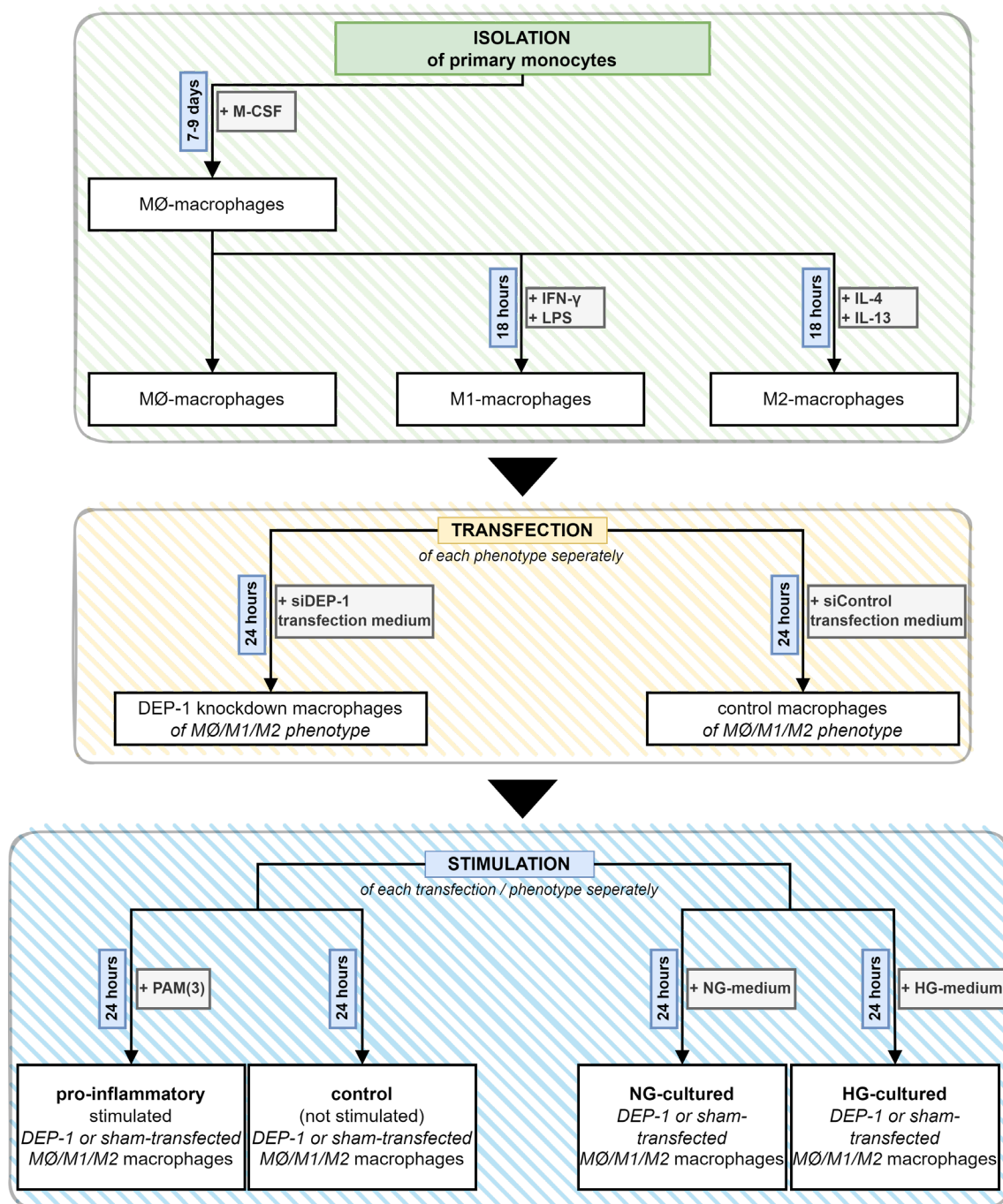


**Figure 6: Established *in-vitro* DEP-1 knockdown model.** The flowchart shows the steps of isolation, differentiation, activation, transfection, and stimulation, as well as the required incubation times in the established DEP-1 knockdown model.

Several transfection reagents for chemical transfection and electroporation were assessed for knockdown efficiency (**chapter 4.5.1**) and toxicity (**chapter 4.5.2**). A stable, constantly low knockdown for 72 hours was required to perform functional readout experiments, especially scratch migration, and viability assays. In the pre-treated cells as

described above, multiple tested transfection methods either led to early cell death or could not achieve a stable knockdown of the above-described criteria.

This methodologic part of this work could identify two chemical transfection methods which fulfilled the requirements: Either Lipofectamine® RNAiMAX (Thermo Fisher Scientific) or Viromer® Blue (Lipocalyx) chemical lipid-based transfection was then used for the functional experiments of this work. The protocol was changed to Viromer® Blue later due to higher knockdown efficiencies.

#### 4.5.1 Knockdown efficiency

DEP-1 specific knockdown efficiencies were evaluated for different chemical transfection reagents. **Figure 7A and Figure 7B** show that RNAiMAX reached DEP-1 mRNA knockdown efficiencies of averagely  $53.7 \% \pm 11.9 \%$  ( $p=0.0159$ ). RNAiMAX (protein knockdown efficiency  $63.8\% \pm 11.4\%$ ,  $n=5$ , one-sample t-test  $p=0.0363$ ) regulated DEP-1 protein expression slightly better compared to Oligofectamine® (protein knockdown efficiency  $46.7\% \pm 6.7\%$ , one-sample t-test  $p=0.0804$ ) and two more worse performing transfection reagents (efficiencies not shown). These tests were performed when Viromer® Blue was not yet established. Therefore, RNAiMAX was used for the first preliminary experiments as it delivered most consistently and satisfying DEP-1 knockdown.

First publications featuring Viromer® Blue as a transfection reagent for macrophages were released during experimental time of this work. DEP-1 mRNA knockdown efficiencies with Viromer® Blue were reassessed and compared to RNAiMAX which revealed much better and even more consistent efficiencies with lower variations for Viromer® Blue (SD  $4.0 \%$  vs.  $11.4 \%$ ). DEP-1 knockdown efficiency employing Viromer® Blue was  $85.9 \% \pm 4.0 \%$  ( $p=0.0079$ , **Figure 7A and Figure 7B**). Therefore, Viromer® Blue was used for further experiments.

Within one experiment series, the same knockdown technique was used for all reported cases and is described for each experiment individually.

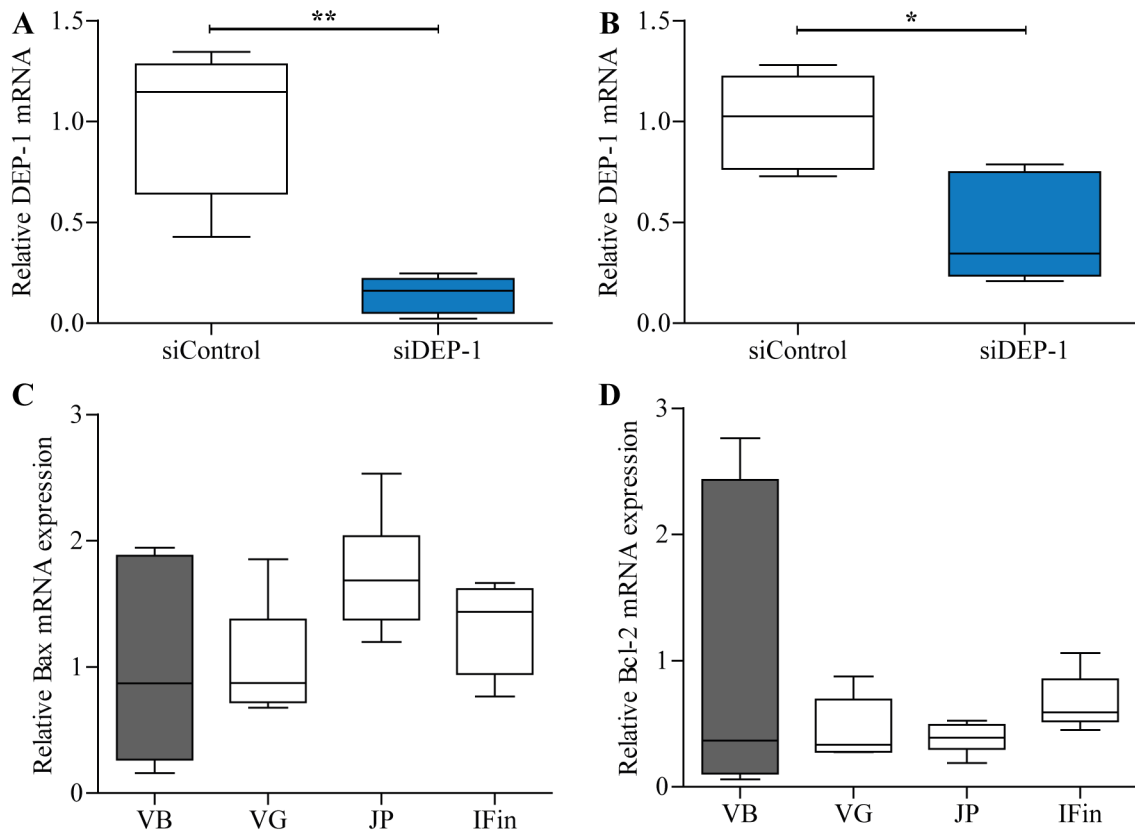


**Figure 7: Knockdown efficiencies and toxicity evaluation.** Commercially available knockdown reagents Lipofectamine<sup>®</sup> RNAiMAX, Viomer<sup>®</sup> Blue (VB), Viomer<sup>®</sup> Green (VG), JetPrime<sup>®</sup> (JP) and INTERFERin<sup>®</sup> (IFin) were assessed regarding their knockdown efficiency of DEP-1 in primary human monocyte-derived macrophages, as well as regarding their toxicity via rt-qPCR-analysis of apoptosis gene regulation. Knockdown was performed according to manufacturer's instruction employing DEP-1 siRNA (**chapter 3.5**) in primary monocyte-derived macrophages immediately after 7-9 days differentiation. After a standardized transfection incubation time of 24 hours, macrophages were lysed and RNA respectively proteins (as indicated in sub-figures) were extracted. Plotted in all sub-figures are box plots with Minimum-to-Maximum-Whiskers. Mann-Whitney-U tests were employed at a significance level of  $\alpha=0.05$ . A: VB reached a mean mRNA knockdown efficiency of 85.9 % (A, SEM=4.0%, n=5 biological replicates, p=0.0079). B: Lipofectamine<sup>®</sup> RNAiMAX reached a mean knockdown efficiency 53.7 % for mRNA (B, SEM=11.9%, n=5 biological replicates, p=0.0159) and a mean protein knockdown efficiency of 63.8 % (not shown, SEM=11.4%, n=5 biological replicates, one-sample t-test p=0.0363). C, D: Expression of apoptosis regulators Bax and Bcl-2 was assessed in n=6 biological replicates via rt-qPCR for transfection reagents VB, VG, JP and IFin. Mean relative Bax- and Bcl-2-mRNA-expression per transfection reagent are normalized to the mean relative expression in Viomer<sup>®</sup> Blue transfected samples. \* p<0.05, \*\* p<0.01.

#### 4.5.2 Knockdown toxicity

Toxicity of Viomer<sup>®</sup> Blue in the given setup was assessed against three other transfection reagents Viomer<sup>®</sup> Green, INTERFERin<sup>®</sup> and JetPrime<sup>®</sup> in this work's specific use case of DEP-1 siRNA-based knockdown in primary human monocyte-derived macrophages with a sufficient knockdown required to last at least 48 hours (**chapter 4.5, Figure 6**). The transfection reagents were used according to their manuals, but siRNA concentration was equalized (25 nM) for all reagents in this assessment to exclude siRNA-related

toxicity effects. Bax is a pro-apoptotic protein which is typically upregulated when a cell is exposed to toxic substances while Bcl-2 acts as an anti-apoptotic regulator against cell death. Bax expression was lowest in cells transfected with Viromer<sup>®</sup> Blue, whereas Bcl-2 expression was higher compared to the other transfection reagents, indicating that Viromer<sup>®</sup> Blue comes with the relatively lowest toxicity against macrophages. However, Bcl-2 expression was most variable for Viromer<sup>®</sup> Blue (**Figure 7C, Figure 7D and Table 15**).

**Table 15: Comparison of knockdown reagent toxicity against Viromer<sup>®</sup> Blue.**

	Relative expression relative to Viromer <sup>®</sup> Blue	
	Bax	Bcl-2
<b>Viromer<sup>®</sup> Blue</b>	100.0 % ± 32.1 %	100.0 % ± 45.4 %
<b>Viromer<sup>®</sup> Green</b>	103.8 % ± 18.1 %	45.4 % ± 10.0 %
<b>INTERFERin<sup>®</sup></b>	131.8 % ± 14.5 %	67.0 % ± 09.0 %
<b>JetPrime<sup>®</sup></b>	173.4 % ± 18.6 %	38.5 % ± 04.9 %

*Primary human monocyte-derived macrophages from healthy donors (n=6 biological replicates) were transfected with the given reagents and control siRNA according to manufacturer's instructions. Viromer<sup>®</sup> Blue showed the highest expression of anti-apoptotic Bcl-2 while expression of pro-apoptotic Bax protein was the lowest for Viromer<sup>®</sup> Blue. The values are shown as percental relative expressions normalized to Viromer<sup>®</sup> Blue which was set to 100 % and SEM.*

#### 4.6 DEP-1 knockdown negatively influences macrophage migration

Leukocyte migration is a crucial factor in mediating the pathology of arteriosclerosis (72, 73). Therefore, this key function was analyzed under DEP-1 knockdown circumstances.

Primary monocytes were isolated, differentiated into MØ-macrophages and then activated to M1- and M2-macrophages for 18 hours or kept at the MØ-stage. The macrophages were then stimulated in either NG or HG for 24 hours. Now, knockdown was performed with either Lipofectamine<sup>®</sup> RNAiMAX or later Viromer<sup>®</sup> Blue and cells were incubated with the transfection components in the medium for 24 hours. A central scar was scratched using a pipette tip (approximately 1mm distal diameter) and the medium was changed twice to wash out non-adherent cells. NG and HG conditions were kept in the final reaction medium. The open area was photographed and quantified in ImageJ at 0, (6, 12), 24 and 48 hours after creating the scar. Reported are fractional open areas (FOA) at every time point, normalized to the initial open area at the beginning of the experiment.

**Table 16: Comparison of fractional open areas (FOA) during a wound healing assay of primary human monocyte-derived macrophages after siRNA-mediated knockdown of DEP-1 in normoglycemia (NG).**

	Fractional open area after 48 hours			
	siControl	siDEP-1	Fold-increase	p-value
<b>M0</b>	17.0 % ± 2.9 %	31.4 % ± 8.7 %	1.85	0.1789
<b>M1</b>	60.4 % ± 6.7 %	79.7 % ± 5.1 %	1.32	0.0208
<b>M2</b>	20.2 % ± 5.9 %	41.6 % ± 6.1 %	2.06	0.0150
<b>combined</b>	32.5 % ± 5.1 %	50.9 % ± 5.7 %	1.59	0.0003

A scratch assay of confluent primary monocyte-derived macrophages isolated freshly from healthy donors ( $n=8$  biological replicates) was performed in the implemented DEP-1 knockdown model in NG medium. FOA were calculated comparing the 48-hour open area with the initial ( $t = 0$  h) open area for each sample individually. The table shows mean FOA and SEM for the different macrophage phenotypes in NG after siDEP-1 and siControl transfection. Mean FOA varied significantly for M1- and M2-macrophages, as well as in the combined analysis. There was a trend of impaired migration in M0-phenotype. Statistical analysis was performed for each phenotype individually and in a combined analysis of all datasets using a two-sided paired Student's  $t$ -test at a significance level of  $\alpha=0.05$ .

Independent of DEP-1 knockdown, Macrophage migration was much more effective in the non-treated NG group of the M0- and M2-phenotype with average FOA after 48 hours of 17.0 % and 20.2 %, respectively, compared to the non-treated M1-phenotype with a mean FOA of 60.4 % after 48 hours.

DEP-1 knockdown lead to a significantly 1.32-fold in M1- and 2.06-fold increased FOA, therefore impaired migration, in M2-macrophages. In M1-macrophages, the FOA was 60.4 % without treatment and 79.7 % after DEP-1 knockdown ( $p=0.0208$ ). In M2-macrophages the open area doubled from 20.2 % to 41.6 % ( $p=0.0150$ ). There was a non-significant increase of FOA from 17.0 % to 31.4 % ( $p=0.1789$ ) in M0-macrophages.

Combining all three macrophages-phenotypes, DEP-1 knockdown impaired migration with a 1.59-fold increase in the remaining FOA ( $p=0.0003$ ).

**Table 17: Comparison of fractional open areas (FOA) during a wound healing assay of primary human monocyte-derived macrophages between normoglycemic (NG) and hyperglycemic (HG) culturing.**

	Fractional open area after 48 hours			
	NG	HG	Fold-increase	p-value
<b>M0</b>	17.0 % ± 2.9 %	30.5 % ± 8.5 %	1.80	0.1590
<b>M1</b>	60.4 % ± 6.7 %	68.9 % ± 6.8 %	1.14	0.1963
<b>M2</b>	20.2 % ± 5.9 %	22.7 % ± 7.5 %	1.20	0.6395
<b>combined</b>	32.5 % ± 5.1 %	40.7 % ± 6.0 %	1.25	0.0429

A scratch assay of confluent primary monocyte-derived macrophages isolated freshly from healthy donors ( $n=8$  biological replicates) was performed in the implemented DEP-1 knockdown model in normo- (NG) and hyperglycemia (HG). Macrophages were siControl-transfected; therefore, DEP-1 is normally expressed. FOA were calculated comparing the 48-hour open area with the initial ( $t = 0$  h) open area for each sample individually. The table shows mean FOA and SEM for the different macrophage phenotypes in NG and HG. Mean FOA varied significantly when comparing all phenotypes in a combined analysis with a 1.25-fold increased FOA, therefore impaired migration, in HG. This was – although not significant – measurable in all phenotypes individually. Statistical analysis was performed for each phenotype and in a combined analysis of all phenotypes by two-sided paired Student's  $t$ -test at a significance level  $\alpha=0.05$ .

The experiment was performed in normoglycemic (NG) and hyperglycemic (HG) conditions. Therefore, combined effects of DEP-1 knockdown and metabolic stress were assessed, as well. There was significantly impaired migration in HG, measurable by a 1.25-fold increase of the FOA in the combined non-stratified sample ( $p=0.0429$ , **Table 17**). Although not significant, this effect was measurable in all macrophage phenotypes individually, as well, with a 1.14-fold increase ( $p=0.1963$ ) of FOA in hyperglycemic cultured M1-macrophages, 1.20-fold increased FOA ( $p=0.6395$ ) in M2-macrophages and even 1.80-fold increased FOA in M0-macrophages ( $p=0.1590$ ).

Analyzing the 48-hour FOA of each phenotype and glucose concentration subgroup individually, significant differences were obtained in three groups: In M1-macrophages, migration was significantly impaired by DEP-1 knockdown in NG ( $60.4\% \pm 6.7\%$  vs.  $79.7\% \pm 5.1\%$ , 1.32-fold increased FOA,  $p=0.0208$ ). In M2-macrophages, mean FOA varied significantly in DEP-1-depleted macrophages in both NG ( $20.2\% \pm 5.9\%$  vs.  $41.6\% \pm 6.1\%$ , 2.07-fold increased FOA,  $p=0.0150$ ) and HG ( $22.6\% \pm 7.5\%$  vs.  $46.5\% \pm 9.7\%$ , 2.05-fold increased FOA,  $p=0.0099$ ). All other subgroups had the same trends as shown in the corresponding figure panel (**Figure 8**).

In summary, this experiment conducted in monocyte-derived macrophages from 8 individual healthy donors provided good evidence that knockdown of DEP-1 in macrophages (**Table 16**, **Figure 8**) as well as HG (**Table 17**) both negatively influence these cells' migratory capabilities. Additionally, it could be shown that migration is generally impaired in the M1-phenotype of macrophages (**Table 16**). This phenotype is a result of foregone inflammatory stimulation and signaling.

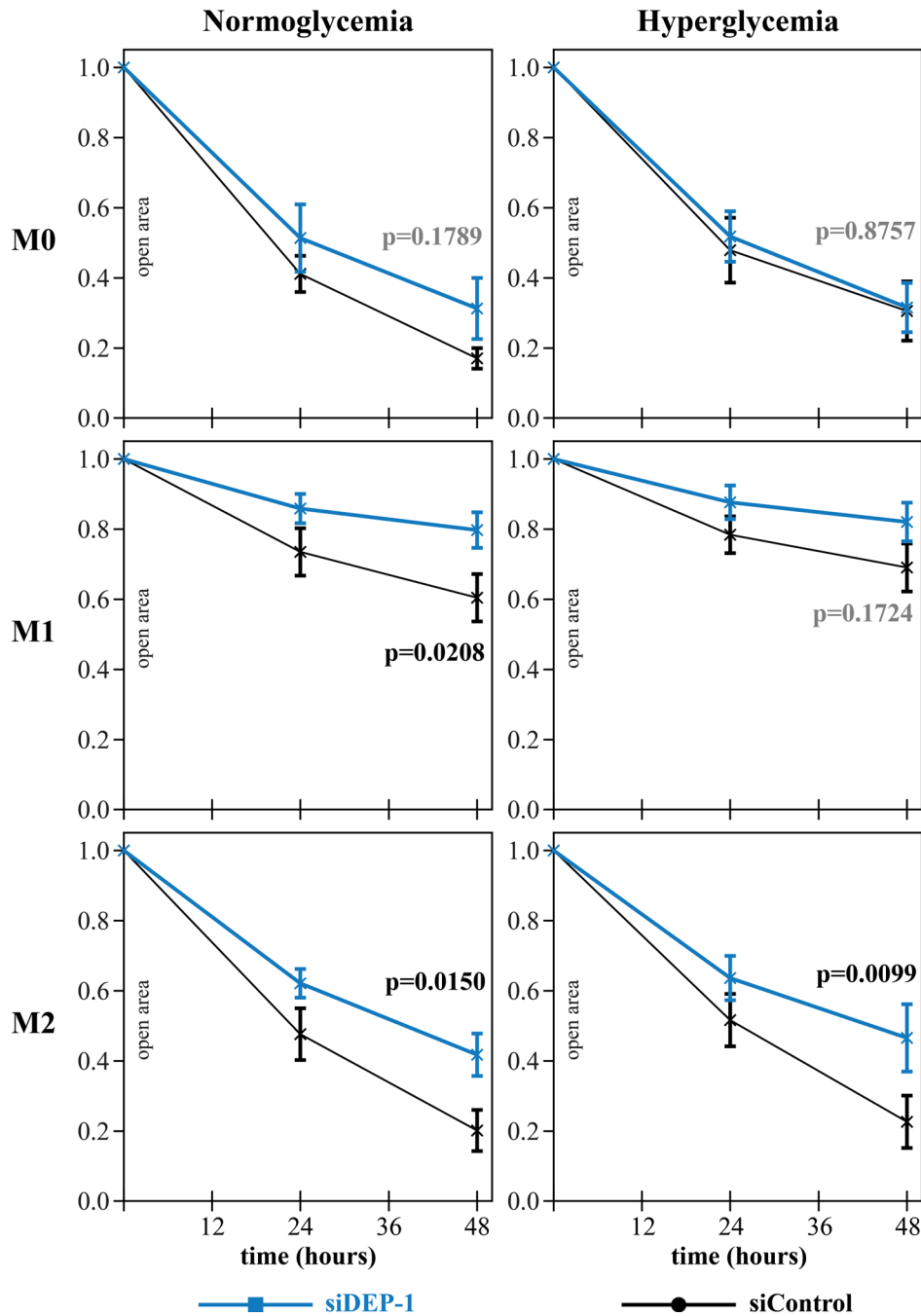


**Figure 8: DEP-1 knockdown migration assays.** Migration assays were performed as a wound healing assay in a confluent layer of primary human monocyte-derived macrophages isolated from healthy donors (n=8 biological replicates), differentiated, transfected, and stimulated by normoglycemia (NG) and hyperglycemia (HG) according to the described, established DEP-1 knockdown model. Independent from glucose treatment, knockdown of DEP-1 led to an increased open area after 48 hours (Table 16). Hyperglycemic culturing led to impaired migration (Table 17). The graph-set shows mean fractional, per-experiment-normalized open areas (FOA) with SEM as error bars for DEP-1 transfected (---blue lines---) and control transfected cells (---black lines---). DEP-1 knockdown impaired migration in NG M1- (19% FOA-difference, SEM of difference 6.5%, p=0.0208) and M2-phenotype (21% FOA-difference, SEM of difference 6.7%, p=0.0150), as well as in the HG-cultured M2-phenotype (24% FOA-difference, SEM of difference 6.8%, p=0.0099). Statistical analysis was performed for each stratified subgroup in a two-sided paired Student's t-test at a significance level  $\alpha=0.05$ . Exact p-values are reported in the graph and significant p-values are also reported in this figure legend.



#### 4.7 DEP-1 knockdown did not reveal significant differences in macrophage proliferation nor viability

The previous experiment showed that macrophage migration is negatively affected after DEP-1 knockdown. Because migration in a scratch assay is not always easily distinguishable from proliferation and since macrophage proliferation is – as well as – migration itself an important cell function and therefore relevant in pathological conditions, cell proliferation in DEP-1 knockdown conditions was assessed.

Therefore, primary monocytes were isolated and seeded in 96-well plates, differentiated into MØ-macrophages, activated as described previously and then stimulated in either NG or HG for 24 hours. Knockdown was performed with Lipofectamine<sup>®</sup> RNAiMAX. Afterwards, medium was changed to a proliferation medium supplemented with 20 ng/ml recombinant human PDGF-BB. Absorbance was measured after 24 hours and after 48 hours.

The data was analyzed regarding differences in the absorbance means in the six different subgroups defined by macrophage polarization and glucose stimulation. The measured mean absorbances varied only slightly between the groups and were not significantly different in a two-way ANOVA statistical testing for time and knockdown. This experiment could show that DEP-1 knockdown in the fashion it was performed in the migration experiments does not influence macrophage proliferation or viability (**Figure 9**). It can be assumed, that measured differences in scratch open area are only due to altered migration.

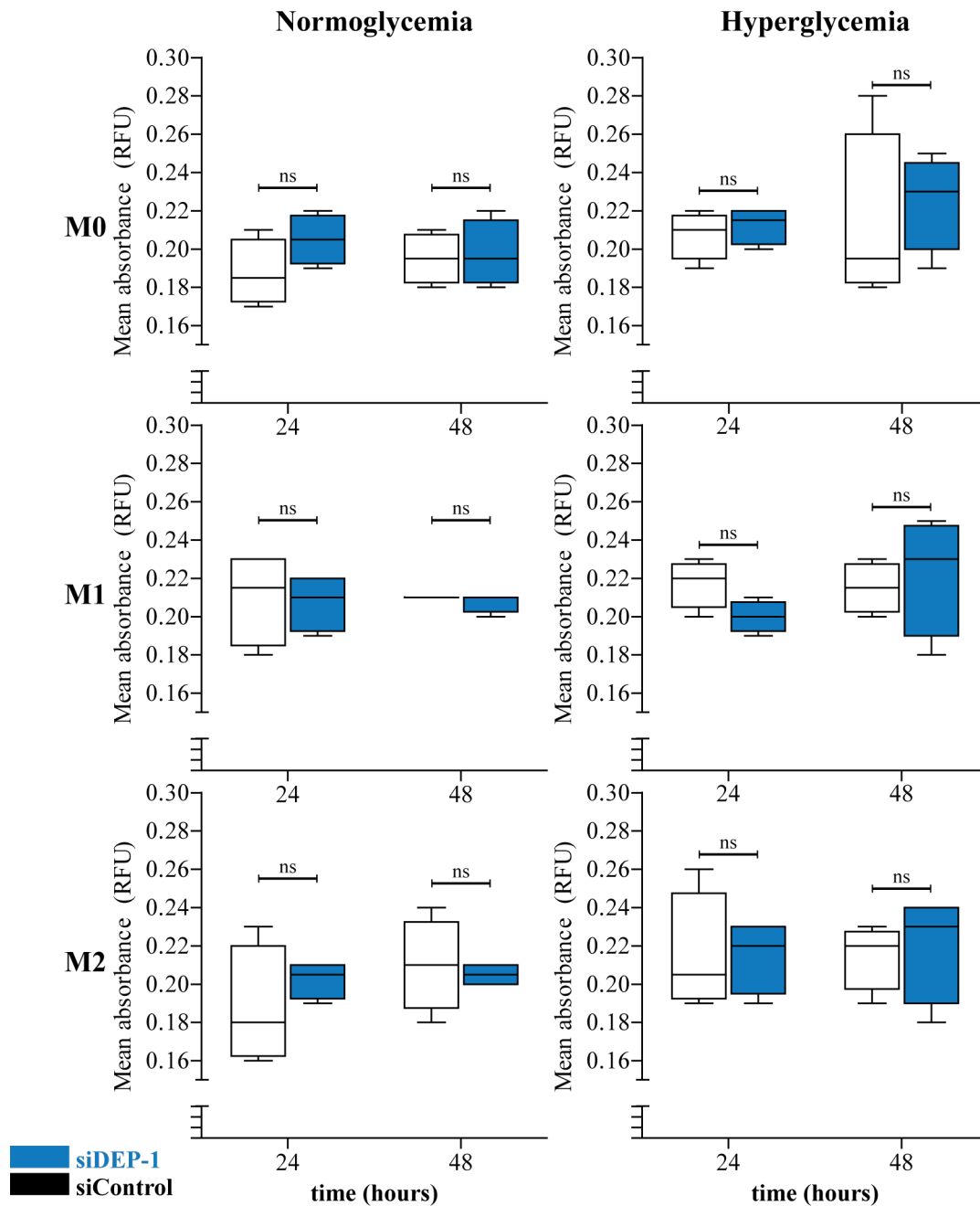


**Figure 9: DEP-1 knockdown proliferation and viability assay.** A proliferation and viability assay was performed in primary human monocyte-derived macrophages isolated from healthy individuals (n=4 biological replicates) after differentiation, activation and DEP-1 knockdown through the established protocol. Proliferation was stimulated with 20 ng/ml recombinant human PDGF-BB. Absorbance was measured 24 and 48 hours after addition of PDGF-BB. In all six stratified groups (macrophage phenotypes and glucose conditions) there were no significant differences between the absorbance means of the control and DEP-1 knockdown group. Statistical analysis was performed in a two-way ANOVA test for time and knockdown at a significance level  $\alpha=0.05$ . ns not significant.

## 4.8 DEP-1 knockdown mediates NF- $\kappa$ B transcription factor upregulation in inflammatory macrophages

Stimulants HG, possibly MG and oxLDL *in-vitro*, as well as T2DM *in-vivo*, were identified as regulators of DEP-1 expression (**chapters 4.1 and 4.2**). Pro-inflammatory stimulation with TNF- $\alpha$  lead to upregulation of DEP-1 most likely through the NF- $\kappa$ B signaling pathway (**chapter 4.3**). If DEP-1 plays a role in pro-inflammatory signaling which is also associated with HG, DEP-1 might also influence downstream inflammatory signaling. Therefore, regulation of the NF- $\kappa$ B signaling pathway was assessed, as it is one of the most important inflammatory signaling pathways, as well as a downstream target of NF- $\kappa$ B signaling the TNF- $\alpha$  expression.

Primary monocytes were isolated, differentiated and activated into M1-macrophages. After 18 hours, medium was replaced with culturing medium and the cells were transfected with either siControl or siDEP-1 siRNA by Viromer<sup>®</sup> Blue with the transfection reagent in the medium for at least 24 hours. After 24 hours, medium was replaced with new culturing medium containing 100 ng/ml of the synthetic TLR1 and TLR2 ligand Pam3CSK4 (PAM3). Cells were lysed after 6-12 hours stimulation time, RNA was extracted, and cDNA was analyzed by rt-qPCR regarding the mRNA expression of the p65-subunit which is a member of the NF- $\kappa$ B family and involved in the dimerization, nuclear translocation and activation of NF- $\kappa$ B (**Figure 10A**). Besides, the expression of TNF- $\alpha$  which is a target gene of the NF- $\kappa$ B transcription factor, was measured (**Figure 10B**). DEP-1 mRNA expression itself served as an internal control to evaluate whether knockdown is still effective under stimulation with PAM3.

To evaluate the phosphorylation state of NF- $\kappa$ B's p65 subunit, the same experiment as described above were performed with an incubation time for PAM3 stimulation of 24 hours and lysed the cells, extracted protein and ran SDS-PAGE and Western Blot with antibodies against total p65 and phosphorylated p65 to densitometrically quantify a ratio of phosphorylated versus non-phosphorylated p65 after DEP-1 knockdown and PAM3 stimulation (**Figure 10C+D**).

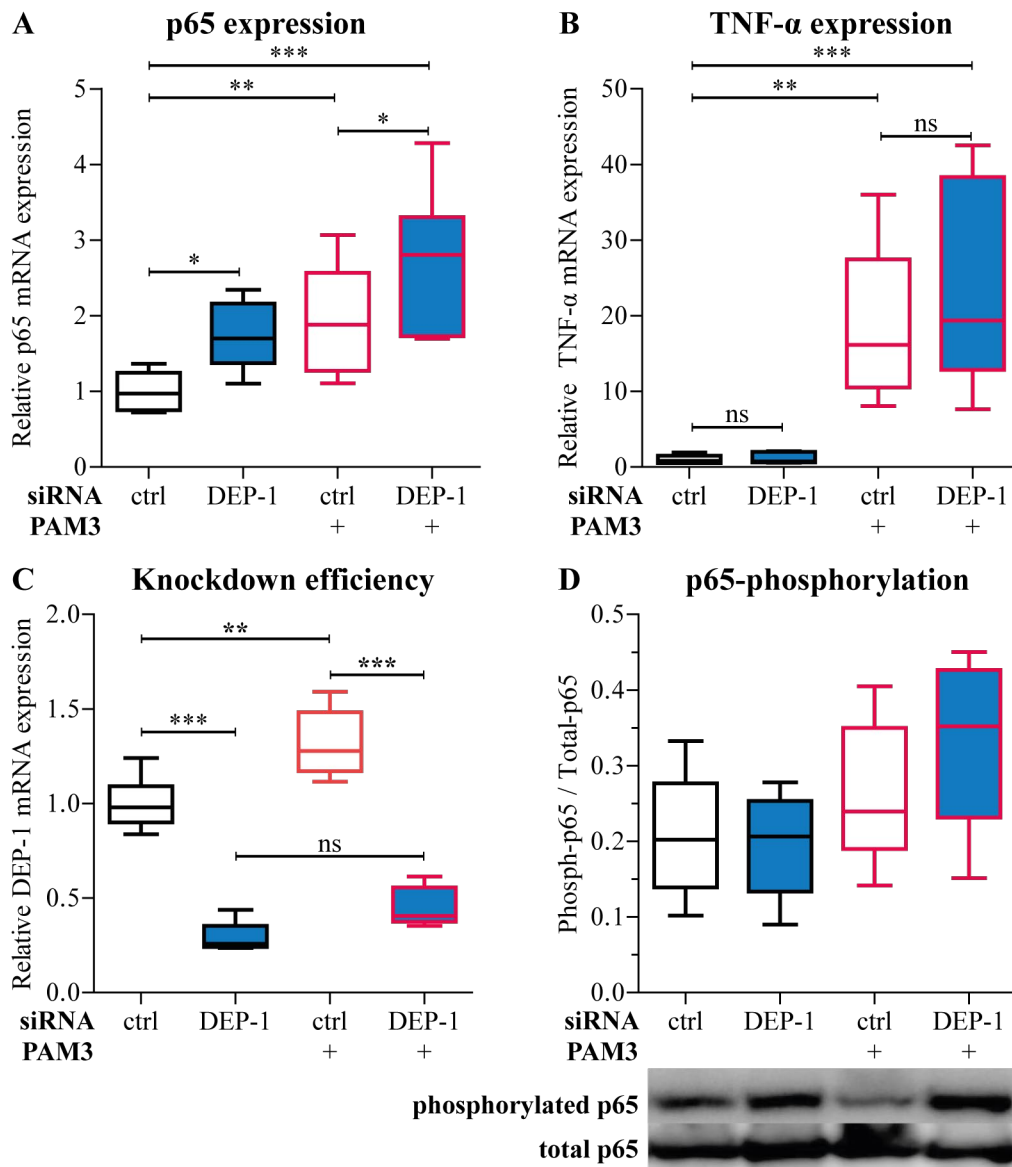


**Figure 10: Downstream signaling effects of siRNA-mediated DEP-1 knockdown in M1 macrophages.** Primary human monocytes from healthy donors (n=6 biological replicates) were isolated, differentiated and activated into M1-macrophages. DEP-1 knockdown was achieved via Viromer Blue<sup>®</sup> transfection for 24 hours. Macrophages were stimulated 6 hours for RNA analysis and 24 hours for protein analysis, respectively, with 100 ng/ml PAM3. Plotted in all sub-figures are boxplots with minimum- to maximum whiskers. Multiple comparisons were tested via ordinary or repeated-measures ANOVA as indicated and Bonferroni post-hoc tests at a significance level of  $\alpha=0.05$ . **A:** DEP-1 knockdown lead to a significant increase in basal (73.5%,  $p=0.0371$ ) and PAM3-stimulated (39.8%,  $p=0.0269$ , repeated-measures ANOVA) p65-expression. **B:** Expression of TNF- $\alpha$  mRNA increased after PAM3-stimulation. TNF- $\alpha$  mRNA expression increased by 25.0% under PAM3-stimulation in DEP-1 depleted M1-macrophages ( $p=0.0470$  in paired t-test, not significant in post-hoc test of repeated-measures ANOVA). **C:** Knockdown was consistently stable throughout all experiments. PAM3 stimulation did not increase DEP-1 expression significantly during knockdown ( $p=0.2828$ , ordinary ANOVA). **D:** The quotient of phosphorylated p65 and total p65 as a measure for NF- $\kappa$ B activation increased under PAM3-stimulation in DEP1-knockdown. Exemplary western blots are shown. However, repeated-measures ANOVA of semi-quantified western blot data was not significant at a significance level of  $\alpha=0.05$  ( $p=0.1018$ ). Therefore, post-hoc testing was not performed. \*  $p<0.05$ , \*\*  $p<0.01$ , \*\*\*  $p<0.001$ .

This data suggests that NF- $\kappa$ B expression and phosphorylation is – among of course many other regulatory cascades – to some extent dependent on DEP-1 expression. DEP-1 knockdown led to a 73.5% increase of basal p65 housekeeping-gene-relative mRNA-expression in M1-activated macrophages ( $0.1342 \pm 0.0339$  vs.  $0.2329 \pm 0.0624$ ,  $p=0.0371$ ) and to a 39.8% increase during 100 ng/ml PAM3-stimulation ( $0.2610 \pm 0.0980$  vs.  $0.3649 \pm 0.1280$ ,  $p=0.0269$ ) (**Figure 10A**). NF- $\kappa$ B especially effects pro-inflammatory cytokine regulation. This was assessed next: TNF- $\alpha$  mRNA was non-significant without PAM3-stimulation. However, during stimulation, differences were observed: DEP-1 knockdown led to an 25.0% increased TNF- $\alpha$  mRNA expression ( $0.0949 \pm 0.0532$  vs.  $0.1186 \pm 0.0685$ ,  $p=0.0470$ , paired t-test) (**Figure 10B**). This indirectly confirms that besides p65 mRNA also the functional NF- $\kappa$ B protein complex is upregulated in DEP-1 knockdown. In western blot analysis, protein concentrations of phosphorylation of p65 and total p65 were measured semi-quantitatively. The quotient may be interpreted as a measure for NF- $\kappa$ B activation. Interestingly, this quotient also increased in DEP-1 knockdown and PAM3-stimulation by 26.5% ( $0.2638 \pm 0.0963$  vs.  $0.3337 \pm 0.1145$ ) (**Figure 10D**). However, repeated-measures ANOVA of semi-quantified western blot data was not significant and therefore no post-hoc testing was performed. The described effect was only observed in four out of totally six independent experiments. Nevertheless, it may – after further validation – support the idea that DEP-1 negatively regulates NF- $\kappa$ B expression and alters its phosphorylation.

As a control, DEP-1 mRNA-expression was determined in all tested conditions to verify that knockdown was efficient and PAM3-stimulated does not attenuate knockdown. In average, knockdown efficiencies of 70.7 % and 65.8 % were reached without and with PAM3-stimulation, respectively. Although PAM3-stimulation as a ligand of TLR2 decreased knockdown efficiency slightly, they were still acceptable.

## 5 Discussion

This work aimed to investigate the functional role of DEP-1 in diabetic monocytes and macrophages. It was shown *ex-vivo* that DEP-1 is upregulated in monocytes from diabetic hyperglycemic patients compared to non-diabetic patients which underlines the phosphatase's clinical relevance (**chapter 4.1**). This effect was also shown in *in-vitro* experiments employing hyperglycaemic stimulation (**chapter 4.2**). Besides, DM and HG, other regulatory stimuli of DEP-1 could be identified and partly validated (**chapters 4.2, 4.3, 4.8**). Next, an easily in S1-laboratories performable, low toxic, stable and reproducible siRNA-mediated knockdown protocol for DEP-1 in primary monocyte-derived macrophages was established and validated (**chapter 4.5**). This allowed investigation of downstream functions and signaling pathways of the phosphatase in longer lasting experiments. Here it was shown that macrophage migration was impaired after DEP-1 knockdown which may allow to conclude a positive regulatory role of DEP-1 in this context (**chapter 4.6**). Proliferation was not altered after knockdown of the phosphatase. An increase of baseline and PAM3-stimulated NF- $\kappa$ B expression was observed in DEP-1 knockdown macrophages, which – at least – questions the model of DEP-1 as a pro-inflammatory mediator of immune cells (**chapter 4.8**).

### 5.1 DEP-1 protein expression can be efficiently reduced by siRNA-mediated knockdown in a time-efficient, reproducible and easily performable approach

Transfection of cells with small nucleic acids which mediate gene silencing is called RNA interference (RNAi) (57, 61). RNAi is a commonly used laboratory technique to study cell function and signaling under altered gene expression (55). *In-vitro* transfection techniques are either virus-mediated, chemical or physical techniques (reviewed by Kim and Eberwine 2010 (121)) and although many protocols for different cell types have been published, transfection can remain challenging depending on cell type, siRNA and circumstances related to cell culture and experimental read-out. From an ideal transfection method, one would expect high delivery efficiency with minimal peripheral effects of the transfection itself on the transfected cells.

Macrophages, especially primary macrophages, are considered to be harder to transfect than other cell types because of their natural immunological function (117, 260, 262).

Especially viral vectors and in general uptake of foreign nucleic acids have been discussed to activate macrophages and trigger immune responses which alter experimental conditions and outcomes on the one hand and lead to degradation of the foreign nucleic acids on the other hand (40). Uptake and degradation of transfection components through macrophages' phagocytotic pathways can limit transfection efficiencies. Additionally, especially primary cells are highly sensitive to damage through changes of their environment which was also observed in experiments carried for this work (105, 228).

An important prerequisite and goal of this work was to establish and validate a high-efficient protocol for knocking down DEP-1 in primary human monocyte-derived macrophages with a low primary macrophage-specific toxicity which does not trigger immune responses by itself since immunological function itself was subject to analysis.

Primary cells do not carry significant genetic changes as cell lines usually do. Besides, they can be obtained from multiple different healthy donors and can therefore be used to validate and statistically test observed effects in multiple individuals. Cell lines lack this feature. A knockdown of a protein in primary cells comes closer to targeting this protein with inhibitors *in-vivo* and observed results might suggest druggable pathways to treat malfunctions. This requires specific and cell-targeted siRNA delivery *in-vivo* which is part of ongoing research (216, 225).

Lee et al. obtained high knockdown efficiencies using lentivirus-delivered shRNA in primary bovine macrophages (140). However, virus-based transfection was not an option for this work since immunological stress needed to be kept as low as possible. Besides the laboratory in which the experiments were carried out is – as a significant number of laboratories – not certified for work with lentiviral vectors. Electroporation and nucleofection were assessed in macrophages. While reasonable results were obtainable in macrophage cell lines, electroporation and nucleofection, respectively, seem to remain a challenge when dealing with primary macrophages (155, 228). However, Wiese *et al.* were able to transfect bone-marrow derived macrophages from mice with efficiencies over 95 % using electroporation while observing no differences in cell viability (266). Electroporation was briefly tested in this work as well, but was not successful due to high toxicity and cell death within 24 hours was observed which is why this method was not

further considered<sup>3</sup>. Wiese's results, however, suggest that although electroporation was not an option in this work's specific context, different protocols deserve assessment for their usability, quality, and efficiency in other contexts as electroporation may be a helpful tool in other experimental conditions.

These own findings and already published evaluated transfection protocols set the focus for the search for a durable and evenly gentle transfection method for transfecting DEP-1 silencing siRNA into primary human macrophages on chemical transfection methods, especially lipofection. Commercially available transfection reagents which were priorly shown or advertised to be compatible with and effectful in primary human monocytes were in general used according to their manufacturers' instructions; however, adjustments were made regarding siRNA concentrations, transfection during serum-free or low-serum starvation periods. Since not all transfection reagents were available at the beginning of this work, the screening for a suitable agent was done twice and subsequently. In the first screening, Lipofectamine RNAiMAX (ThermoFisher Scientific, USA) was found to be most effective throughout the tested substances and was therefore used for preliminary experiments as shown in Figure 7C of this thesis. Shortly after, the Viromer® transfection line (Lipocalyx, Germany) came to the investigator's attention and even better transfection efficiencies of up to 90 % were reached using Viromer® Blue. Additionally, Viromer® Blue showed comparably low toxicity compared to other reagents which is summarized in Table 15 of this thesis. A shortcoming here is the missing head-to-head comparison of Viromer® Blue and Lipofectamine RNAiMAX. With recently published protocols, other groups reached comparably high transfection efficiencies, however below 80 % in most cases, among different siRNAs transfection reagents which were also evaluated in this work (16, 131, 144, 251). It is remarkable that Wati *et al.* reached a transfection efficiency above 90 % using Lipofectamine RNAiMAX and a fluorescent oligonucleotide for testing purposes. As in this work, Wati *et al.* used RNAiMAX transfection in combination with cell starvation for 4 hours but they added an additional 4-hour transfection period after allowing the cells to recover from the first transfection for 18 hours (261). This interesting concept deserves a validation in the experimental conditions of the here established model in the future course.

---

<sup>3</sup> Own, unpublished, preliminary data



Reaching high-enough DEP-1 knockdown efficiency by testing different transfection techniques was one out of several steps in the development and optimization of the described *in-vitro* experimental model used in this work. The model required a sufficient knockdown for at least 96 hours, since effects of 48 hours glucose stimulation needed to be evaluated and experimental readouts took up to 48 hours (scratch assay, proliferation and viability assay). Against all optimizations, only 72 hours of highly efficient knockdown were reachable with the described protocol. Therefore, glucose stimulation was added already during the 24-hour transfection incubation time which may be interpreted as an additional stressor for the cells during transfection. The experimental model was carefully validated as described in chapter 4.5 and knockdown efficiencies were constantly monitored, since evenly treated and transfected samples were split and used for both functional assays and RNA readouts in which analysis of DEP-1 mRNA was always included. Nevertheless, instabilities of the experimental model were experienced during the experiments which had to result in repetition of the experiment set for single monocyte donors. Observed instabilities were mainly cell death which led to non-confluent cell layers necessary for scratch assays over the long culturing time of up to 14 days. These observations were attributed to frequent media changes and cell-stress during transfection, starvation, and glucose stimulation. In part, insufficient media quality or possibly insufficient precise and careful handling during cell culture cannot be excluded as reasons here. However, included in analysis were only those experiments which met the described quality standards.

## 5.2 DEP-1 expression is a target of metabolic stress and pro-inflammatory stimulation in type 2 diabetes mellitus

This work revealed altered *ex-vivo* and *in-vitro* DEP-1 expression in different physiological conditions, elucidating the phosphatase's relevance in pathological contexts, especially in DM in which both metabolic stress through HG and side products of HG-metabolism, as well as inflammation are relevant mediators. Both mediators have been investigated separately but are also dependent on each other which will be discussed.

### 5.2.1 DEP-1 is elevated in the hyperglycemic diabetic disease

DEP-1 mRNA expression was significantly higher in primary monocytes isolated from hyperglycemic diabetic patients compared to control subjects while a linear correlation

of HbA<sub>1C</sub> and DEP-1 mRNA expression normalized to the mean expression within the investigated cohort could not be determined in regression analysis. The study population had an HbA<sub>1C</sub> lower cut-off of 7.5 % together with the diagnosis of T2DM as inclusion criteria for the diabetes group and an HbA<sub>1C</sub> upper cut-off of 6.5 % for the control group. HbA<sub>1C</sub> values above 6.5 and below 7.5 with or without a diagnosis of T2DM were excluded, ensuring an active diabetic disease in a hyperglycemic metabolic situation in the T2DM cohort. The observed DEP-1 upregulation is therefore associated with the combination of T2DM and a hyperglycemic metabolic situation rather than the clinical diagnose of T2DM itself. This also needs to be considered when results are interpreted. Interestingly, CRP levels were lower in the low-glycemic-index diet group in a controlled trial comparing a low- and high-glycemic-index diet, although HbA<sub>1C</sub> levels did not differ significantly (269). This, however, supports the idea that glycemic load can have an impact on the level of inflammation independent of the diagnose of T2DM itself.

It is remarkable and a limitation that the two groups of the study populations did not only differ from each other regarding the diagnosed T2DM and associated conditions such as an elevated HbA<sub>1C</sub> but also in co-morbidities, ex-smoking status and age. The main reason for this may be that control patients were recruited in another center as were the diabetic individuals. Therefore, these *ex-vivo* results are limited in their reliability and their interpretative value may be more suggestive than confirmatory. However, reliability is increased by this work's *in-vitro* data and already published *in-vivo* results from other groups which observed an increased DEP-1 activity in high-fat dieted obese mice (126). Further testing in a larger cohort of human patients suffering from T2DM, ideally at a disease progression state without any yet developed complications. Also, other relevant attributes with impact on systemic inflammation such as nicotine, alcohol, or any other drug abuse, free from systemic infections and immune activation could ideally be excluded. A comparison between at least age- and sex-matched healthy controls seems interesting and rational. A suitable cohort for such a diabetic study population may be patients at the time of initial diagnosis which happens most likely in ambulatory care.

Several research groups have shown PTPs such as PTP1B (132) and SHP-1 (273) to be upregulated in mice fed with high-fat. In line with that and with this work's results, DEP-1 was upregulated in this type of animal model for T2DM (126). Dorenkamp *et al.* have recently shown, that SHP-2, another PTP, is upregulated in monocytes from diabetic

patients (52). Except for the latter study, PTP expression in diabetic disease conditions was analyzed in liver, muscle and adipose tissue samples but not in immune cells before (1, 86). Addressing this cell type is important since immune cells play a role in diabetes itself but especially in atherosclerosis as one of its clinical manifestations. Insofar this study adds relevant knowledge about potential roles of DEP-1 in diabetes.

Only from this work's *ex-vivo* data it remains unclear which signaling pathway(s) is/are activated by HG and mediate(s) the observed upregulation of DEP-1 in diabetic patients' monocytes. Chronic systemic inflammation measured exemplarily by elevated serum acute-phase proteins such as CRP was found to be a co-pathology associated with an active diabetes disease: Festa et al. showed a correlation between inflammatory markers and insulin sensitivity, systolic blood pressure and body-mass index (59) and Pradhan et al. found that serum hs-CRP is elevated in patients with T2DM (197). It was later added that an elevated hs-CRP only above 0.3 mg/dl in diabetic individuals is associated with a higher risk of death from coronary artery disease (224). Therefore, inflammation and associated signaling pathways are – also from a clinical point of view – possible mediators of DEP-1 upregulation through HG in diabetic individuals.

### 5.2.2 Inflammation and related pathways are potential mediators of elevated DEP-1 expression in diabetic individuals

*In-vitro*, hyperglycemic culturing of a monoculture of primary monocytes from healthy donors for 48 hours showed a non-significant but 5.6-fold DEP-1 upregulation and a less strong trend of increased expression was observed in hyperglycemic-cultured macrophages. This supports but due to a lack of statistical significance does not prove the idea that HG can activate signaling pathways that exist in monocytes as well as in macrophages which in turn mediate the regulation of DEP-1 expression.

*In-vivo*, HG may also affect DEP-1 expression indirectly by increasing the level of systemic inflammation which is known for decades from diabetic subjects (reviewed by Greenberg and Obin 2008 (84)). Lowering of glycemic index was even shown to reduce TNF- $\alpha$  in mononuclear cells of obese patients (119). However, systemic effects of hyperglycemia are by-design excluded in this study of a monoculture of monocytes or macrophages which means that all regulating pathways leading to hyperglycemia-induced elevated DEP-1 expression these investigated cells must reside within this specific cell type.

Since effects were seen in both monocytes and macrophages and both cell types are dependents within the mononuclear lineage one may assume that the same pathways are responsible in both cell types.

Normoglycemic and hyperglycemic cultured monocytes were also stimulated with MG, a side metabolite of glycolysis and significantly enhanced in non-insulin-dependent and insulin-dependent DM (161, 215, 246). It has been described to be a mediator of diabetes complications such as impaired wound healing and microvascular diseases (19) or neuropathy (20). More recently, Khan *et al.* reported that MG – through generation of advanced glycation end products (AGEs) – decreases the number of anti-inflammatory macrophages in hyperglycemic stroke (120). Newer studies discuss elevated MG levels as a cause for instead of a consequence of diabetes (168). In this work, MG was used to check whether glucose itself or its metabolites are responsible for elevated DEP-1 levels in diabetics. In NG alone, as well as in combination with HG, trends but no significant effects of DEP-1 induction through MG were shown. It may be concluded that MG is a further mediator between glucose and DEP-1 regulation. However, MG did not enhance DEP-1 expression beyond HG alone which is contradictory to the hypothesis.

MG can indirectly upregulate NF- $\kappa$ B as a precursor of AGEs which then bind to proteins and alter their function. These can in turn bind to and activate the receptor for AGE (RAGE) (48, 49). Activation of NF- $\kappa$ B by RAGE is mediated through the mitogen-activated protein kinases (MAPKs) pathway (199). Conclusively, suggesting MG and more downstream NF- $\kappa$ B- and MAPK-signaling as further links between HG and regulation of DEP-1 expression is reasonable.

OxLDL is an essential pro-atherosclerotic product as it is the main component of foam cells which in turn are the main component of fatty streaks, the early manifestations of atherosclerosis in the vascular wall (74). Circulating oxLDL is associated with T2DM, obesity and T2DM-related traits (174, 176), LDL-oxidization is enhanced in diabetes-typical HG (116) and in serum from T2DM patients (66). This work found a trend of DEP-1 induction by oxLDL stimulation in both NG and HG. However, no additive effects of HG and oxLDL were observed. In fact, upregulation through HG alone seemed attenuated under additional oxLDL stimulation. Literature research could not reveal earlier studies testing oxLDL stimulation on DEP-1 expression. Nevertheless, an enhanced SHP-

2 and ERK phosphorylation upon oxLDL stimulation was shown in vascular smooth muscle cells (33) and CD45 is upregulated in atherosclerotic arteries from hamsters on a high-cholesterol diet (222). As DEP-1 was shown to be upregulated in inflammatory diseases, one of the major inflammatory transcription factors in macrophages, NF- $\kappa$ B, may be a potential mediator of its regulation. OxLDL was shown to activate NF- $\kappa$ B signaling in macrophages through CD36 and a TLR4-TLR6-heterodimer (235), as well as through enhancing TLR-signaling when lipids accumulate in the cell membrane (279, 285). Besides, oxLDL was shown to induce macrophage activation (31) which was discussed to be mediated through TNF- $\alpha$  release (107) and subsequent NF- $\kappa$ B activation which again causes a release of cytokines, that trigger macrophage activation. Indeed, DEP-1 expression and activity was shown to be increased in activated macrophages in this work. OxLDL is usually used for stimulation of macrophages in doses between 10 and 100  $\mu$ g/ml without relevant differences in cell viability, however with dose-dependent increasing effects in several studies, demonstrated exemplarily by Lara-Guzmàn et al. (135). In this work, 20  $\mu$ g/ml were used which is rather in the lower compartment of possible doses. Further investigation of this question including dose-response curves of DEP-1 expression upon oxLDL stimulation and use of NF- $\kappa$ B signaling pathway inhibitors, as well as increased biological replicates due to high inter-subject variability in experiments with primary human monocyte-derived macrophages seems rational.

Conclusively, this work identified stimulators of DEP-1 (HG and very likely MG and oxLDL) present in DM and discusses how inflammation is a potential link between pathways activated by these stimulants.

### 5.2.3 TNF- $\alpha$ stimulation showed strongest capabilities of DEP-1 induction in monocytes *in-vitro* and the NF- $\kappa$ B pathway is a potential mediator in between

The pro-inflammatory cytokine TNF- $\alpha$  activates NF- $\kappa$ B through its receptors of the TNF-receptor-superfamily (TNFR), especially TNFR1, and is therefore a potent trigger of immune cell's inflammatory response (113, 256). TNF- $\alpha$  stimulated monocytes gave further evidence for the involvement of pro-inflammatory signaling pathways in regulation of the DEP-1 phosphatase's expression: TNF- $\alpha$  led to a significant 3.6-fold increased expression of DEP-1 while this induction was impaired at co-incubation with an NF- $\kappa$ B

activation inhibitor. It was even more drastically reduced by nearly 50 % in co-culture with the PKC inhibitor GF 109203X.

These results confirm again the ability of pro-inflammatory cytokines, in this case TNF- $\alpha$ , to upregulate DEP-1 expression which is in line with very early results from Osborne et al. (180) who showed DEP-1 induction in murine macrophages after stimulation with LPS. This work adds, that not only toll-like receptors (TLR) – e. g. TLR4 for LPS – and TLR-specific adapter proteins or TLR-specific downstream pathways but also TNFRs, here TNFR1 and TNFR2, are mediating the observed effects on DEP-1 expression. Therefore it is most likely that common downstream signaling pathways of TLRs and TNFRs regulate DEP-1 expression in inflammatory contexts. Possible candidates are particularly the MAPK and the NF- $\kappa$ B signaling pathway (115, 256). It was earlier shown that the promoter of the PTPRJ gene has NF- $\kappa$ B binding sites (44) which makes especially NF- $\kappa$ B a likely upstream regulator of DEP-1 expression. NF- $\kappa$ B activation was previously shown to be catalyzed by PKC  $\delta$  and  $\epsilon$  which positively contribute to I $\kappa$ B kinase degradation and therefore to nuclear translocation of NF- $\kappa$ B (255). Therefore, both used inhibitors impair NF- $\kappa$ B signaling and DEP-1 expression was reduced in both inhibitor-treated samples independently which provides good evidence that NF- $\kappa$ B is at least one important mediator in regulation of DEP-1 expression.

This work supports the concept that the DEP-1 phosphatase is upregulated especially in inflammatory contexts. HG itself *in-vivo* and *in-vitro*, as well as side products accumulating in HG may also be able to upregulate DEP-1 expression while stimulation with TNF- $\alpha$  showed the strongest effects. *In-vivo*, systemic inflammatory effects of HG may play an important role. Therefore, it can be assumed that both glucose and MG trigger inflammation which subsequently regulates DEP-1 expression particularly via NF- $\kappa$ B signaling. This, however, does not exclude involvement of other, even more direct acting, transcription and translation regulating pathways.

Naive macrophages stimulated with LPS and IFN- $\gamma$  can be activated into a sustained inflammatory, so called classical, phenotype. Classically activated M1-macrophages showed the highest DEP-1 expression among non- and alternatively activated macrophages. Besides, HG enhanced DEP-1 expression slightly in all phenotypes. Induced DEP-1 expression in pro-inflammatory M1-macrophages is in line with induced

monocytic DEP-1 expression by the pro-inflammatory cytokine TNF- $\alpha$ , as seen in this work. However, both results did not test significant in statistical analysis. Standard deviations were comparably high due to a small sample size which is a limitation of this experiment. However, DEP-1's phosphatase activity was strongly and significantly elevated in M1-macrophages compared to M2- and M0-macrophages. It is therefore assumable that M1-macrophages express DEP-1 to a higher extent. This is in line with very initial findings of DEP-1's regulation in primary mouse macrophages (180) which was confirmed later by Stuart Kellie's group in the murine RAW264.7 macrophage cell line and thioglycolate-elicited peritoneal macrophages (45). This group also confirmed reduced DEP-1-inducibility by LPS after M-CSF starvation followed by M-CSF repletion (44). Divergent to some extent is their finding that overnight priming of macrophages with 500 pg/ml IFN- $\gamma$  limited the phosphatase's inducibility by 10 ng/ml LPS within the first 24 hours after stimulation compared to the unprimed cells, as IFN- $\gamma$  is used commonly for M1-action. Yet, concentrations of LPS and IFN- $\gamma$  were twice and 100-times as high, respectively, for M1-activation of macrophages in this work and were both applied at the same time for 18 hours while the cells were lysed 48 hours after removal of the ligands. Therefore, this study provides further knowledge about DEP-1 expression in M1- compared to M2-activated primary human monocyte-derived macrophages in the time period starting 24 hours after activation. In any way these findings support the hypothesis of DEP-1's role in inflammation in mononuclear cells and fit in line with the *in-vivo* and *in-vitro* results generated in monocytes.

### 5.3 DEP-1 depletion impairs macrophage migration, possibly by dephosphorylating and activating SFKs

This work investigated migration in DEP-1 depleted macrophages and found it reduced in the M1- and M2-activated phenotype while DEP-1 depletion had no effect in M0-macrophages. Migration was investigated because macrophage's migratory capabilities play a role in regression of atherosclerotic plaques, monocyte migration plays an important role in plaque progression (167).

Reduced migration of M1- and M2-activated macrophages after DEP-1 knockdown suggests a pro-migratory regulatory role of DEP-1 in these macrophage phenotypes. Similar results were obtained by Schneble *et al.* in primary microglial cells from DEP-1-deficient

mice, as well as in a DEP-1-knockdown microglial cell line (212). Antibody-based DEP-1 inhibition reduced migration, as well as formation of membrane ruffles and filopodia, in primary bone-marrow derived mouse macrophages in response to M-CSF (45). Impaired migration has also been observed upon DEP-1 depletion in a human megakaryocytic cell line (158). There against, Jandt et al. suggested DEP-1 to be a negative regulator of migration towards a PDGF- and a serum-gradient in an porcine aortic endothelial cell line (X23) and in 3T3 fibroblasts (102). The latter finding was confirmed by Kellie et al. in 2004, showing impaired migration of fibroblasts towards a PDGF-gradient in a cell line with mifepristone-inducible DEP-1 expression (118). Overexpression of DEP-1 lead to decreased HUVEC transmigration in a Boyden-chamber assay, as well as decreased proliferation (23). Alteration of endothelial cell migration was discussed to be mediated through inhibitory effects of DEP-1 on VEGFR2-, ERK- and Akt-signaling (29).

Migration as part of tumor metastasis was intensively studied in cancer cells and respective cell lines. In most assayed cancer types, e.g. colon carcinoma (12), hepatocellular carcinoma (152), lung carcinoma (41) and esophageal squamous cell carcinoma (198), DEP-1 inhibition lead to enhanced cell migration and invasion.

Although DEP-1 seems to regulate cell migration of many cell types in different pathological and physiological conditions, this function of the phosphatase is complex and not yet fully understood. It also remains unclear whether has a pro- or anti-migratory role and the question may not be answerable in a dichotomous manner. Previous studies including this work suggest a highly context-dependent phenotype: Interestingly, studies which have suggested DEP-1 to be a positive regulator of cell migration were mainly conducted in cell types descending from the hematopoietic lineage (45, 158, 212). There against, studies showing anti-migratory capabilities of DEP-1 were conducted in either mesenchymal (102, 118) or epithelial cell types (12, 23, 41, 152, 198).

It is worth to consider that regulation of directed sheet migration, as studied in this work, is an extremely complex signaling process involving cell polarization, different states of adhesion and morphological changes like formation of lamellipodia and filopodia and cytoskeletal re-arrangements (reviewed in (192)).

Among the already tested conditions, this work adds knowledge about migration of primary human monocyte-derived macrophages under DEP-1 depletion and different serum



glucose levels. In these conditions, impaired wound healing was observed which suggests a generally positive regulatory role of DEP-1. Compared to a few other experiments mentioned before which were conducted *in-vitro* but with fully DEP-1 depleted cells from knockout mice, DEP-1 was not completely abolished in this study's experiments but expression was rather reduced to approximately 14 % (**Figure 7**). Of note, PDGF-BB-stimulated cell proliferation and viability was not altered by DEP-1 knockdown in this work (**chapter 4.7**). This underlines on the one hand that proliferation may be excluded as a factor other than migration leading to differing closure times in the scratch assays (**chapter 4.6**). On the other hand, this result is contradictory to results obtained in endothelial cells in which DEP-1 was crucial for serum- and VEGF-induced proliferation (23, 83, 241) but in line with results from Stuart Kellie's group which found that CSF-1R-mediated proliferation and survival was not affected by DEP-1 inhibition by a monoclonal antibody in murine bone-marrow derived macrophages (45). Therefore, proliferation and survival might be differently controlled by DEP-1 depending on stimulating growth factors and cell type.

Different downstream pathways of DEP-1 have been identified and suggested to interfere with migration. It has been shown in two studies that DEP-1 impairs PDGF-stimulated migration. Both studies were conducted in fibroblast cell lines. The authors suggested PDGFR which was shown before to be dephosphorylated by DEP-1 (122, 188) to be one major signaling component downstream of DEP-1 in regulation of cell migration (102, 118).

In this work, migration was measured in M-CSF supplemented medium but without a concentration gradient. M-CSF is a ligand of CSF-1R and is known to be an important regulator of cell functions including cell migration (193) and its transient depletion in tumor associated macrophages was shown to impair migration in a scratch assay (124). Inhibition via a pan-SFK small molecule inhibitor significantly reduced macrophage motility in response to M-CSF and subcellular re-localization of SFKs was observed in M-CSF-stimulated human macrophages (54) which both indicates a significant relevance of SFKs in M-CSF induced migration. Regulation of macrophage motility is thought to be regulated to a relevant extent through two downstream cascades: 1) activation of SFKs and in turn Pyk2 (179) which activates Paxillin and 2) activation of PI3K through its regulatory p85 subunit (211). Subsequently, both pathways activate signaling

downstream of Rho GTPases Rho, Rac and Cdc42 (194, 202) which includes activation of Wiskott–Aldrich syndrome protein (WASP) and WASP-family verprolin homologous (WAVE) which were shown to induce pro-migratory actin-cytoskeleton remodeling (192, 209). Notably, activation of PI3K was achievable both Src-mediated and as a direct effect of CSF-1R phosphorylation (138). Akt2 is a downstream target of PI3K which was also shown to be relevant (281), however not crucial, for macrophage motility. Not only CSF-1R but also other immune receptors may be located upstream of SFKs and therefore at the top of the described signaling cascades (14, 100).

DEP-1 was shown to be able to interfere with all above mentioned pathways proximally. While Tsuboi *et al.* described DEP-1 to attenuate PI3K activity (249) it was also shown that DEP-1 and CD45 dephosphorylate the inhibitory N-terminal tyrosine phosphorylation site of SFKs (91, 137, 284) which – enhanced by trans-autophosphorylation of the conserved activation loop – activates SFKs (148). Very recently but of importance, Nagy *et al.* suggested an inhibitory-autophosphorylation effect of the different SFKs on each other. They found that in a triple knockout of Csk, Chk, the two known kinases that phosphorylate the inhibitory N-terminal tyrosine phosphorylation site of SFKs, and DEP-1, phosphorylation of the inhibitory tyrosine residues of Src and Fyn was slightly higher than in a Csk Chk double knockout which means that a third player can phosphorylate this site and is probably inhibited by DEP-1. This effect was abolished under inhibition of SFK by small molecules (172). Therefore, DEP-1 seems to have both activating and inhibiting functions in regulation of SFKs. Also of note, it was recently shown that DEP-1 can directly dephosphorylate CSF-1R at Y723 in osteoclasts and therefore inhibit downstream signaling of M-CSF stimulation (217).

However, it was hypothesized that DEP-1 has a predominantly activating effect on the above-described pathways by activation of SFKs which in this work's experimental conditions leads to activation of pro-migratory cytoskeletal re-arrangement via signaling processes downstream of Rho GTPases. Observed, rather mild changes in motility are in line with only mild alterations in cellular function when depleting cells of either CD45 or DEP-1 in Zhu *et al.*'s study which suggested that both phosphatases together are required for optimal dephosphorylation of the N-terminal inhibitory tyrosine phosphorylation site in SFKs (284). Further reasons for only mild functional effects may be that the inhibitory effect of DEP-1 on PI3K is attenuated under DEP-1 depletion leading to enhanced pro-

migratory signaling of PI3K in opposite to anti-migratory signaling of the depleted DEP-1 itself. Besides, DEP-1 depletion was incomplete (**chapters 4.5.1 and 4.8**). DEP-1 was recently shown to be important for Src and Akt activation in endothelial cells (63). However, to reason this model of explaining involved signaling, it must be assumed that direct effects of DEP-1 activated SFKs on migration through at least direct activation of Pyk2 and PI3K exceed inhibitory effects of DEP-1 on PI3K and its downstream signaling.

A shortcoming of this study is the missing verification of the here proposed signaling processes which was initiated in preliminary experiments but not finished sufficiently. However, rescue experiments in the tested conditions would be interesting to validate these ideas. Small-molecule activation or overexpression of SFKs in macrophages should rescue their motility during DEP-1 depletion. Besides, SFK depletion or chemical inhibition should lead to a similar migratory phenotype. Additionally, direct effects of DEP-1 on CSF-1R observed in osteoclasts (217) require confirmation in monocytes and macrophages. If direct effects of DEP-1 on CSF-1R are responsible for upregulation of macrophage migration in DEP-1 knockdown, then this effect would not be observed in DEP-1 CSF-1R double knockdown cells.

#### 5.4 DEP-1 depletion enhances NF- $\kappa$ B expression and activation possibly as a feedback regulation

This study revealed significant effects of TNF- $\alpha$  stimulation on DEP-1 expression which could be attenuated by inhibition of the NF- $\kappa$ B signaling pathway employing two independent inhibitors. Likewise, metabolic stress increased DEP-1 expression. DEP-1 expression and activity were enhanced in classically, pro-inflammatory activated macrophages, as well and NF- $\kappa$ B seemed to be a very likely candidate regulating DEP-1 transcription in the context of inflammation and metabolic stress.

In atherosclerosis, NF- $\kappa$ B activation and subsequent transcription of pro-inflammatory cytokines leads to plaque progression through induced monocyte recruitment (220, 258). However, there is also evidence for a regulatory role of NF- $\kappa$ B in atherosclerosis as NF- $\kappa$ B depletion was shown to increase lesion size and cell death in atherosclerotic plaques (111). Studying further effects of DEP-1 on NF- $\kappa$ B seemed therefore rational:

This study showed that DEP-1 itself significantly affects expression of the NF- $\kappa$ B regulatory subunit p65. p65 mRNA was upregulated in DEP-1 depleted macrophages. Simultaneously, p65 protein-phosphorylation, measured via western blotting, was increased relevantly and significantly in basal, as well as TLR-stimulated conditions. TLR-stimulation in this work was achieved via the synthetic TLR1 and TLR2 ligand Pam3CSK4 (4). TNF- $\alpha$ , which is one of the main cytokine-type transcription products of NF- $\kappa$ B, was also increased at mRNA level in the same DEP-1 depleted macrophages (**chapter 4.8**). These results suggest that DEP-1 may inhibit NF- $\kappa$ B signaling on a basis of gene expression and activity, at least in the conditions tested. Occurrence of the same effect in basal and TLR1/2-stimulated conditions suggests that NF- $\kappa$ B signaling is DEP-1 dependent since TLR1/2-stimulated induction of TNF- $\alpha$  gene expression requires NF- $\kappa$ B activation, strictly dependent on the myeloid differentiation primary-response gene 88 (MyD88) signaling pathway (242).

Pro-inflammatory stimuli and stressors lead to upregulation of the DEP-1 (**chapters 4.1 - 4.3**) and DEP-1 was expressed at highest levels, as well as most active in pro-inflammatory M1-activated macrophages (**chapter 4.4**). Therefore, and in regard of DEP-1's association with auto-inflammatory diseases Morbus Crohn and Cogan's syndrome (**chapter 1.4**), DEP-1's role in immunity was assumed to be also pro-inflammatory.

The described regulation of p65, TNF- $\alpha$  and p-65 phosphorylation, however, suggests a potential regulatory role in inflammation for DEP-1: As knockdown leads to activation of these inflammatory mediators, DEP-1 itself might be negatively regulating NF- $\kappa$ B expression and activation under the given circumstances. However, this does not imply that DEP-1 is only anti-inflammatory: TLR- and NF- $\kappa$ B signaling is extremely complex, variable and context dependent itself (53). Also, for DEP-1 it was shown already that its function is highly context-dependent.

Effects of DEP-1 on NF- $\kappa$ B signaling have not been extensively studied but it was identified as a potential activator of NF- $\kappa$ B binding activity in a large screen for NF- $\kappa$ B-regulating phosphatases in astrocytes. Out of 250 screened (putative) phosphatase genes, knockdown of only 19 showed a relevant fold-change of NF- $\kappa$ B and only 6 out of these 19, including DEP-1, showed inhibition of NF- $\kappa$ B activity, indicating a relevant role of these phosphatases in activating NF- $\kappa$ B signaling (142). This result is opposite to what

was seen in this work, although the approach of siRNA-mediated knockdown was similar. The readout, in contrast, differed as Li et al. employed NF- $\kappa$ B reporter assay and an NF- $\kappa$ B DNA-binding assay and this work employed rather functional read-outs, measuring NF- $\kappa$ B activity by p65-phosphorylation and TNF- $\alpha$  mRNA expression which is a result of NF- $\kappa$ B transcription factor binding. Also, Li et al. employed TNF- $\alpha$  stimulation, a TNFR ligand, while Pam3Csk4, a TLR1/2, ligand was employed in this work. However, basal, unstimulated rates changed in both works as well.

Similarly, Wen *et al.* found overexpression of Ptprij-as1, a long noncoding RNA (lncRNA) which is transcribed antisense to PTPRJ and inducible by TLR-ligands with a similar time course compared to PTPRJ itself (44), to promote migration of BV2 microglial cells and induce expression levels of inflammatory cytokines dependent on intracellular NF- $\kappa$ B signaling (263). LncRNA are a heterogeneous group of RNAs longer than 200 nucleotides, transcribed from the nuclear genome in different manners which allocates them into different classes that act regulatory at different levels of gene expression, post-translational modification (275) and even as direct interaction partners of proteins, such as lnc-DC, which prevents STAT3-dephosphorylation by SHP1 (259) or NKILA which is an NF- $\kappa$ B activator, upregulated upon stimulation with IL-1 $\beta$  and TNF- $\alpha$  (147). Several lncRNA were shown to interfere with the immune system (8). Exemplarily, lincRNA-Cox2, induced by LPS, were attributed both inflammation driving and repressing capabilities in TLR signaling, highly dependent on multiple interaction partners (26). Therefore, one may assume that Ptprij-as1's positive regulation of NF- $\kappa$ B signaling as shown by Wen et al. may not be exclusive.

Assuming roles of DEP-1 itself in NF- $\kappa$ B signaling by looking at its antisense-transcribed lncRNA may be too primitive; However, if Ptprij-as1 regulates balancing to PTPRJ, this would indicate an anti-inflammatory role of DEP-1 itself under certain circumstances. In contrast, if Ptprij-as1 is co-operative to DEP-1, this would indicate a pro-inflammatory role of DEP-1. At least, involvement of Ptprij-as1 in NF- $\kappa$ B signaling supports the existing evidence that DEP-1 itself also influences NF- $\kappa$ B signaling in a yet elusive way.

CD45, another transmembrane PTP, which was shown to have overlapping and co-operative roles with DEP-1 in regulating SFK signaling (284), was investigated regarding its regulatory impact on TLR-mediated cytokine secretion and found to both positively and

negative influence NF- $\kappa$ B signaling, depending on the activated TLR. In short, CD45 was shown to be upregulated upon LPS stimulation, similar to DEP-1 being induced by LPS (180) and NF- $\kappa$ B dependently by TNF- $\alpha$  (**chapter 4.3**). Pro-inflammatory cytokine production upon TLR2 (via PAM3) and TLR 9 stimulation (via CpG 1668) in CD45<sup>-/-</sup> bone-marrow derived dendritic cells was significantly increased compared to wildtypes, while no difference was seen upon TLR4 stimulation (via LPS). Similar results were obtained by Piercy et al. (190). TLR2 and TLR9 are strictly MyD88-dependent (242) while LPS-stimulated TLR4 signals MyD88-dependent and -independent.

Cross et al. also found distinct effects of CD45 in bone-marrow derived dendritic cells and BMDMs, suggesting a cell-type specific behavior (39) which might also apply for DEP-1 and explain opposite findings of this work and Li et al.'s screen in astrocytes (142).

In this work, effects of DEP-1 knockdown on LPS-induced NF- $\kappa$ B activation were not investigated. TNF- $\alpha$  was the only used TLR ligand. However, Cross et al.'s study gives reason to assume that DEP-1's effects on NF- $\kappa$ B signaling may similarly be dependent either on which TLR is activated or dependent on whether that TLR is strictly MyD88-dependent or not.

SFKs were shown to interact with TLR signaling in different manners which suggests this interaction to be very complex and possibly also indirect via paracrine and autocrine effects. This includes the kinases themselves, as well as their upstream regulators, among them CD45 and DEP-1 (91). Mitchell et al. used chemical rescue techniques to investigate Src effects on TLR4 signaling without potential compensation of other SFK members. SFK rescue disrupted MyD88 association with TLR4 while alternative Toll-like downstream signaling remained unchanged. Rescue of SFK activity lead to decreased LPS-induced, therefore TLR4-dependent, inflammatory responses (162). That study suggests that MyD88 and SFKs may be important mediators between DEP-1 and NF- $\kappa$ B signaling. Of note, it was mostly conducted in epithelial cell lines.

Further experiments investigating the interplay between the MyD88-dependent TLR-signaling pathway, SFKs and DEP-1 are likely to bring further understanding of DEP-1's effects on TLR-signaling and NF- $\kappa$ B activation. Also, effects within tonic signaling needs to be investigated in macrophages to understand the differences in basal rates of NF- $\kappa$ B activation seen in this work and oppositely in astrocytes (142).

This work identified, however elusive, an anti-inflammatory regulatory role of DEP-1 in NF- $\kappa$ B signaling when stimulated by the TLR1/2 ligand PAM3 which lead to attenuated TNF- $\alpha$  mRNA production. A mediator between signaling cascades downstream of TLR dephosphorylated by DEP-1 and thus inhibiting the process was not identified but SFKs may play a role. It is important to consider the exact circumstances and timings, mechanism and efficiency of knockdown and all involved factors when interpreting this result and when it comes to planning further experiments, as this signaling process is assumed to be rather complex and indirect, not mentioned or thought of components may be furtherly involved.

### 5.5 DEP-1's role in atherosclerosis

Atherosclerosis is a highly complex, intensively regulated process which includes hundreds of involved signaling proteins and pathways. This work investigated DEP-1's role in atherosclerosis-related cellular processes: macrophage migration and immune signaling.

In case DEP-1's role in immunity will be confirmed to be rather anti-inflammatory than pro-inflammatory and taking into account its rather pro-migratory role of which this work's migration experiments informed, DEP-1's role in atherosclerosis may be anti-atherosclerotic and/or it may contribute to plaque resolving, as it may attenuate inflammatory processes within the atherosclerotic plaque and promote a migratory phenotype which could lead to emigration of foam cells from atherosclerotic lesion.

Therefore, DEP-1's upregulation in diabetic monocytes and macrophages may have a protective, balancing purpose. However, this hypothesis remains speculative and requires further, detailed research, not only on DEP-1 itself but also on exact signaling processes involving TLR-signaling and other immunoreceptors that regulate the atherosclerotic inflammation during plaque regression.

## 6 Conclusions

This work identified DEP-1 as a novel target regulating diabetic monocytes and macrophages and provides evidence for its involvement in NF- $\kappa$ B signaling and macrophage migration. As DEP-1 was shown to be upregulated in monocytes from diabetic patients and could be induced in HG-cultured monocytes and macrophages, as well as by glycolysis side product methylglyoxal, oxLDL and pro-inflammatory stimuli depending on NF- $\kappa$ B signaling, its role in these cells may be assumed to be of high relevance in immune signaling processes. This was confirmed by knockdown experiments, showing an increased NF- $\kappa$ B activity and TNF- $\alpha$  mRNA production which suggested an anti-inflammatory role of DEP-1 in the conditions tested. However, DEP-1's impact on NF- $\kappa$ B signaling remains highly elusive and requires detailed further research in different contexts as its function seems highly context-dependent. A second function of DEP-1 in regulating macrophage migration without interfering with cell viability was confirmed by similar methods. DEP-1 knockdown led to a phenotype of impaired macrophage migration. Signaling via SFKs was suggested to be mediating these effects. Therefore, further research is required in confirming this by employing Src-inhibition, -activation and -overexpression. The latter ones should restore migration in DEP-1 knockdown conditions.

This work analyzed DEP-1's functional role in the context of DM and atherosclerosis as a main consequence of longer lasting DM. Analyzing DEP-1 expression in diabetic hyperglycemic patients revealed a potential importance of the phosphatase in this context. These functional impacts on macrophage function, regulation of migration and NF- $\kappa$ B, were discussed regarding a chance to play a role in plaque regression by enhancement of emigration of foam cells and limiting the atherosclerotic inflammation. However, results are preliminary and require further confirmation. An advantage of this work is, that all experiments were performed in primary human monocytes and monocyte derived macrophages therefore being conducted without the need to use less precise models. Conducting experiments in primary cells in turn brings in higher interindividual variabilities which are reflected in higher standard deviations. Experiments in cell lines and mouse models would be able to overcome this limitation and confirm this work's results in further models. Being a cell regulating molecule, mechanistic research and identification of other involved signaling pathways will inform further understanding of DEP-1.



## 7 References

- (1) Ahmad F, Goldstein BJ (1995) Increased abundance of specific skeletal muscle protein-tyrosine phosphatases in a genetic model of insulin-resistant obesity and diabetes mellitus. *Metabolism* 44, 9: 1175–1184, doi: 10.1016/0026-0495(95)90012-8
- (2) Ahmad F, Li PM, Meyerovitch J, Goldstein BJ (1995) Osmotic loading of neutralizing antibodies demonstrates a role for protein-tyrosine phosphatase 1B in negative regulation of the insulin action pathway. *J Biol Chem* 270, 35: 20503–20508, doi: 10.1074/jbc.270.35.20503
- (3) Ajami B, Bennett JL, Krieger C, Tetzlaff W, Rossi FMV (2007) Local self-renewal can sustain CNS microglia maintenance and function throughout adult life. *Nat Neurosci* 10, 12: 1538–1543, doi: 10.1038/nn2014
- (4) Aliprantis AO, Yang RB, Mark MR, Suggett S, Devaux B, Radolf JD, Klimpel GR, Godowski P, Zychlinsky A (1999) Cell activation and apoptosis by bacterial lipoproteins through toll-like receptor-2. *Science* 285, 5428: 736–739, doi: 10.1126/science.285.5428.736
- (5) Alonso A, Sasin J, Bottini N, Friedberg I, Friedberg I, Osterman A, Godzik A, Hunter T, Dixon J, Mustelin T (2004) Protein tyrosine phosphatases in the human genome. *Cell* 117, 6: 699–711, doi: 10.1016/j.cell.2004.05.018
- (6) Arora D, Stopp S, Böhmer S-A, Schons J, Godfrey R, Masson K, Razumovskaya E, Rönstrand L, Tänzer S, Bauer R, Böhmer F-D, Müller JP (2011) Protein-tyrosine phosphatase DEP-1 controls receptor tyrosine kinase FLT3 signaling. *J Biol Chem* 286, 13: 10918–10929, doi: 10.1074/jbc.M110.205021
- (7) Assmann G, Schulte H, Eckardstein A von (1996) Hypertriglyceridemia and elevated lipoprotein (a) are risk factors for major coronary events in middle-aged men. *Am J Cardiol* 77, 14: 1179–1184, doi: 10.1016/S0002-9149(96)00159-2
- (8) Atianand MK, Fitzgerald KA (2014) Long non-coding RNAs and control of gene expression in the immune system. *Trends Mol Med* 20, 11: 623–631, doi: 10.1016/j.molmed.2014.09.002
- (9) Auffray C, Fogg D, Garfa M, Elain G, Join-Lambert O, Kayal S, Sarnacki S, Cumano A, Lauvau G, Geissmann F (2007) Monitoring of blood vessels and tissues by a population of monocytes with patrolling behavior. *Science* 317, 5838: 666–670, doi: 10.1126/science.1142883
- (10) Autschbach F, Palou E, Mechttersheimer G, Rohr C, Piroto F, Gassler N, Otto HF, Schraven B, Gaya A (1999) Expression of the membrane protein tyrosine phosphatase CD148 in human tissues. *Tissue Antigens* 54, 5: 485–498, doi: 10.1034/j.1399-0039.1999.540506.x
- (11) Babaev VR, Gleaves LA, Carter KJ, Suzuki H, Kodama T, Fazio S, Linton MF (2000) Reduced atherosclerotic lesions in mice deficient for total or macrophage-specific expression of scavenger receptor-A. *Arterioscl Throm Vas* 20, 12: 2593–2599, doi: 10.1161/01.atv.20.12.2593
- (12) Balavenkatraman KK, Jandt E, Friedrich K, Kautenburger T, Pool-Zobel BL, Ostman A, Böhmer FD (2006) DEP-1 protein tyrosine phosphatase inhibits proliferation and migration of colon carcinoma cells and is upregulated by protective nutrients. *Oncogene* 25, 47: 6319–6324, doi: 10.1038/sj.onc.1209647
- (13) Baltimore D (1970) RNA-dependent DNA polymerase in virions of RNA tumour viruses. *Nature* 226, 5252: 1209–1211, doi: 10.1038/2261209a0
- (14) Baruzzi A, Cavegion E, Berton G (2008) Regulation of phagocyte migration and recruitment by Src-family kinases. *Cell Mol Life Sci* 65, 14: 2175–2190, doi: 10.1007/s00018-008-8005-6
- (15) Bays HE, Chapman RH, Grandy S (2007) The relationship of body mass index to diabetes mellitus, hypertension and dyslipidaemia: comparison of data from two national surveys. *Int J Clin Pract* 61, 5: 737–747, doi: 10.1111/j.1742-1241.2007.01336.x
- (16) Behmoaras J, Bhangal G, Smith J, McDonald K, Mutch B, Lai PC, Domin J, Game L, Salama A, Foxwell BM, Pusey CD, Cook HT, Aitman TJ (2008) Jund is a determinant of macrophage activation and is associated with glomerulonephritis susceptibility. *Nat Genet* 40, 5: 553–559, doi: 10.1038/ng.137

- (17) Benoit M, Desnues B, Mege J-L (2008) Macrophage polarization in bacterial infections. *J Immunol* 181, 6: 3733–3739, doi: 10.4049/jimmunol.181.6.3733
- (18) Bentzon JF, Otsuka F, Virmani R, Falk E (2014) Mechanisms of plaque formation and rupture. *Circ Res* 114, 12: 1852–1866, doi: 10.1161/CIRCRESAHA.114.302721
- (19) Berlanga J, Cibrian D, Guillén I, Freyre F, Alba JS, Lopez-Saura P, Merino N, Aldama A, Quintela AM, Triana ME, Montequin JF, Ajamieh H, Urquiza D, Ahmed N, Thornalley PJ (2005) Methylglyoxal administration induces diabetes-like microvascular changes and perturbs the healing process of cutaneous wounds. *Clin Sci* 109, 1: 83–95, doi: 10.1042/CS20050026
- (20) Bierhaus A, Fleming T, Stoyanov S, et al. (2012) Methylglyoxal modification of Nav1.8 facilitates nociceptive neuron firing and causes hyperalgesia in diabetic neuropathy. *Nat Med* 18, 6: 926–933, doi: 10.1038/nm.2750
- (21) Borges LG, Seifert RA, Grant FJ, Hart CE, Disteché CM, Edelhoff S, Solca FF, Lieberman MA, Lindner V, Fischer EH, Lok S, Bowen-Pope DF (1996) Cloning and characterization of rat density-enhanced phosphatase-1, a protein tyrosine phosphatase expressed by vascular cells. *Circ Res* 79, 3: 570–580, doi: 10.1161/01.res.79.3.570
- (22) Brown MS, Goldstein JL, Krieger M, Ho YK, Anderson RG (1979) Reversible accumulation of cholesteryl esters in macrophages incubated with acetylated lipoproteins. *J Cell Biol* 82, 3: 597–613, doi: 10.1083/jcb.82.3.597
- (23) Brunner PM, Heier PC, Mihaly-Bison J, Priglinger U, Binder BR, Prager GW (2011) Density-enhanced phosphatase-1 down-regulates urokinase receptor surface expression in confluent endothelial cells. *Blood* 117, 15: 4154–4161, doi: 10.1182/blood-2010-09-307694
- (24) Burger-Kentischer A, Goebel H, Seiler R, Fraedrich G, Schaefer HE, Dimmeler S, Kleemann R, Bernhagen J, Ihling C (2002) Expression of macrophage migration inhibitory factor in different stages of human atherosclerosis. *Circulation* 105, 13: 1561–1566, doi: 10.1161/01.cir.0000012942.49244.82
- (25) Burgess AW, Metcalf D (1980) The nature and action of granulocyte-macrophage colony stimulating factors. *Blood* 56, 6: 947–958, doi: 10.1182/blood.V56.6.947.947
- (26) Carpenter S, Aiello D, Atianand MK, Ricci EP, Gandhi P, Hall LL, Byron M, Monks B, Henry-Bezy M, Lawrence JB, O'Neill LAJ, Moore MJ, Caffrey DR, Fitzgerald KA (2013) A long non-coding RNA mediates both activation and repression of immune response genes. *Science* 341, 6147: 789–792, doi: 10.1126/science.1240925
- (27) Carréno S, Caron E, Cougoule C, Emorine LJ, Maridonneau-Parini I (2002) p59Hck isoform induces F-actin reorganization to form protrusions of the plasma membrane in a Cdc42- and Rac-dependent manner. *J Biol Chem* 277, 23: 21007–21016, doi: 10.1074/jbc.M201212200
- (28) Centers for Disease Control and Prevention National Diabetes Statistics Report, 2020: Centers for Disease Control and Prevention, U.S. Dept of Health and Human Services, Atlanta, GA, <https://www.cdc.gov/diabetes/data/statistics-report/index.html> [Retrieval date: 05.02.2022]
- (29) Chabot C, Spring K, Gratton J-P, Elchebly M, Royal I (2009) New role for the protein tyrosine phosphatase DEP-1 in Akt activation and endothelial cell survival. *Mol Cell Biol* 29, 1: 241–253, doi: 10.1128/MCB.01374-08
- (30) Chávez-Galán L, Olleros ML, Vesin D, Garcia I (2015) Much More than M1 and M2 Macrophages, There are also CD169(+) and TCR(+) Macrophages. *Front Immunol* 6: 263, doi: 10.3389/fimmu.2015.00263
- (31) Chen C, Khismatullin DB (2015) Oxidized low-density lipoprotein contributes to atherogenesis via co-activation of macrophages and mast cells. *PLoS One* 10, 3: e0123088, doi: 10.1371/journal.pone.0123088
- (32) Chen C-Y, Lin L-I, Tang J-L, Tsay W, Chang H-H, Yeh Y-C, Huang C-F, Chiou R-J, Yao M, Ko B-S, Chen Y-C, Lin K-H, Lin D-T, Tien H-F (2006) Acquisition of JAK2, PTPN11, and RAS mutations during disease progression in primary myelodysplastic syndrome. *Leukemia* 20, 6: 1155–1158, doi: 10.1038/sj.leu.2404190

- (33) Chen J, Cao Z, Guan J (2018) SHP2 inhibitor PHPS1 protects against atherosclerosis by inhibiting smooth muscle cell proliferation. *BMC Cardiovasc Disord* 18, 1: 72, doi: 10.1186/s12872-018-0816-2
- (34) Clarke R, Halsey J, Lewington S, Lonn E, Armitage J, Manson JE, Bønaa KH, Spence JD, Nygård O, Jamison R, Gaziano JM, Guarino P, Bennett D, Mir F, Peto R, Collins R (2010) Effects of lowering homocysteine levels with B vitamins on cardiovascular disease, cancer, and cause-specific mortality: Meta-analysis of 8 randomized trials involving 37 485 individuals. *Arch Intern Med* 170, 18: 1622–1631, doi: 10.1001/archinternmed.2010.348
- (35) Collaboration TERF (2010) Diabetes mellitus, fasting blood glucose concentration, and risk of vascular disease: a collaborative meta-analysis of 102 prospective studies. *Lancet* 375, 9733: 2215–2222, doi: 10.1016/S0140-6736(10)60484-9
- (36) Cominacini L, Rigoni A, Pasini AF, Garbin U, Davoli A, Campagnola M, Pastorino AM, Lo Cascio V, Sawamura T (2001) The binding of oxidized low density lipoprotein (ox-LDL) to ox-LDL receptor-1 reduces the intracellular concentration of nitric oxide in endothelial cells through an increased production of superoxide. *J Biol Chem* 276, 17: 13750–13755, doi: 10.1074/jbc.M010612200
- (37) Cory G (2011) Scratch-wound assay. *Methods Mol Biol* 769: 25–30, doi: 10.1007/978-1-61779-207-6\_2
- (38) Cros J, Cagnard N, Woollard K, Patey N, Zhang S-Y, Senechal B, Puel A, Biswas SK, Moshous D, Picard C, Jais J-P, D'Cruz D, Casanova J-L, Trouillet C, Geissmann F (2010) Human CD14<sup>dim</sup> monocytes patrol and sense nucleic acids and viruses via TLR7 and TLR8 receptors. *Immunity* 33, 3: 375–386, doi: 10.1016/j.immuni.2010.08.012
- (39) Cross JL, Kott K, Miletic T, Johnson P (2008) CD45 regulates TLR-induced proinflammatory cytokine and IFN- $\beta$  secretion in dendritic cells. *J Immunol* 180, 12: 8020–8029, doi: 10.4049/jimmunol.180.12.8020
- (40) Crowl JT, Gray EE, Pestal K, Volkman HE, Stetson DB (2017) Intracellular Nucleic Acid Detection in Autoimmunity. *Annu Rev Immunol* 35: 313–336, doi: 10.1146/annurev-immunol-051116-052331
- (41) D'Agostino S, Lanzillotta D, Varano M, Botta C, Baldrini A, Bilotta A, Scalise S, Dattilo V, Amato R, Gaudio E, Paduano F, Palmieri C, Iuliano R, Perrotti N, Indiveri C, Fusco A, Gaspari M, Trapasso F (2018) The receptor protein tyrosine phosphatase PTPRJ negatively modulates the CD98hc oncoprotein in lung cancer cells. *Oncotarget* 9, 34: 23334–23348, doi: 10.18632/oncotarget.25101
- (42) Dai X-M, Ryan GR, Hapel AJ, Dominguez MG, Russell RG, Kapp S, Sylvestre V, Stanley ER (2002) Targeted disruption of the mouse colony-stimulating factor 1 receptor gene results in osteopetrosis, mononuclear phagocyte deficiency, increased primitive progenitor cell frequencies, and reproductive defects. *Blood* 99, 1: 111–120, doi: 10.1182/blood.v99.1.111
- (43) Dalton DK, Pitts-Meek S, Keshav S, Figari IS, Bradley A, Stewart TA (1993) Multiple defects of immune cell function in mice with disrupted interferon- $\gamma$  genes. *Science* 259, 5102: 1739–1742, doi: 10.1126/science.8456300
- (44) Dave RK, Dinger ME, Andrew M, Askarian-Amiri M, Hume DA, Kellie S (2013) Regulated expression of PTPRJ/CD148 and an antisense long noncoding RNA in macrophages by proinflammatory stimuli. *PLoS One* 8, 6: e68306, doi: 10.1371/journal.pone.0068306
- (45) Dave RK, Hume DA, Elsegood C, Kellie S (2009) CD148/DEP-1 association with areas of cytoskeletal organisation in macrophages. *Exp Cell Res* 315, 10: 1734–1744, doi: 10.1016/j.yexcr.2009.02.023
- (46) Dave RK, Naylor AJ, Young SP, Bayley R, Hardie DL, Haworth O, Rider DA, Cook AD, Buckley CD, Kellie S (2013) Differential expression of CD148 on leukocyte subsets in inflammatory arthritis. *Arthritis Res Ther* 15, 5: R108, doi: 10.1186/ar4288
- (47) Davies MJ (2000) The pathophysiology of acute coronary syndromes. *Heart* 83, 3: 361–366, doi: 10.1136/heart.83.3.361

- (48) Dhar A, Dhar I, Bhat A, Desai KM (2016) Alagebrium attenuates methylglyoxal induced oxidative stress and AGE formation in H9C2 cardiac myocytes. *Life Sci* 146: 8–14, doi: 10.1016/j.lfs.2016.01.006
- (49) Dhar I, Dhar A, Wu L, Desai KM (2014) Methylglyoxal, a reactive glucose metabolite, increases renin angiotensin aldosterone and blood pressure in male Sprague-Dawley rats. *Am J Hypertens* 27, 3: 308–316, doi: 10.1093/ajh/hpt281
- (50) Digenio A, Pham NC, Watts LM, Morgan ES, Jung SW, Baker BF, Geary RS, Bhanot S (2018) Antisense Inhibition of Protein Tyrosine Phosphatase 1B With IONIS-PTP-1BRx Improves Insulin Sensitivity and Reduces Weight in Overweight Patients With Type 2 Diabetes. *Diabetes Care* 41, 4: 807–814, doi: 10.2337/dc17-2132
- (51) Donath MY, Meier DT, Böni-Schnetzler M (2019) Inflammation in the Pathophysiology and Therapy of Cardiometabolic Disease. *Endocr Rev* 40, 4: 1080–1091, doi: 10.1210/er.2019-00002
- (52) Dorenkamp M, Müller JP, Shanmuganathan KS, Schulten H, Müller N, Löffler I, Müller UA, Wolf G, Böhmer F-D, Godfrey R, Waltenberger J (2018) Hyperglycaemia-induced methylglyoxal accumulation potentiates VEGF resistance of diabetic monocytes through the aberrant activation of tyrosine phosphatase SHP-2/SRC kinase signalling axis. *Sci Rep* 8, 1: 14684, doi: 10.1038/s41598-018-33014-9
- (53) Dorrington MG, Fraser IDC (2019) NF- $\kappa$ B Signaling in Macrophages: Dynamics, Crosstalk, and Signal Integration. *Front Immunol* 10: 705, doi: 10.3389/fimmu.2019.00705
- (54) Dwyer AR, Mouchemore KA, Steer JH, Sunderland AJ, Sampaio NG, Greenland EL, Joyce DA, Pixley FJ (2016) Src family kinase expression and subcellular localization in macrophages: implications for their role in CSF-1-induced macrophage migration. *J Leukoc Biol* 100, 1: 163–175, doi: 10.1189/jlb.2A0815-344RR
- (55) Dykxhoorn DM, Lieberman J (2005) The silent revolution: RNA interference as basic biology, research tool, and therapeutic. *Annu Rev Med* 56: 401–423, doi: 10.1146/annurev.med.56.082103.104606
- (56) Ebert RH, Florey HW (1939) The Extravascular Development of the Monocyte Observed In vivo. *Br J Exp Pathol* 20, 4: 342–356, <https://www.ncbi.nlm.nih.gov/pmc/articles/PMC2065374/pdf/brjexpathol00196-0047.pdf>
- (57) Elbashir SM, Harborth J, Lendeckel W, Yalcin A, Weber K, Tuschl T (2001) Duplexes of 21-nucleotide RNAs mediate RNA interference in cultured mammalian cells. *Nature* 411, 6836: 494–498, doi: 10.1038/35078107
- (58) Fernández GC, Ramos MV, Gómez SA, Dran GI, Exeni R, Alduncín M, Grimoldi I, Vallejo G, Elías-Costa C, Isturiz MA, Palermo MS (2005) Differential expression of function-related antigens on blood monocytes in children with hemolytic uremic syndrome. *J Leukoc Biol* 78, 4: 853–861, doi: 10.1189/jlb.0505251
- (59) Festa A, D'Agostino R, Howard G, Mykkänen L, Tracy RP, Haffner SM (2000) Chronic subclinical inflammation as part of the insulin resistance syndrome: the Insulin Resistance Atherosclerosis Study (IRAS). *Circulation* 102, 1: 42–47, doi: 10.1161/01.cir.102.1.42
- (60) Fingerle G, Pforte A, Passlick B, Blumenstein M, Strobel M, Ziegler-Heitbrock HW (1993) The novel subset of CD14<sup>+</sup>/CD16<sup>+</sup> blood monocytes is expanded in sepsis patients. *Blood* 82, 10: 3170–3176, doi: 10.1182/blood.V82.10.3170.3170
- (61) Fire A, Xu S, Montgomery MK, Kostas SA, Driver SE, Mello CC (1998) Potent and specific genetic interference by double-stranded RNA in *Caenorhabditis elegans*. *Nature* 391, 6669: 806–811, doi: 10.1038/35888
- (62) Fournier P, Dussault S, Fusco A, Rivard A, Royal I (2016) Tyrosine Phosphatase PTPRJ/DEP-1 Is an Essential Promoter of Vascular Permeability, Angiogenesis, and Tumor Progression. *Cancer Res* 76, 17: 5080–5091, doi: 10.1158/0008-5472.CAN-16-1071

- (63) Fournier P, Viallard C, Dejda A, Sapieha P, Larrivée B, Royal I (2020) The protein tyrosine phosphatase PTPRJ/DEP-1 contributes to the regulation of the Notch-signaling pathway and sprouting angiogenesis. *Angiogenesis* 23, 2: 145–157, doi: 10.1007/s10456-019-09683-z
- (64) Fowler S, Shio H, Haley NJ (1979) Characterization of lipid-laden aortic cells from cholesterol-fed rabbits. IV. Investigation of macrophage-like properties of aortic cell populations. *Lab Invest* 41, 4: 372–378. PMID: 491545
- (65) Fruchart J-C, Nierman MC, Stroes ESG, Kastelein JJP, Duriez P (2004) New risk factors for atherosclerosis and patient risk assessment. *Circulation* 109, 23 Suppl 1: III15-9, doi: 10.1161/01.CIR.0000131513.33892.5b
- (66) Ganjifrockwala F, Joseph J, George G (2016) Serum Oxidized LDL Levels in Type 2 Diabetic Patients with Retinopathy in Mthatha Region of the Eastern Cape Province of South Africa. *Oxid Med Cell Longev* 2016: 2063103, doi: 10.1155/2016/2063103
- (67) Gao S, Zhao D, Wang M, Zhao F, Han X, Qi Y, Liu J (2017) Association Between Circulating Oxidized LDL and Atherosclerotic Cardiovascular Disease: A Meta-analysis of Observational Studies. *Can J Cardiol* 33, 12: 1624–1632, doi: 10.1016/j.cjca.2017.07.015
- (68) Gautier EL, Shay T, Miller J, Greter M, Jakubzick C, Ivanov S, Helft J, Chow A, Elpek KG, Gordonov S, Mazloom AR, Ma'ayan A, Chua W-J, Hansen TH, Turley SJ, Merad M, Randolph GJ (2012) Gene-expression profiles and transcriptional regulatory pathways that underlie the identity and diversity of mouse tissue macrophages. *Nat Immunol* 13, 11: 1118–1128, doi: 10.1038/ni.2419
- (69) Gayà A, Pirotto F, Palou E, Autschbach F, Del Pozo V, Solé J, Serra-Pages C (1999) CD148, a new membrane tyrosine phosphatase involved in leukocyte function. *Leuk Lymphoma* 35, 3-4: 237–243, doi: 10.3109/10428199909145726
- (70) Geissmann F, Jung S, Littman DR (2003) Blood monocytes consist of two principal subsets with distinct migratory properties. *Immunity* 19, 1: 71–82, doi: 10.1016/s1074-7613(03)00174-2
- (71) Geissmann F, Manz MG, Jung S, Sieweke MH, Merad M, Ley K (2010) Development of monocytes, macrophages, and dendritic cells. *Science* 327, 5966: 656–661, doi: 10.1126/science.1178331
- (72) Gerrity RG (1981) The role of the monocyte in atherogenesis: I. Transition of blood-borne monocytes into foam cells in fatty lesions. *Am J Pathol* 103, 2: 181–190. PMID: 7234961
- (73) Gerrity RG (1981) The role of the monocyte in atherogenesis: II. Migration of foam cells from atherosclerotic lesions. *Am J Pathol* 103, 2: 191–200. PMID: 7234962
- (74) Gerrity RG, Naito HK (1980) Lipid clearance from fatty streak lesions by foam cell migration. *Artery* 8, 3: 215–219. PMID: 7213031
- (75) Ginhoux F, Greter M, Leboeuf M, Nandi S, See P, Gokhan S, Mehler MF, Conway SJ, Ng LG, Stanley ER, Samokhvalov IM, Merad M (2010) Fate mapping analysis reveals that adult microglia derive from primitive macrophages. *Science* 330, 6005: 841–845, doi: 10.1126/science.1194637
- (76) Ginhoux F, Guilliams M (2016) Tissue-Resident Macrophage Ontogeny and Homeostasis. *Immunity* 44, 3: 439–449, doi: 10.1016/j.immuni.2016.02.024
- (77) Godfrey R, Arora D, Bauer R, Stopp S, Müller JP, Heinrich T, Böhmer S-A, Dagnell M, Schnetzke U, Scholl S, Östman A, Böhmer F-D (2012) Cell transformation by FLT3 ITD in acute myeloid leukemia involves oxidative inactivation of the tumor suppressor protein-tyrosine phosphatase DEP-1/PTPRJ. *Blood* 119, 19: 4499–4511, doi: 10.1182/blood-2011-02-336446
- (78) Goossens P, Gijbels MJJ, Zerneck A, Eijgelaar W, Vergouwe MN, van der Made I, Vanderlocht J, Beckers L, Buurman WA, Daemen MJAP, Kalinke U, Weber C, Lutgens E, Winther MPJ de (2010) Myeloid type I interferon signaling promotes atherosclerosis by stimulating macrophage recruitment to lesions. *Cell Metab* 12, 2: 142–153, doi: 10.1016/j.cmet.2010.06.008
- (79) Gordon S (1998) The role of the macrophage in immune regulation. *Res Immunol* 149, 7-8: 685–688, doi: 10.1016/s0923-2494(99)80039-x
- (80) Gordon S (2003) Alternative activation of macrophages. *Nat Rev Immunol* 3, 1: 23–35, doi: 10.1038/nri978

- (81) Gordon S, Plüddemann A (2017) Tissue macrophages: heterogeneity and functions. *BMC Biol* 15, 1: 53, doi: 10.1186/s12915-017-0392-4
- (82) Gordon S, Taylor PR (2005) Monocyte and macrophage heterogeneity. *Nat Rev Immunol* 5, 12: 953–964, doi: 10.1038/nri1733
- (83) Grazia Lampugnani M, Zanetti A, Corada M, Takahashi T, Balconi G, Breviario F, Orsenigo F, Cattelino A, Kemler R, Daniel TO, Dejana E (2003) Contact inhibition of VEGF-induced proliferation requires vascular endothelial cadherin, beta-catenin, and the phosphatase DEP-1/CD148. *J Cell Biol* 161, 4: 793–804, doi: 10.1083/jcb.200209019
- (84) Greenberg AS, Obin MS (2006) Obesity and the role of adipose tissue in inflammation and metabolism. *Am J Clin Nutr* 83, 2: 461S–465S, doi: 10.1093/ajcn/83.2.461S
- (85) Gritte RB, Souza-Siqueira T, Masi LN, Germano JdF, Murata GM, Machado MCC, Pithon-Curi TC, Curi R, Soriano FG (2020) Reference Genes for Quantitative qPCR Analyses in Monocytes of Septic Patients, preprint, doi: 10.21203/rs.3.rs-34928/v1
- (86) Gurzov EN, Tran M, Fernandez-Rojo MA, Merry TL, Zhang X, Xu Y, Fukushima A, Waters MJ, Watt MJ, Andrikopoulos S, Neel BG, Tiganis T (2014) Hepatic oxidative stress promotes insulin-STAT-5 signaling and obesity by inactivating protein tyrosine phosphatase N2. *Cell Metab* 20, 1: 85–102, doi: 10.1016/j.cmet.2014.05.011
- (87) Hazen SL, Heinecke JW (1997) 3-Chlorotyrosine, a specific marker of myeloperoxidase-catalyzed oxidation, is markedly elevated in low density lipoprotein isolated from human atherosclerotic intima. *J Clin Invest* 99, 9: 2075–2081, doi: 10.1172/JCI119379
- (88) Heine GH, Ortiz A, Massy ZA, Lindholm B, Wiecek A, Martínez-Castelao A, Covic A, Goldsmith D, Süleymanlar G, London GM, Parati G, Sicari R, Zoccali C, Fliser D (2012) Monocyte subpopulations and cardiovascular risk in chronic kidney disease. *Nat Rev Nephrol* 8, 6: 362–369, doi: 10.1038/nrneph.2012.41
- (89) Hemling P, Zibrova D, Strutz J, Sohrabi Y, Desoye G, Schulten H, Findeisen H, Heller R, Godfrey R, Waltenberger J (2020) Hyperglycemia-induced endothelial dysfunction is alleviated by thioredoxin mimetic peptides through the restoration of VEGFR-2-induced responses and improved cell survival. *Int J Cardiol* 308: 73–81, doi: 10.1016/j.ijcard.2019.12.065
- (90) Herijgers N, Winther MP de, van Eck M, Havekes LM, Hofker MH, Hoogerbrugge PM, van Berkel TJ (2000) Effect of human scavenger receptor class A overexpression in bone marrow-derived cells on lipoprotein metabolism and atherosclerosis in low density lipoprotein receptor knockout mice. *J Lipid Res* 41, 9: 1402–1409. PMID: 10974047
- (91) Hermiston ML, Zikherman J, Zhu JW (2009) CD45, CD148, and Lyp/Pep: critical phosphatases regulating Src family kinase signaling networks in immune cells. *Immunol Rev* 228, 1: 288–311, doi: 10.1111/j.1600-065X.2008.00752.x
- (92) Hochreiter-Hufford A, Ravichandran KS (2013) Clearing the dead: apoptotic cell sensing, recognition, engulfment, and digestion. *Cold Spring Harb Perspect Biol* 5, 1: a008748, doi: 10.1101/cshperspect.a008748
- (93) Holsinger LJ, Ward K, Duffield B, Zachwieja J, Jallal B (2002) The transmembrane receptor protein tyrosine phosphatase DEP1 interacts with p120(ctn). *Oncogene* 21, 46: 7067–7076, doi: 10.1038/sj.onc.1205858
- (94) Holvoet P, Lee D-H, Steffes M, Gross M, Jacobs DR (2008) Association between circulating oxidized low-density lipoprotein and incidence of the metabolic syndrome. *JAMA* 299, 19: 2287–2293, doi: 10.1001/jama.299.19.2287
- (95) Honda H, Inazawa J, Nishida J, Yazaki Y, Hirai H (1994) Molecular cloning, characterization, and chromosomal localization of a novel protein-tyrosine phosphatase, HPTP etc. *Blood* 84, 12: 4186–4194. PMID: 7994032
- (96) Hopkinson-Woolley J, Hughes D, Gordon S, Martin P (1994) Macrophage recruitment during limb development and wound healing in the embryonic and foetal mouse. *J Cell Sci* 107 (Pt 5), 5: 1159–1167. PMID: 7929625

- (97) Hou H-A, Chou W-C, Lin L-I, Chen C-Y, Tang J-L, Tseng M-H, Huang C-F, Chiou R-J, Lee F-Y, Liu M-C, Tien H-F (2008) Characterization of acute myeloid leukemia with PTPN11 mutation: the mutation is closely associated with NPM1 mutation but inversely related to FLT3/ITD. *Leukemia* 22, 5: 1075–1078, doi: 10.1038/sj.leu.2405005
- (98) Hume DA (2006) The mononuclear phagocyte system. *Curr Opin Immunol* 18, 1: 49–53, doi: 10.1016/j.coi.2005.11.008
- (99) International Diabetes Federation (2019) *IDF Diabetes Atlas*, 9th edition. Brussels, Belgium, 9th edition, <http://www.diabetesatlas.org> [Retrieval date: 05.02.2022]
- (100) Isakov N (1997) Immunoreceptor tyrosine-based activation motif (ITAM), a unique module linking antigen and Fc receptors to their signaling cascades. *J Leukoc Biol* 61, 1: 6–16, doi: 10.1002/jlb.61.1.6
- (101) Jacob F, Guertler R, Naim S, Nixdorf S, Fedier A, Hacker NF, Heinzelmann-Schwarz V (2013) Careful selection of reference genes is required for reliable performance of RT-qPCR in human normal and cancer cell lines. *PLoS One* 8, 3: e59180, doi: 10.1371/journal.pone.0059180
- (102) Jandt E, Denner K, Kovalenko M, Ostman A, Böhmer F-D (2003) The protein-tyrosine phosphatase DEP-1 modulates growth factor-stimulated cell migration and cell-matrix adhesion. *Oncogene* 22, 27: 4175–4185, doi: 10.1038/sj.onc.1206652
- (103) Jenkins DJA, Dehghan M, Mente A, et al. (2021) Glycemic Index, Glycemic Load, and Cardiovascular Disease and Mortality. *N Engl J Med* 384, 14: 1312–1322, doi: 10.1056/NEJMoa2007123
- (104) Jenkins SJ, Ruckerl D, Cook PC, Jones LH, Finkelman FD, van Rooijen N, MacDonald AS, Allen JE (2011) Local macrophage proliferation, rather than recruitment from the blood, is a signature of TH2 inflammation. *Science* 332, 6035: 1284–1288, doi: 10.1126/science.1204351
- (105) Jensen K, Anderson JA, Glass EJ (2014) Comparison of small interfering RNA (siRNA) delivery into bovine monocyte-derived macrophages by transfection and electroporation. *Vet Immunol Immunopathol* 158, 3-4: 224–232, doi: 10.1016/j.vetimm.2014.02.002
- (106) Jones GE (2000) Cellular signaling in macrophage migration and chemotaxis. *J Leukoc Biol* 68, 5: 593–602, doi: 10.1189/jlb.68.5.593
- (107) Jovinge S, Ares MP, Kallin B, Nilsson J (1996) Human monocytes/macrophages release TNF-alpha in response to Ox-LDL. *Arterioscl Throm Vas* 16, 12: 1573–1579, doi: 10.1161/01.atv.16.12.1573
- (108) Kahn SE, Cooper ME, Del Prato S (2014) Pathophysiology and treatment of type 2 diabetes: perspectives on the past, present, and future. *Lancet* 383, 9922: 1068–1083, doi: 10.1016/S0140-6736(13)62154-6
- (109) Kahn SE, Prigeon RL, McCulloch DK, Boyko EJ, Bergman RN, Schwartz MW, Neifing JL, Ward WK, Beard JC, Palmer JP (1993) Quantification of the relationship between insulin sensitivity and beta-cell function in human subjects. Evidence for a hyperbolic function. *Diabetes* 42, 11: 1663–1672, doi: 10.2337/diab.42.11.1663
- (110) Kannel WB, McGee DL (1979) Diabetes and glucose tolerance as risk factors for cardiovascular disease: the Framingham study. *Diabetes Care* 2, 2: 120–126, doi: 10.2337/diacare.2.2.120
- (111) Kanters E, Pasparakis M, Gijbels MJJ, Vergouwe MN, Partouns-Hendriks I, Fijneman RJA, Clausen BE, Förster I, Kockx MM, Rajewsky K, Kraal G, Hofker MH, Winther MPJ de (2003) Inhibition of NF-kappaB activation in macrophages increases atherosclerosis in LDL receptor-deficient mice. *J Clin Invest* 112, 8: 1176–1185, doi: 10.1172/JCI18580
- (112) Karagyozov L, Godfrey R, Böhmer S-A, Petermann A, Hölters S, Ostman A, Böhmer F-D (2008) The structure of the 5'-end of the protein-tyrosine phosphatase PTPRJ mRNA reveals a novel mechanism for translation attenuation. *Nucleic Acids Res* 36, 13: 4443–4453, doi: 10.1093/nar/gkn391
- (113) Karin M (1999) How NF-kappaB is activated: the role of the IkappaB kinase (IKK) complex. *Oncogene* 18, 49: 6867–6874, doi: 10.1038/sj.onc.1203219
- (114) Karmali KN, Lloyd-Jones DM, Berendsen MA, Goff DC, Sanghavi DM, Brown NC, Korenovska L, Huffman MD (2016) *Drugs for Primary Prevention of Atherosclerotic Cardiovascular Disease*:

An Overview of Systematic Reviews. *JAMA Cardiol* 1, 3: 341–349, doi: 10.1001/jamacardio.2016.0218

- (115) Kawai T, Akira S (2005) Toll-like receptor downstream signaling. *Arthritis Res Ther* 7, 1: 12–19, doi: 10.1186/ar1469
- (116) Kawamura M, Heinecke JW, Chait A (1994) Pathophysiological concentrations of glucose promote oxidative modification of low density lipoprotein by a superoxide-dependent pathway. *J Clin Invest* 94, 2: 771–778, doi: 10.1172/JCI117396
- (117) Keller A-A, Maeß MB, Schnoor M, Scheiding B, Lorkowski S (2018) Transfecting Macrophages. *Methods Mol Biol* 1784: 187–195, doi: 10.1007/978-1-4939-7837-3\_18
- (118) Kellie S, Craggs G, Bird IN, Jones GE (2004) The tyrosine phosphatase DEP-1 induces cytoskeletal rearrangements, aberrant cell-substratum interactions and a reduction in cell proliferation. *J Cell Sci* 117, Pt 4: 609–618, doi: 10.1242/jcs.00879
- (119) Kelly KR, Haus JM, Solomon TPJ, Patrick-Melin AJ, Cook M, Rocco M, Barkoukis H, Kirwan JP (2011) A low-glycemic index diet and exercise intervention reduces TNF(alpha) in isolated mononuclear cells of older, obese adults. *J Nutr* 141, 6: 1089–1094, doi: 10.3945/jn.111.139964
- (120) Khan MA, Schultz S, Othman A, Fleming T, Lebrón-Galán R, Rades D, Clemente D, Nawroth PP, Schwaninger M (2016) Hyperglycemia in Stroke Impairs Polarization of Monocytes/Macrophages to a Protective Noninflammatory Cell Type. *J Neurosci* 36, 36: 9313–9325, doi: 10.1523/JNEUROSCI.0473-16.2016
- (121) Kim TK, Eberwine JH (2010) Mammalian cell transfection: the present and the future. *Anal Bioanal Chem* 397, 8: 3173–3178, doi: 10.1007/s00216-010-3821-6
- (122) Kovalenko M, Denner K, Sandström J, Persson C, Gross S, Jandt E, Vilella R, Böhmer F, Ostman A (2000) Site-selective dephosphorylation of the platelet-derived growth factor beta-receptor by the receptor-like protein-tyrosine phosphatase DEP-1. *J Biol Chem* 275, 21: 16219–16226, doi: 10.1074/jbc.275.21.16219
- (123) Kozicky LK, Sly LM (2015) Phosphatase regulation of macrophage activation. *Semin Immunol* 27, 4: 276–285, doi: 10.1016/j.smim.2015.07.001
- (124) Król M, Majchrzak K, Mucha J, Homa A, Bulkowska M, Jakubowska A, Karwicka M, Pawłowski KM, Motyl T (2013) CSF-1R as an inhibitor of apoptosis and promoter of proliferation, migration and invasion of canine mammary cancer cells. *BMC Vet Res* 9: 65, doi: 10.1186/1746-6148-9-65
- (125) Krüger J, Brachs S, Trappiel M, Kintscher U, Meyborg H, Wellnhofer E, Thöne-Reineke C, Stawowy P, Östman A, Birkenfeld AL, Böhmer FD, Kappert K (2015) Enhanced insulin signaling in density-enhanced phosphatase-1 (DEP-1) knockout mice. *Mol Metab* 4, 4: 325–336, doi: 10.1016/j.molmet.2015.02.001
- (126) Krüger J, Trappiel M, Dagnell M, Stawowy P, Meyborg H, Böhm C, Bhanot S, Ostman A, Kintscher U, Kappert K (2013) Targeting density-enhanced phosphatase-1 (DEP-1) with antisense oligonucleotides improves the metabolic phenotype in high-fat diet-fed mice. *Cell Commun Signal* 11, 1: 49, doi: 10.1186/1478-811X-11-49
- (127) Kruskal WH, Wallis WA (1952) Use of Ranks in One-Criterion Variance Analysis. *J Am Stat Assoc* 47, 260: 583, doi: 10.2307/2280779
- (128) Krychtiuk KA, Kastl SP, Hofbauer SL, Wonnerth A, Goliasch G, Ozsvar-Kozma M, Katsaros KM, Maurer G, Huber K, Dostal E, Binder CJ, Pfaffenberger S, Oravec S, Wojta J, Speidl WS (2015) Monocyte subset distribution in patients with stable atherosclerosis and elevated levels of lipoprotein(a). *J Clin Lipidol* 9, 4: 533–541, doi: 10.1016/j.jacl.2015.04.005
- (129) La Fuente-García MA de, Nicolás JM, Freed JH, Palou E, Thomas AP, Vilella R, Vives J, Gayá A (1998) CD148 is a membrane protein tyrosine phosphatase present in all hematopoietic lineages and is involved in signal transduction on lymphocytes. *Blood* 91, 8: 2800–2809. PMID: 9531590
- (130) Laemmli UK (1970) Cleavage of structural proteins during the assembly of the head of bacteriophage T4. *Nature* 227, 5259: 680–685, doi: 10.1038/227680a0



- (131) Lai Y, Xu X, Zhu Z, Hua Z (2018) Highly efficient siRNA transfection in macrophages using apoptotic body-mimic Ca-PS lipopolyplex. *Int J Nanomedicine* 13: 6603–6623, doi: 10.2147/IJN.S176991
- (132) Lam NT, Covey SD, Lewis JT, Oosman S, Webber T, Hsu EC, Cheung AT, Kieffer TJ (2006) Leptin resistance following over-expression of protein tyrosine phosphatase 1B in liver. *J Mol Endocrinol* 36, 1: 163–174, doi: 10.1677/jme.1.01937
- (133) Lampugnani MG, Orsenigo F, Gagliani MC, Tacchetti C, Dejana E (2006) Vascular endothelial cadherin controls VEGFR-2 internalization and signaling from intracellular compartments. *J Cell Biol* 174, 4: 593–604, doi: 10.1083/jcb.200602080
- (134) Landsman L, Bar-On L, Zerneck A, Kim K-W, Krauthgamer R, Shagdarsuren E, Lira SA, Weissman IL, Weber C, Jung S (2009) CX3CR1 is required for monocyte homeostasis and atherogenesis by promoting cell survival. *Blood* 113, 4: 963–972, doi: 10.1182/blood-2008-07-170787
- (135) Lara-Guzmán OJ, Gil-Izquierdo Á, Medina S, Osorio E, Álvarez-Quintero R, Zuluaga N, Oger C, Galano J-M, Durand T, Muñoz-Durango K (2018) Oxidized LDL triggers changes in oxidative stress and inflammatory biomarkers in human macrophages. *Redox Biol* 15: 1–11, doi: 10.1016/j.redox.2017.11.017
- (136) Lawrence T (2009) The nuclear factor NF-kappaB pathway in inflammation. *Cold Spring Harb Perspect Biol* 1, 6: a001651, doi: 10.1101/cshperspect.a001651
- (137) Le Pera I, Iuliano R, Florio T, Susini C, Trapasso F, Santoro M, Chiariotti L, Schettini G, Viglietto G, Fusco A (2005) The rat tyrosine phosphatase eta increases cell adhesion by activating c-Src through dephosphorylation of its inhibitory phosphotyrosine residue. *Oncogene* 24, 19: 3187–3195, doi: 10.1038/sj.onc.1208510
- (138) Lee AW, States DJ (2000) Both src-dependent and -independent mechanisms mediate phosphatidylinositol 3-kinase regulation of colony-stimulating factor 1-activated mitogen-activated protein kinases in myeloid progenitors. *Mol Cell Biol* 20, 18: 6779–6798, doi: 10.1128/MCB.20.18.6779-6798.2000
- (139) Lee J, Tam H, Adler L, Istad-Minnihan A, Macaubas C, Mellins ED (2017) The MHC class II antigen presentation pathway in human monocytes differs by subset and is regulated by cytokines. *PLoS One* 12, 8: e0183594, doi: 10.1371/journal.pone.0183594
- (140) Lee M-TM, Coburn GA, McClure MO, Cullen BR (2003) Inhibition of human immunodeficiency virus type 1 replication in primary macrophages by using Tat- or CCR5-specific small interfering RNAs expressed from a lentivirus vector. *J Virol* 77, 22: 11964–11972, doi: 10.1128/jvi.77.22.11964-11972.2003
- (141) Levitan I, Volkov S, Subbaiah PV (2010) Oxidized LDL: diversity, patterns of recognition, and pathophysiology. *Antioxid Redox Signal* 13, 1: 39–75, doi: 10.1089/ars.2009.2733
- (142) Li S, Wang L, Berman MA, Zhang Y, Dorf ME (2006) RNAi screen in mouse astrocytes identifies phosphatases that regulate NF-kappaB signaling. *Mol Cell* 24, 4: 497–509, doi: 10.1016/j.molcel.2006.10.015
- (143) Libby P, Ridker PM, Hansson GK (2011) Progress and challenges in translating the biology of atherosclerosis. *Nature* 473, 7347: 317–325, doi: 10.1038/nature10146
- (144) Lietzén N, Ohman T, Rintahaka J, Julkunen I, Aittokallio T, Matikainen S, Nyman TA (2011) Quantitative subcellular proteome and secretome profiling of influenza A virus-infected human primary macrophages. *PLoS Pathog* 7, 5: e1001340, doi: 10.1371/journal.ppat.1001340
- (145) Lin J, Zhu JW, Baker JE, Weiss A (2004) Regulated expression of the receptor-like tyrosine phosphatase CD148 on hemopoietic cells. *J Immunol* 173, 4: 2324–2330, doi: 10.4049/jimmunol.173.4.2324
- (146) Linton MF, Fazio S (2001) Class A scavenger receptors, macrophages, and atherosclerosis. *Curr Opin Lipidol* 12, 5: 489–495, doi: 10.1097/00041433-200110000-00003

- (147) Liu B, Sun L, Liu Q, Gong C, Yao Y, Lv X, Lin L, Yao H, Su F, Li D, Zeng M, Song E (2015) A cytoplasmic NF- $\kappa$ B interacting long noncoding RNA blocks I $\kappa$ B phosphorylation and suppresses breast cancer metastasis. *Cancer Cell* 27, 3: 370–381, doi: 10.1016/j.ccell.2015.02.004
- (148) Lowell CA (2011) Src-family and Syk kinases in activating and inhibitory pathways in innate immune cells: signaling cross talk. *Cold Spring Harb Perspect Biol* 3, 3: 1–16, doi: 10.1101/cshperspect.a002352
- (149) Lowry OH, Rosebrough NJ, Farr AL, Randall RJ (1951) Protein measurement with the Folin phenol reagent. *J Biol Chem* 193, 1: 265–275, doi: 10.1074/jbc.H118.005121
- (150) Luca C de, Olefsky JM (2008) Inflammation and insulin resistance. *FEBS Lett* 582, 1: 97–105, doi: 10.1016/j.febslet.2007.11.057
- (151) Lunardi C, Bason C, Leandri M, Navone R, Lestani M, Millo E, Benatti U, Cilli M, Beri R, Corrocher R, Puccetti A (2002) Autoantibodies to inner ear and endothelial antigens in Cogan's syndrome. *Lancet* 360, 9337: 915–921, doi: 10.1016/S0140-6736(02)11028-2
- (152) Luo X, Yang S, Zhou C, Pan F, Li Q, Ma S (2015) MicroRNA-328 enhances cellular motility through posttranscriptional regulation of PTPRJ in human hepatocellular carcinoma. *OncoTargets Ther* 8: 3159–3167, doi: 10.2147/OTT.S93056
- (153) Lusis AJ (2000) Atherosclerosis. *Nature* 407, 6801: 233–241, doi: 10.1038/35025203
- (154) Mackaness GB (1962) Cellular resistance to infection. *J Exp Med* 116: 381–406, doi: 10.1084/jem.116.3.381
- (155) Maeß MB, Wittig B, Lorkowski S (2014) Highly efficient transfection of human THP-1 macrophages by nucleofection. *J Vis Exp*, 91: e51960, doi: 10.3791/51960
- (156) Mann HB, Whitney DR (1947) On a Test of Whether one of Two Random Variables is Stochastically Larger than the Other. *Ann Math Statist* 18, 1: 50–60, doi: 10.1214/aoms/1177730491
- (157) Mantovani A, Sica A, Sozzani S, Allavena P, Vecchi A, Locati M (2004) The chemokine system in diverse forms of macrophage activation and polarization. *Trends Immunol* 25, 12: 677–686, doi: 10.1016/j.it.2004.09.015
- (158) Marconi C, Di Buduo CA, LeVine K, Barozzi S, Faleschini M, Bozzi V, Palombo F, McKinstry S, Lassandro G, Giordano P, Noris P, Balduini CL, Savoia A, Balduini A, Pippucci T, Seri M, Katsanis N, Pecci A (2019) Loss-of-function mutations in PTPRJ cause a new form of inherited thrombocytopenia. *Blood* 133, 12: 1346–1357, doi: 10.1182/blood-2018-07-859496
- (159) Martinez FO, Gordon S (2014) The M1 and M2 paradigm of macrophage activation: time for reassessment. *F1000Prime Rep* 6: 13, doi: 10.12703/P6-13
- (160) Maxfield FR, Tabas I (2005) Role of cholesterol and lipid organization in disease. *Nature* 438, 7068: 612–621, doi: 10.1038/nature04399
- (161) McLellan AC, Thornalley PJ, Benn J, Sonksen PH (1994) Glyoxalase system in clinical diabetes mellitus and correlation with diabetic complications. *Clin Sci* 87, 1: 21–29, doi: 10.1042/cs0870021
- (162) Mitchell J, Kim SJ, Seelmann A, Veit B, Shepard B, Im E, Rhee SH (2018) Src family kinase tyrosine phosphorylates Toll-like receptor 4 to dissociate MyD88 and Mal/Tirap, suppressing LPS-induced inflammatory responses. *Biochem Pharmacol* 147: 119–127, doi: 10.1016/j.bcp.2017.11.015
- (163) Mizutani S, Boettiger D, Temin HM (1970) A DNA-dependent DNA polymerase and a DNA endonuclease in virions of Rous sarcoma virus. *Nature* 228, 5270: 424–427, doi: 10.1038/228424a0
- (164) Modolell M, Corraliza IM, Link F, Soler G, Eichmann K (1995) Reciprocal regulation of the nitric oxide synthase/arginase balance in mouse bone marrow-derived macrophages by TH1 and TH2 cytokines. *Eur J Immunol* 25, 4: 1101–1104, doi: 10.1002/eji.1830250436
- (165) Moganti K, Li F, Schmuttmaier C, Riemann S, Klüter H, Gratchev A, Harmsen MC, Kzhyshkowska J (2017) Hyperglycemia induces mixed M1/M2 cytokine profile in primary human monocyte-derived macrophages. *Immunobiology* 222, 10: 952–959, doi: 10.1016/j.imbio.2016.07.006

- (166) Moore KJ, Freeman MW (2006) Scavenger receptors in atherosclerosis: beyond lipid uptake. *Arterioscl Throm Vas* 26, 8: 1702–1711, doi: 10.1161/01.ATV.0000229218.97976.43
- (167) Moore KJ, Sheedy FJ, Fisher EA (2013) Macrophages in atherosclerosis: a dynamic balance: A dynamic balance. *Nat Rev Immunol* 13, 10: 709–721, doi: 10.1038/nri3520
- (168) Moraru A, Wiederstein J, Pfaff D, Fleming T, Miller AK, Nawroth P, Teleanu AA (2018) Elevated Levels of the Reactive Metabolite Methylglyoxal Recapitulate Progression of Type 2 Diabetes. *Cell Metab* 27, 4: 926–934.e8, doi: 10.1016/j.cmet.2018.02.003
- (169) Mosser DM, Edwards JP (2008) Exploring the full spectrum of macrophage activation. *Nat Rev Immunol* 8, 12: 958–969, doi: 10.1038/nri2448
- (170) Murphy JE, Tedbury PR, Homer-Vanniasinkam S, Walker JH, Ponnambalam S (2005) Biochemistry and cell biology of mammalian scavenger receptors. *Atherosclerosis* 182, 1: 1–15, doi: 10.1016/j.atherosclerosis.2005.03.036
- (171) Murray PJ, Allen JE, Biswas SK, et al. (2014) Macrophage activation and polarization: nomenclature and experimental guidelines. *Immunity* 41, 1: 14–20, doi: 10.1016/j.immuni.2014.06.008
- (172) Nagy Z, Mori J, Ivanova V-S, Mazharian A, Senis YA (2020) Interplay between the tyrosine kinases Chk and Csk and phosphatase PTPRJ is critical for regulating platelets in mice. *Blood* 135, 18: 1574–1587, doi: 10.1182/blood.2019002848
- (173) Naito M, Takahashi K, Nishikawa S (1990) Development, differentiation, and maturation of macrophages in the fetal mouse liver. *J Leukoc Biol* 48, 1: 27–37, doi: 10.1002/jlb.48.1.27
- (174) Nakhjavani M, Khalilzadeh O, Khajeali L, Esteghamati A, Morteza A, Jamali A, Dadkhaipour S (2010) Serum oxidized-LDL is associated with diabetes duration independent of maintaining optimized levels of LDL-cholesterol. *Lipids* 45, 4: 321–327, doi: 10.1007/s11745-010-3401-8
- (175) Nicholson AC, Frieda S, Pearce A, Silverstein RL (1995) Oxidized LDL binds to CD36 on human monocyte-derived macrophages and transfected cell lines. Evidence implicating the lipid moiety of the lipoprotein as the binding site. *Arterioscl Throm Vas* 15, 2: 269–275, doi: 10.1161/01.atv.15.2.269
- (176) Njajou OT, Kanaya AM, Holvoet P, Connelly S, Strotmeyer ES, Harris TB, Cummings SR, Hsueh W-C (2009) Association between oxidized LDL, obesity and type 2 diabetes in a population-based cohort, the Health, Aging and Body Composition Study. *Diabetes Metab Res Rev* 25, 8: 733–739, doi: 10.1002/dmrr.1011
- (177) Nordestgaard BG, Chapman MJ, Ray K, Borén J, Andreotti F, Watts GF, Ginsberg H, Amarencu P, Catapano A, Descamps OS, Fisher E, Kovanen PT, Kuivenhoven JA, Lesnik P, Masana L, Reiner Z, Taskinen M-R, Tokgözoğlu L, Tybjaerg-Hansen A (2010) Lipoprotein(a) as a cardiovascular risk factor: current status. *Eur Heart J* 31, 23: 2844–2853, doi: 10.1093/eurheartj/ehq386
- (178) Ogurtsova K, da Rocha Fernandes JD, Huang Y, Linnenkamp U, Guariguata L, Cho NH, Cavan D, Shaw JE, Makaroff LE (2017) IDF Diabetes Atlas: Global estimates for the prevalence of diabetes for 2015 and 2040: Global estimates for the prevalence of diabetes for 2015 and 2040. *Diabetes Res Clin Pract* 128: 40–50, doi: 10.1016/j.diabres.2017.03.024
- (179) Okigaki M, Davis C, Falasca M, Harroch S, Felsenfeld DP, Sheetz MP, Schlessinger J (2003) Pyk2 regulates multiple signaling events crucial for macrophage morphology and migration. *PNAS* 100, 19: 10740–10745, doi: 10.1073/pnas.1834348100
- (180) Osborne JM, Elzen N den, Lichanska AM, Costelloe EO, Yamada T, Cassady AI, Hume DA (1998) Murine DEP-1, a receptor protein tyrosine phosphatase, is expressed in macrophages and is regulated by CSF-1 and LPS. *J Leukoc Biol* 64, 5: 692–701, doi: 10.1002/jlb.64.5.692
- (181) Ostman A, Böhmer FD (2001) Regulation of receptor tyrosine kinase signaling by protein tyrosine phosphatases. *Trends Cell Biol* 11, 6: 258–266, doi: 10.1016/s0962-8924(01)01990-0
- (182) Ostman A, Yang Q, Tonks NK (1994) Expression of DEP-1, a receptor-like protein-tyrosine-phosphatase, is enhanced with increasing cell density. *PNAS* 91, 21: 9680–9684, doi: 10.1073/pnas.91.21.9680

- (183) Palka HL, Park M, Tonks NK (2003) Hepatocyte growth factor receptor tyrosine kinase met is a substrate of the receptor protein-tyrosine phosphatase DEP-1. *J Biol Chem* 278, 8: 5728–5735, doi: 10.1074/jbc.M210656200
- (184) Pardali E, Waltenberger J (2012) Monocyte function and trafficking in cardiovascular disease. *Thromb Haemost* 108, 5: 804–811, doi: 10.1160/TH12-04-0276
- (185) Park YM, Drazba JA, Vasanji A, Egelhoff T, Febbraio M, Silverstein RL (2012) Oxidized LDL/CD36 interaction induces loss of cell polarity and inhibits macrophage locomotion. *Mol Biol Cell* 23, 16: 3057–3068, doi: 10.1091/mbc.E11-12-1051
- (186) Patel AA, Zhang Y, Fullerton JN, Boelen L, Rongvaux A, Maini AA, Bigley V, Flavell RA, Gilroy DW, Asquith B, Macallan D, Yona S (2017) The fate and lifespan of human monocyte subsets in steady state and systemic inflammation. *J Exp Med* 214, 7: 1913–1923, doi: 10.1084/jem.20170355
- (187) Perdiguero EG, Geissmann F (2016) The development and maintenance of resident macrophages. *Nat Immunol* 17, 1: 2–8, doi: 10.1038/ni.3341
- (188) Persson C, Engström U, Mowbray SL, Ostman A (2002) Primary sequence determinants responsible for site-selective dephosphorylation of the PDGF beta-receptor by the receptor-like protein tyrosine phosphatase DEP-1. *FEBS Lett* 517, 1-3: 27–31, doi: 10.1016/s0014-5793(02)02570-x
- (189) Pfaffl MW (2001) A new mathematical model for relative quantification in real-time RT-PCR. *Nucleic Acids Res* 29, 9: e45, doi: 10.1093/nar/29.9.e45
- (190) Piercy J, Petrova S, Tchilian EZ, Beverley PCL (2006) CD45 negatively regulates tumour necrosis factor and interleukin-6 production in dendritic cells. *Immunology* 118, 2: 250–256, doi: 10.1111/j.1365-2567.2006.02363.x
- (191) Pirro M, Bagaglia F, Paoletti L, Razzi R, Mannarino MR (2008) Hypercholesterolemia-associated endothelial progenitor cell dysfunction. *Ther Adv Cardiovasc Dis* 2, 5: 329–339, doi: 10.1177/1753944708094769
- (192) Pixley FJ (2012) Macrophage Migration and Its Regulation by CSF-1. *Int J Cell Biol* 2012: 501962, doi: 10.1155/2012/501962
- (193) Pixley FJ, Lee PS, Condeelis JS, Stanley ER (2001) Protein tyrosine phosphatase phi regulates paxillin tyrosine phosphorylation and mediates colony-stimulating factor 1-induced morphological changes in macrophages. *Mol Cell Biol* 21, 5: 1795–1809, doi: 10.1128/MCB.21.5.1795-1809.2001
- (194) Pixley FJ, Stanley ER (2004) CSF-1 regulation of the wandering macrophage: complexity in action. *Trends Cell Biol* 14, 11: 628–638, doi: 10.1016/j.tcb.2004.09.016
- (195) Plüddemann A, Neyen C, Gordon S (2007) Macrophage scavenger receptors and host-derived ligands. *Methods* 43, 3: 207–217, doi: 10.1016/j.ymeth.2007.06.004
- (196) Porcheray F, Viaud S, Rimaniol A-C, Léone C, Samah B, Dereuddre-Bosquet N, Dormont D, Gras G (2005) Macrophage activation switching: an asset for the resolution of inflammation. *Clin Exp Immunol* 142, 3: 481–489, doi: 10.1111/j.1365-2249.2005.02934.x
- (197) Pradhan AD, Manson JE, Rifai N, Buring JE, Ridker PM (2001) C-reactive protein, interleukin 6, and risk of developing type 2 diabetes mellitus. *JAMA* 286, 3: 327–334, doi: 10.1001/jama.286.3.327
- (198) Qiao D, Li M, Pu J, Wang W, Zhu W, Liu H (2016) Loss of Protein Tyrosine Phosphatase Receptor J Expression Predicts an Aggressive Clinical Course in Patients with Esophageal Squamous Cell Carcinoma. *Pathol Oncol Res* 22, 3: 541–547, doi: 10.1007/s12253-015-0036-3
- (199) Rasheed Z, Akhtar N, Haqqi TM (2011) Advanced glycation end products induce the expression of interleukin-6 and interleukin-8 by receptor for advanced glycation end product-mediated activation of mitogen-activated protein kinases and nuclear factor- $\kappa$ B in human osteoarthritis chondrocytes. *Rheumatology* 50, 5: 838–851, doi: 10.1093/rheumatology/keq380
- (200) Ridker PM (2016) A Test in Context: High-Sensitivity C-Reactive Protein. *J Am Coll Cardiol* 67, 6: 712–723, doi: 10.1016/j.jacc.2015.11.037

- (201) Ridker PM, Everett BM, Thuren T, et al. (2017) Antiinflammatory Therapy with Canakinumab for Atherosclerotic Disease. *N Engl J Med* 377, 12: 1119–1131, doi: 10.1056/NEJMoa1707914
- (202) Ridley AJ (2015) Rho GTPase signalling in cell migration. *Curr Opin Cell Biol* 36: 103–112, doi: 10.1016/j.ceb.2015.08.005
- (203) Ririe KM, Rasmussen RP, Wittwer CT (1997) Product differentiation by analysis of DNA melting curves during the polymerase chain reaction. *Anal Biochem* 245, 2: 154–160, doi: 10.1006/abio.1996.9916
- (204) Robbins CS, Chudnovskiy A, Rauch PJ, Figueiredo J-L, Iwamoto Y, Gorbatov R, Eitzrodt M, Weber GF, Ueno T, van Rooijen N, Mulligan-Kehoe MJ, Libby P, Nahrendorf M, Pittet MJ, Weissleder R, Swirski FK (2012) Extramedullary hematopoiesis generates Ly-6C(high) monocytes that infiltrate atherosclerotic lesions. *Circulation* 125, 2: 364–374, doi: 10.1161/CIRCULATION-NAHA.111.061986
- (205) Robbins CS, Hilgendorf I, Weber GF, Theurl I, Iwamoto Y, Figueiredo J-L, Gorbatov R, Sukhova GK, Gerhardt LMS, Smyth D, Zavitz CCJ, Shikatani EA, Parsons M, van Rooijen N, Lin HY, Husain M, Libby P, Nahrendorf M, Weissleder R, Swirski FK (2013) Local proliferation dominates lesional macrophage accumulation in atherosclerosis. *Nat Med* 19, 9: 1166–1172, doi: 10.1038/nm.3258
- (206) Robertson AL, Holmes GR, Bojarczuk AN, et al. (2014) A zebrafish compound screen reveals modulation of neutrophil reverse migration as an anti-inflammatory mechanism. *Sci Transl Med* 6, 225: 225ra29, doi: 10.1126/scitranslmed.3007672
- (207) Ross R (1999) Atherosclerosis is an inflammatory disease. *Am Heart J* 138, 5: S419–S420, doi: 10.1016/S0002-8703(99)70266-8
- (208) Ross R, Glomset J, Harker L (1977) Response to injury and atherogenesis. *Am J Pathol* 86, 3: 675–684. PMID: 842616
- (209) Rougerie P, Miskolci V, Cox D (2013) Generation of membrane structures during phagocytosis and chemotaxis of macrophages: role and regulation of the actin cytoskeleton. *Immunol Rev* 256, 1: 222–239, doi: 10.1111/imr.12118
- (210) Ruivenkamp CAL, van Wezel T, Zanon C, Stassen APM, Vlcek C, Csikós T, Klous AM, Tripodis N, Perrakis A, Boerrigter L, Groot PC, Lindeman J, Mooi WJ, Meijjer GA, Scholten G, Dauwerse H, Paces V, van Zandwijk N, van Ommen GJB, Demant P (2002) Ptpnj is a candidate for the mouse colon-cancer susceptibility locus Sccl and is frequently deleted in human cancers. *Nat Genet* 31, 3: 295–300, doi: 10.1038/ng903
- (211) Sampaio NG, Yu W, Cox D, Wyckoff J, Condeelis J, Stanley ER, Pixley FJ (2011) Phosphorylation of CSF-1R Y721 mediates its association with PI3K to regulate macrophage motility and enhancement of tumor cell invasion. *J Cell Sci* 124, 12: 2021–2031, doi: 10.1242/jcs.075309
- (212) Schneble N, Müller J, Kliche S, Bauer R, Wetzker R, Böhmer F-D, Wang Z-Q, Müller JP (2017) The protein-tyrosine phosphatase DEP-1 promotes migration and phagocytic activity of microglial cells in part through negative regulation of fyn tyrosine kinase. *Glia* 65, 2: 416–428, doi: 10.1002/glia.23100
- (213) Schulz C, Gomez Perdiguero E, Chorro L, Szabo-Rogers H, Cagnard N, Kierdorf K, Prinz M, Wu B, Jacobsen SEW, Pollard JW, Frampton J, Liu KJ, Geissmann F (2012) A lineage of myeloid cells independent of Myb and hematopoietic stem cells. *Science* 336, 6077: 86–90, doi: 10.1126/science.1219179
- (214) Scott CL, Henri S, Guillemins M (2014) Mononuclear phagocytes of the intestine, the skin, and the lung. *Immunol Rev* 262, 1: 9–24, doi: 10.1111/imr.12220
- (215) Sena CM, Matafome P, Crisóstomo J, Rodrigues L, Fernandes R, Pereira P, Seiça RM (2012) Methylglyoxal promotes oxidative stress and endothelial dysfunction. *Pharmacol Res* 65, 5: 497–506, doi: 10.1016/j.phrs.2012.03.004
- (216) Setten RL, Rossi JJ, Han S (2019) The current state and future directions of RNAi-based therapeutics. *Nat Rev Drug Discov* 18, 6: 421–446, doi: 10.1038/s41573-019-0017-4

- (217) Shalev M, Arman E, Stein M, Cohen-Sharir Y, Brumfeld V, Kapishnikov S, Royal I, Tuckermann J, Elson A (2021) PTPRJ promotes osteoclast maturation and activity by inhibiting Cbl-mediated ubiquitination of NFATc1 in late osteoclastogenesis. *FEBS J* 288, 15: 4702–4723, doi: 10.1111/febs.15778
- (218) Shintani T, Higashi S, Suzuki R, Takeuchi Y, Ikaga R, Yamazaki T, Kobayashi K, Noda M (2017) PTPRJ Inhibits Leptin Signaling, and Induction of PTPRJ in the Hypothalamus Is a Cause of the Development of Leptin Resistance. *Sci Rep* 7, 1: 11627, doi: 10.1038/s41598-017-12070-7
- (219) Sica A, Mantovani A (2012) Macrophage plasticity and polarization: in vivo veritas. *J Clin Invest* 122, 3: 787–795, doi: 10.1172/JCI159643
- (220) Sica A, Wang JM, Colotta F, Dejana E, Mantovani A, Oppenheim JJ, Larsen CG, Zachariae CO, Matsushima K (1990) Monocyte chemotactic and activating factor gene expression induced in endothelial cells by IL-1 and tumor necrosis factor. *J Immunol* 144, 8: 3034–3038. PMID: 2182712
- (221) Silverman MG, Ference BA, Im K, Wiviott SD, Giugliano RP, Grundy SM, Braunwald E, Sabatine MS (2016) Association Between Lowering LDL-C and Cardiovascular Risk Reduction Among Different Therapeutic Interventions: A Systematic Review and Meta-analysis. *JAMA* 316, 12: 1289–1297, doi: 10.1001/jama.2016.13985
- (222) Singh V, Rana M, Jain M, Singh N, Naqvi A, Malasoni R, Dwivedi AK, Dikshit M, Barthwal MK (2015) Curcuma oil attenuates accelerated atherosclerosis and macrophage foam-cell formation by modulating genes involved in plaque stability, lipid homeostasis and inflammation. *Br J Nutr* 113, 1: 100–113, doi: 10.1017/S0007114514003195
- (223) Smythies LE, Sellers M, Clements RH, Mosteller-Barnum M, Meng G, Benjamin WH, Orenstein JM, Smith PD (2005) Human intestinal macrophages display profound inflammatory anergy despite avid phagocytic and bacteriocidal activity. *J Clin Invest* 115, 1: 66–75, doi: 10.1172/JCI19229
- (224) Soinio M, Marniemi J, Laakso M, Lehto S, Rönnemaa T (2006) High-sensitivity C-reactive protein and coronary heart disease mortality in patients with type 2 diabetes: a 7-year follow-up study. *Diabetes Care* 29, 2: 329–333, doi: 10.2337/diacare.29.02.06.dc05-1700
- (225) Song E, Zhu P, Lee S-K, Chowdhury D, Kussman S, Dykxhoorn DM, Feng Y, Palliser D, Weiner DB, Shankar P, Marasco WA, Lieberman J (2005) Antibody mediated in vivo delivery of small interfering RNAs via cell-surface receptors. *Nat Biotechnol* 23, 6: 709–717, doi: 10.1038/nbt1101
- (226) Spring K, Chabot C, Langlois S, Lapointe L, Trinh NTN, Caron C, Hebda JK, Gavard J, Elchebly M, Royal I (2012) Tyrosine phosphorylation of DEP-1/CD148 as a mechanism controlling Src kinase activation, endothelial cell permeability, invasion, and capillary formation. *Blood* 120, 13: 2745–2756, doi: 10.1182/blood-2011-12-398040
- (227) Spring K, Fournier P, Lapointe L, Chabot C, Roussy J, Pommey S, Stagg J, Royal I (2015) The protein tyrosine phosphatase DEP-1/PTPRJ promotes breast cancer cell invasion and metastasis. *Oncogene* 34, 44: 5536–5547, doi: 10.1038/onc.2015.9
- (228) Stacey KJ, Ross IL, Hume DA (1993) Electroporation and DNA-dependent cell death in murine macrophages. *Immunol Cell Biol* 71 (Pt 2): 75–85, doi: 10.1038/icb.1993.8
- (229) Stanley ER, Berg KL, Einstein DB, Lee PS, Pixley FJ, Wang Y, Yeung YG (1997) Biology and action of colony-stimulating factor-1. *Mol Reprod Dev* 46, 1: 4–10, doi: 10.1002/(SICI)1098-2795(199701)46:1<4:AID-MRD2>3.0.CO;2-V
- (230) Stary HC, Chandler AB, Dinsmore RE, Fuster V, Glagov S, Insull W, Rosenfeld ME, Schwartz CJ, Wagner WD, Wissler RW (1995) A definition of advanced types of atherosclerotic lesions and a histological classification of atherosclerosis. A report from the Committee on Vascular Lesions of the Council on Arteriosclerosis, American Heart Association. *Circulation* 92, 5: 1355–1374, doi: 10.1161/01.cir.92.5.1355
- (231) Statistisches Bundesamt (2020) Anzahl der Gestorbenen nach Kapiteln der ICD-10 und nach Geschlecht für 2018, [https://www.destatis.de/DE/Themen/Gesellschaft-Umwelt/Gesundheit/Todesursachen/Tabellen/gestorbene\\_anzahl.html](https://www.destatis.de/DE/Themen/Gesellschaft-Umwelt/Gesundheit/Todesursachen/Tabellen/gestorbene_anzahl.html) [Retrieval date: 05.02.2022]

- (232) Statistisches Bundesamt (2020) Todesursachen in Deutschland 2015, Fachserie 12 Reihe 4 - 2015, <https://www.destatis.de/DE/Themen/Gesellschaft-Umwelt/Gesundheit/Todesursachen/Publikationen/Downloads-Todesursachen/todesursachen-2120400157004.pdf> [Retrieval date: 05.02.2022]
- (233) Steinberg D (1997) Low density lipoprotein oxidation and its pathobiological significance. *J Biol Chem* 272, 34: 20963–20966, doi: 10.1074/jbc.272.34.20963
- (234) Stepanek O, Kalina T, Draber P, Skopцова T, Svojgr K, Angelisova P, Horejsi V, Weiss A, Brdicka T (2011) Regulation of Src family kinases involved in T cell receptor signaling by protein-tyrosine phosphatase CD148. *J Biol Chem* 286, 25: 22101–22112, doi: 10.1074/jbc.M110.196733
- (235) Stewart CR, Stuart LM, Wilkinson K, van Gils JM, Deng J, Halle A, Rayner KJ, Boyer L, Zhong R, Frazier WA, Lacy-Hulbert A, El Khoury J, Golenbock DT, Moore KJ (2010) CD36 ligands promote sterile inflammation through assembly of a Toll-like receptor 4 and 6 heterodimer. *Nat Immunol* 11, 2: 155–161, doi: 10.1038/ni.1836
- (236) Stout RD, Jiang C, Matta B, Tietzel I, Watkins SK, Suttles J (2005) Macrophages sequentially change their functional phenotype in response to changes in microenvironmental influences. *J Immunol* 175, 1: 342–349, doi: 10.4049/jimmunol.175.1.342
- (237) Sun S-C (2012) The noncanonical NF- $\kappa$ B pathway. *Immunol Rev* 246, 1: 125–140, doi: 10.1111/j.1600-065X.2011.01088.x
- (238) Sunderkötter C, Nikolic T, Dillon MJ, van Rooijen N, Stehling M, Drevets DA, Leenen PJM (2004) Subpopulations of mouse blood monocytes differ in maturation stage and inflammatory response. *J Immunol* 172, 7: 4410–4417, doi: 10.4049/jimmunol.172.7.4410
- (239) Swirski FK, Nahrendorf M, Etzrodt M, Wildgruber M, Cortez-Retamozo V, Panizzi P, Figueiredo J-L, Kohler RH, Chudnovskiy A, Waterman P, Aikawa E, Mempel TR, Libby P, Weissleder R, Pittet MJ (2009) Identification of splenic reservoir monocytes and their deployment to inflammatory sites. *Science* 325, 5940: 612–616, doi: 10.1126/science.1175202
- (240) Tacke F, Alvarez D, Kaplan TJ, Jakubzick C, Spanbroek R, Llodra J, Garin A, Liu J, Mack M, van Rooijen N, Lira SA, Habenicht AJ, Randolph GJ (2007) Monocyte subsets differentially employ CCR2, CCR5, and CX3CR1 to accumulate within atherosclerotic plaques. *J Clin Invest* 117, 1: 185–194, doi: 10.1172/JCI28549
- (241) Takahashi T, Takahashi K, Mernaugh RL, Tsuboi N, Liu H, Daniel TO (2006) A monoclonal antibody against CD148, a receptor-like tyrosine phosphatase, inhibits endothelial-cell growth and angiogenesis. *Blood* 108, 4: 1234–1242, doi: 10.1182/blood-2005-10-4296
- (242) Takeda K, Akira S (2004) TLR signaling pathways. *Semin Immunol* 16, 1: 3–9, doi: 10.1016/j.smim.2003.10.003
- (243) Tartaglia M, Mehler EL, Goldberg R, Zampino G, Brunner HG, Kremer H, van der Burgt I, Crosby AH, Ion A, Jeffery S, Kalidas K, Patton MA, Kucherlapati RS, Gelb BD (2001) Mutations in PTPN11, encoding the protein tyrosine phosphatase SHP-2, cause Noonan syndrome. *Nat Genet* 29, 4: 465–468, doi: 10.1038/ng772
- (244) Taylor F, Huffman MD, Macedo AF, Moore THM, Burke M, Davey Smith G, Ward K, Ebrahim S (2013) Statins for the primary prevention of cardiovascular disease. *Cochrane Database Syst Rev*, 1: CD004816, doi: 10.1002/14651858.CD004816.pub5
- (245) Tchaikovski V, Olieslagers S, Böhmer F-D, Waltenberger J (2009) Diabetes mellitus activates signal transduction pathways resulting in vascular endothelial growth factor resistance of human monocytes. *Circulation* 120, 2: 150–159, doi: 10.1161/CIRCULATIONAHA.108.817528
- (246) Thornalley PJ (1996) Pharmacology of methylglyoxal: formation, modification of proteins and nucleic acids, and enzymatic detoxification-A role in pathogenesis and antiproliferative chemotherapy. *Gen Pharmacol* 27, 4: 565–573, doi: 10.1016/0306-3623(95)02054-3
- (247) Tomlin AM, Tilyard MW, Dovey SM, Dawson AG (2006) Hospital admissions in diabetic and non-diabetic patients: a case-control study. *Diabetes Res Clin Pract* 73, 3: 260–267, doi: 10.1016/j.diabetes.2006.01.008

- (248) Tonks NK (2006) Protein tyrosine phosphatases: from genes, to function, to disease. *Nat Rev Mol Cell Biol* 7, 11: 833–846, doi: 10.1038/nrm2039
- (249) Tsuboi N, Utsunomiya T, Roberts RL, Ito H, Takahashi K, Noda M, Takahashi T (2008) The tyrosine phosphatase CD148 interacts with the p85 regulatory subunit of phosphoinositide 3-kinase. *Biochem J* 413, 1: 193–200, doi: 10.1042/BJ20071317
- (250) UK Prospective Diabetes Study (UKPDS) Group (1998) Intensive blood-glucose control with sulphonylureas or insulin compared with conventional treatment and risk of complications in patients with type 2 diabetes (UKPDS 33). UK Prospective Diabetes Study (UKPDS) Group. *Lancet* 352, 9131: 837–853, doi: 10.1016/S0140-6736(98)07019-6
- (251) Unger A, Finkernagel F, Hoffmann N, Neuhaus F, Joos B, Nist A, Stiewe T, Visekruna A, Wagner U, Reinartz S, Müller-Brüsselbach S, Müller R, Adhikary T (2018) Chromatin Binding of c-REL and p65 Is Not Limiting for Macrophage IL12B Transcription During Immediate Suppression by Ovarian Carcinoma Ascites. *Front Immunol* 9: 1425, doi: 10.3389/fimmu.2018.01425
- (252) van Eck M, Winther MP de, Herijgers N, Havekes LM, Hofker MH, Groot PH, van Berkel TJ (2000) Effect of human scavenger receptor class A overexpression in bone marrow-derived cells on cholesterol levels and atherosclerosis in ApoE-deficient mice. *Arterioscl Throm Vas* 20, 12: 2600–2606, doi: 10.1161/01.atv.20.12.2600
- (253) van Furth R, Cohn ZA (1968) The origin and kinetics of mononuclear phagocytes. *J Exp Med* 128, 3: 415–435, doi: 10.1084/jem.128.3.415
- (254) van Furth R, Cohn ZA, Hirsch JG, Humphrey JH, Spector WG, Langevoort HL (1972) The mononuclear phagocyte system: a new classification of macrophages, monocytes, and their precursor cells. *Bull World Health Organ* 46, 6: 845–852. PMID: 4538544
- (255) Vancurova I, Miskolci V, Davidson D (2001) NF-kappa B activation in tumor necrosis factor alpha-stimulated neutrophils is mediated by protein kinase Cdelta. Correlation to nuclear Ikappa Balpha. *J Biol Chem* 276, 23: 19746–19752, doi: 10.1074/jbc.M100234200
- (256) Verstrepen L, Bekaert T, Chau T-L, Tavernier J, Chariot A, Beyaert R (2008) TLR-4, IL-1R and TNF-R signaling to NF-kappaB: variations on a common theme: Variations on a common theme. *Cell Mol Life Sci* 65, 19: 2964–2978, doi: 10.1007/s00018-008-8064-8
- (257) Walker HK, Hall WD, Hurst JW (1990) *Clinical methods: The history, physical, and laboratory examinations*. Butterworths, Boston, 3rd edition
- (258) Wang N, Liang H, Zen K (2014) Molecular mechanisms that influence the macrophage m1-m2 polarization balance. *Front Immunol* 5: 614, doi: 10.3389/fimmu.2014.00614
- (259) Wang P, Xue Y, Han Y, Lin L, Wu C, Xu S, Jiang Z, Xu J, Liu Q, Cao X (2014) The STAT3-binding long noncoding RNA lnc-DC controls human dendritic cell differentiation. *Science* 344, 6181: 310–313, doi: 10.1126/science.1251456
- (260) Warwick CA, Usachev YM (2017) Culture, Transfection, and Immunocytochemical Analysis of Primary Macrophages. *Methods Mol Biol* 1554: 161–173, doi: 10.1007/978-1-4939-6759-9\_9
- (261) Wati S, Li P, Burrell CJ, Carr JM (2007) Dengue virus (DV) replication in monocyte-derived macrophages is not affected by tumor necrosis factor alpha (TNF-alpha), and DV infection induces altered responsiveness to TNF-alpha stimulation. *J Virol* 81, 18: 10161–10171, doi: 10.1128/JVI.00313-07
- (262) Weischenfeldt J, Porse B (2008) Bone Marrow-Derived Macrophages (BMM): Isolation and Applications. *Cold Spring Harb Protoc* 2008: pdb.prot5080, doi: 10.1101/pdb.prot5080
- (263) Wen J, Yang C-Y, Lu J, Wang X-Y (2018) Ptpn22 mediates inflammatory injury after intracerebral hemorrhage by activating NF-κB pathway. *Eur Rev Med Pharmacol Sci* 22, 9: 2817–2823, doi: 10.26355/eurrev\_201805\_14981
- (264) Weyer C, Bogardus C, Mott DM, Pratley RE (1999) The natural history of insulin secretory dysfunction and insulin resistance in the pathogenesis of type 2 diabetes mellitus. *J Clin Invest* 104, 6: 787–794, doi: 10.1172/JCI7231



- (265) Whitelaw DM (1966) The intravascular lifespan of monocytes. *Blood* 28, 3: 455–464, doi: 10.1182/blood.V28.3.455.455
- (266) Wiese M, Castiglione K, Hensel M, Schleicher U, Bogdan C, Jantsch J (2010) Small interfering RNA (siRNA) delivery into murine bone marrow-derived macrophages by electroporation. *J Immunol Methods* 353, 1-2: 102–110, doi: 10.1016/j.jim.2009.12.002
- (267) Wilcoxon F (1945) Individual Comparisons by Ranking Methods. *Biometrics* 1, 6: 80, doi: 10.2307/3001968
- (268) Winther MPJ de, Kanters E, Kraal G, Hofker MH (2005) Nuclear factor kappaB signaling in atherogenesis. *Arterioscl Throm Vas* 25, 5: 904–914, doi: 10.1161/01.ATV.0000160340.72641.87
- (269) Wolever TMS, Gibbs AL, Mehling C, Chiasson J-L, Connelly PW, Josse RG, Leiter LA, Maheux P, Rabasa-Lhoret R, Rodger NW, Ryan EA (2008) The Canadian Trial of Carbohydrates in Diabetes (CCD), a 1-y controlled trial of low-glycemic-index dietary carbohydrate in type 2 diabetes: no effect on glycated hemoglobin but reduction in C-reactive protein. *Am J Clin Nutr* 87, 1: 114–125, doi: 10.1093/ajcn/87.1.114
- (270) Wong KL, Tai JJ-Y, Wong W-C, Han H, Sem X, Yeap W-H, Kourilsky P, Wong S-C (2011) Gene expression profiling reveals the defining features of the classical, intermediate, and nonclassical human monocyte subsets. *Blood* 118, 5: e16-31, doi: 10.1182/blood-2010-12-326355
- (271) Wong KL, Yeap WH, Tai JJY, Ong SM, Dang TM, Wong SC (2012) The three human monocyte subsets: implications for health and disease. *Immunol Res* 53, 1-3: 41–57, doi: 10.1007/s12026-012-8297-3
- (272) Wynn TA, Vannella KM (2016) Macrophages in Tissue Repair, Regeneration, and Fibrosis. *Immunity* 44, 3: 450–462, doi: 10.1016/j.immuni.2016.02.015
- (273) Xu E, Charbonneau A, Rolland Y, Bellmann K, Pao L, Siminovitch KA, Neel BG, Beauchemin N, Marette A (2012) Hepatocyte-specific Ptpn6 deletion protects from obesity-linked hepatic insulin resistance. *Diabetes* 61, 8: 1949–1958, doi: 10.2337/db11-1502
- (274) Yamashita S, Hirano K, Kuwasako T, Janabi M, Toyama Y, Ishigami M, Sakai N (2007) Physiological and pathological roles of a multi-ligand receptor CD36 in atherogenesis; insights from CD36-deficient patients. *Mol Cell Biochem* 299, 1-2: 19–22, doi: 10.1007/s11010-005-9031-4
- (275) Yao R-W, Wang Y, Chen L-L (2019) Cellular functions of long noncoding RNAs. *Nat Cell Biol* 21, 5: 542–551, doi: 10.1038/s41556-019-0311-8
- (276) Ylä-Herttua S, Palinski W, Rosenfeld ME, Parthasarathy S, Carew TE, Butler S, Witztum JL, Steinberg D (1989) Evidence for the presence of oxidatively modified low density lipoprotein in atherosclerotic lesions of rabbit and man. *J Clin Invest* 84, 4: 1086–1095, doi: 10.1172/JCI114271
- (277) Yoshida H, Kisugi R (2010) Mechanisms of LDL oxidation. *Clin Chim Acta* 411, 23-24: 1875–1882, doi: 10.1016/j.cca.2010.08.038
- (278) Yurdagul A, Green J, Albert P, McInnis MC, Mazar AP, Orr AW (2014)  $\alpha 5\beta 1$  integrin signaling mediates oxidized low-density lipoprotein-induced inflammation and early atherosclerosis. *Arterioscl Throm Vas* 34, 7: 1362–1373, doi: 10.1161/ATVBAHA.114.303863
- (279) Yvan-Charvet L, Welch C, Pagler TA, Ranalletta M, Lamkanfi M, Han S, Ishibashi M, Li R, Wang N, Tall AR (2008) Increased inflammatory gene expression in ABC transporter-deficient macrophages: free cholesterol accumulation, increased signaling via toll-like receptors, and neutrophil infiltration of atherosclerotic lesions. *Circulation* 118, 18: 1837–1847, doi: 10.1161/CIRCULATIONAHA.108.793869
- (280) Zawada AM, Rogacev KS, Rotter B, Winter P, Marell R-R, Fliser D, Heine GH (2011) SuperSAGE evidence for CD14<sup>++</sup>CD16<sup>+</sup> monocytes as a third monocyte subset. *Blood* 118, 12: e50-61, doi: 10.1182/blood-2011-01-326827
- (281) Zhang B, Ma Y, Guo H, Sun B, Niu R, Ying G, Zhang N (2009) Akt2 is required for macrophage chemotaxis. *Eur J Immunol* 39, 3: 894–901, doi: 10.1002/eji.200838809

- (282) Zhang J, Li L, Li J, Liu Y, Zhang C-Y, Zhang Y, Zen K (2015) Protein tyrosine phosphatase 1B impairs diabetic wound healing through vascular endothelial growth factor receptor 2 dephosphorylation. *Arterioscl Throm Vas* 35, 1: 163–174, doi: 10.1161/ATVBAHA.114.304705
- (283) Zhao Y, Glesne D, Huberman E (2003) A human peripheral blood monocyte-derived subset acts as pluripotent stem cells. *PNAS* 100, 5: 2426–2431, doi: 10.1073/pnas.0536882100
- (284) Zhu JW, Brdicka T, Katsumoto TR, Lin J, Weiss A (2008) Structurally distinct phosphatases CD45 and CD148 both regulate B cell and macrophage immunoreceptor signaling. *Immunity* 28, 2: 183–196, doi: 10.1016/j.immuni.2007.11.024
- (285) Zhu X, Owen JS, Wilson MD, Li H, Griffiths GL, Thomas MJ, Hiltbold EM, Fessler MB, Parks JS (2010) Macrophage ABCA1 reduces MyD88-dependent Toll-like receptor trafficking to lipid rafts by reduction of lipid raft cholesterol. *J Lipid Res* 51, 11: 3196–3206, doi: 10.1194/jlr.M006486
- (286) Ziegler-Heitbrock L (2015) Blood Monocytes and Their Subsets: Established Features and Open Questions. *Front Immunol* 6: 423, doi: 10.3389/fimmu.2015.00423
- (287) Zwaka TP, Hombach V, Torzewski J (2001) C-reactive protein-mediated low density lipoprotein uptake by macrophages: implications for atherosclerosis. *Circulation* 103, 9: 1194–1197, doi: 10.1161/01.cir.103.9.1194

## 8 Figure directory

<b>Figure 1: Monocyte subpopulations in fluorescence assisted cell sorting.</b> .....	6
<b>Figure 2: DEP-1 expression in patients with T2DM.</b> .....	46
<b>Figure 3: DEP-1 expression in HG-cultured monocytes.</b> .....	47
<b>Figure 4: TNF-<math>\alpha</math> upregulates DEP-1 protein expression in monocytes.</b> .....	49
<b>Figure 5: DEP-1 expression and phosphatase activity in macrophage subpopulations.</b> .....	51
<b>Figure 6: Established <i>in-vitro</i> DEP-1 knockdown model.</b> .....	53
<b>Figure 7: Knockdown efficiencies and toxicity evaluation.</b> .....	55
<b>Figure 8: DEP-1 knockdown migration assays.</b> .....	59
<b>Figure 9: DEP-1 knockdown proliferation and viability assay.</b> .....	61
<b>Figure 10: Downstream signaling effects of siRNA-mediated DEP-1 knockdown in M1 macrophages.</b> .....	63

### 8.1 Figure references

All figures of this work were calculated, designed, and created by the author of this dissertation. An exception to this is Figure 1, which was licensed and taken from a publication (271).

## 9 Table directory

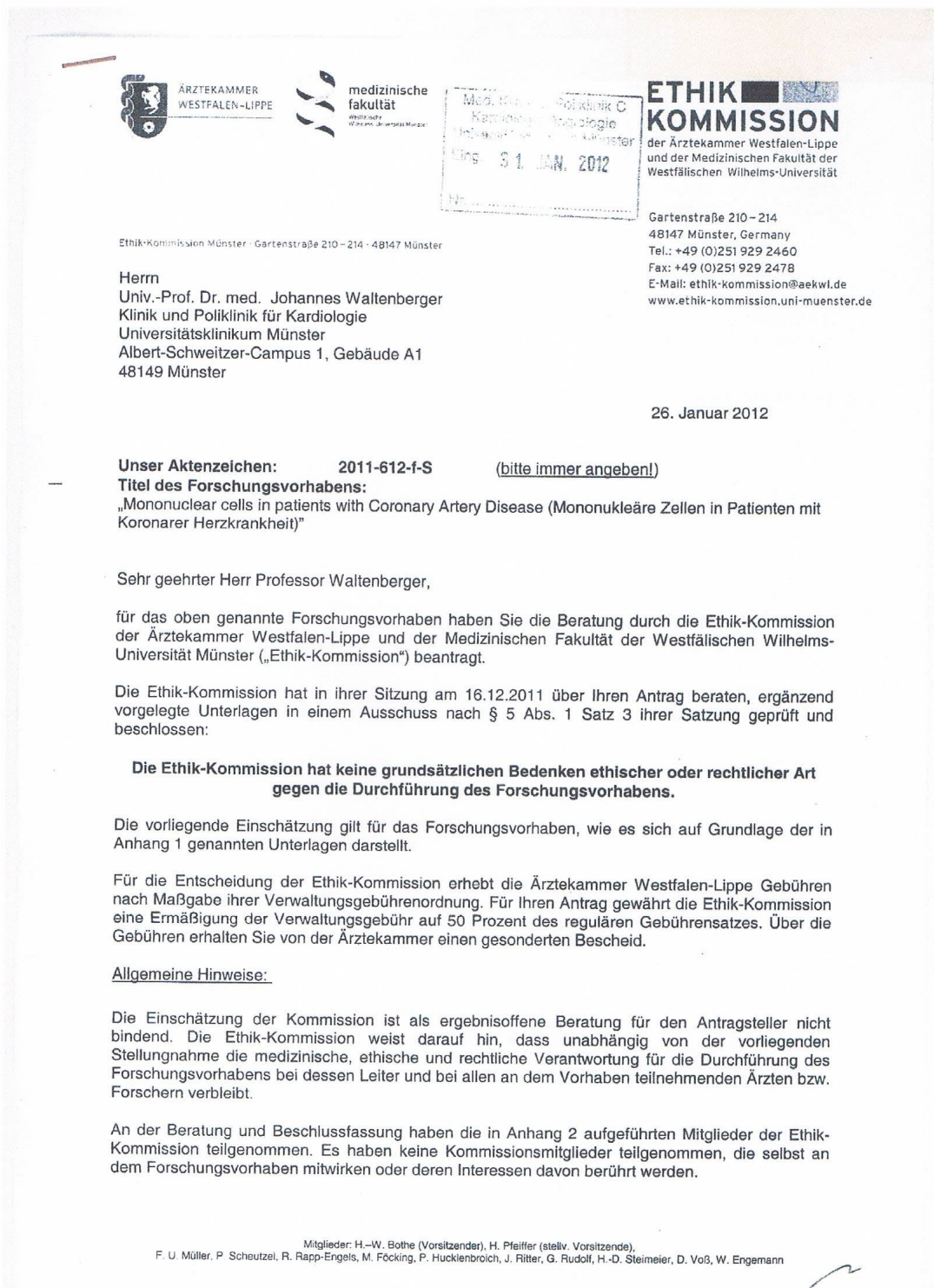
Table 1: Chemicals.....	19
Table 2: Recipes for solutions.....	20
Table 3: Primary antibodies used in Western Blot analyses.....	20
Table 4: Secondary antibodies.....	20
Table 5: Kits and transfection reagents.....	21
Table 6: Plasticware consumables.....	21
Table 7: Laboratory equipment.....	22
Table 8: Software.....	22
Table 9: Reagents and amounts for transfections with Lipofectamine® RNAiMAX. ...	29
Table 10: Reagents and amounts for transfections with Viromer® Blue.....	29
Table 11: Used primers against human target genes.....	33
Table 12: Tabular visualization of the applied PCR program.....	35
Table 13: Components and amounts for casting 7.5% stacking and separating gels.....	38
Table 14: Clinical and biomarker patient characteristics.....	45
Table 15: Comparison of knockdown reagent toxicity against Viromer® Blue.....	56
Table 16: Comparison of fractional open areas (FOA) during a wound healing assay of primary human monocyte-derived macrophages after siRNA-mediated knockdown of DEP-1 in normoglycemia (NG).....	56
Table 17: Comparison of fractional open areas (FOA) during a wound healing assay of primary human monocyte-derived macrophages between normoglycemic (NG) and hyperglycemic (HG) culturing.....	57

## 10 Abbreviations

ANOVA	Analysis of variance
BMDM	Bone-marrow derived macrophage
BSA	Bovine serum albumin
CCR	C-C motif receptor
CD	Cluster of differentiation
CD206, or MRC1	C-Type Mannose Receptor 1
cDNA	complimentary DNA
CI	Confidence interval
CRP	C-reactive protein
CSF-1R	Colony stimulating factor 1 receptor
DEP-1	Density-enhanced phosphatase 1
DKO	Double-knockout
DM	Diabetes mellitus, Diabetes mellitus
DNA	deoxyribonucleic acid
dsDNA	double-stranded deoxyribonucleic acid
ERK	Extracellular signal-regulated kinase
FOA	Fractional open area
GM-CSF	Granulocyte-macrophage colony-stimulating factor
HbA <sub>1c</sub>	Glycated hemoglobin A1C
HDL	High-density lipoprotein
HG	Hyperglycemia
HSC	Hematopoietic stem cell
HUVEC	Human umbilical vein endothelial cell
IDF	International Diabetes Federation
KD	Knock-down
KO	Knockout
LDL	Low-density lipoprotein
lncRNA	Long noncoding RNA
Lp(a)	Lipoprotein(a)
LPS	Lipopolysaccharide
MACS	Magnetic-activated cell sorting
MAPK	Mitogen activated protein kinase
MCP	Monocyte chemoattractant protein
M-CSF	Macrophage colony-stimulating factor
MG	Methylglyoxal
MHC	Major histocompatibility complex
MIF	Macrophage inhibitory factor
MPS	Mononuclear phagocyte system
MRC1, or CD206	C-Type Mannose Receptor 1
mRNA	messenger RNA
MTS	3-(4,5-dimethylthiazol-2-yl)-5-(3-carboxymethoxyphenyl)-2-(4-sulfophenyl)-2H-tetrazolium
NF- $\kappa$ B	Nuclear factor 'kappa-light-chain-enhancer' of activated B-cells
NG	Normoglycemia
oxLDL	Oxidized low-density lipoprotein

PAM3	Synthetic toll like receptor 1 and 2 ligand Pam3CSK4
PBMC	Peripheral blood mononuclear cells
PCR	Polymerase chain reaction
PDGF	Platelet-derived growth factor
PDGF-R	Platelet-derived growth factor receptor
PI3K	Phosphatidylinositol-4,5-bisphosphate 3-kinase
PTP	Protein tyrosine phosphatase
PTPN11, SHP-2	Protein tyrosine phosphatase non-receptor type 11
PVDF	Polyvinylidene fluoride
RFU	Relative fluorescence units
RNA	ribonucleic acid
RNAi	RNA interference
RTK	Receptor tyrosine kinase
rt-qPCR	Real-time quantitative polymerase chain-reaction
Scc1	Susceptibility to colon cancer 1
SD	Standard deviation
SDS-PAGE	Sodium dodecyl sulfate polyacrylamide gel electrophoresis
SEM	Standard error of the mean
SFK	Src-family kinases
siRNA	small-interfering ribonucleic acid
ssDNA	single-stranded desoxyribonucleic acid
T1DM	Type 1 diabetes mellitus
T2DM	Type 2 diabetes mellitus
TGF- $\beta$	Transforming growth-factor beta
TLR	Toll-like receptor
TNF- $\alpha$	Tumor necrosis factor $\alpha$
VEGF	Vascular endothelial growth factor
VEGFR	Vascular endothelial growth factor receptor
VEGF-R2	Vascular endothelial growth factor receptor 2
WASP	Wiskott–Aldrich syndrome protein
WAVE	WASP-family verprolin homologous

# 11 Ethical approvals



Die Ethik-Kommission empfiehlt nachdrücklich die Registrierung klinischer Studien in einem öffentlich zugänglichen Register, das die von der Weltgesundheitsorganisation (WHO) geforderten Voraussetzungen erfüllt, insbesondere deren Mindestangaben enthält. In Betracht kommende Register sowie ausführliche weiterführende Informationen stehen im Internetangebot der WHO zur Verfügung:

<http://www.who.int/ictcp/en/>


Zu den von zahlreichen Fachzeitschriften aufgestellten Anforderungen wird hingewiesen auf:

[http://www.icmje.org/clin\\_trialup.htm](http://www.icmje.org/clin_trialup.htm)

Die Ethik-Kommission der Ärztekammer Westfalen-Lippe und der Medizinischen Fakultät der Westfälischen Wilhelms-Universität Münster ist organisiert und arbeitet gemäß den nationalen gesetzlichen Bestimmungen und den GCP-Richtlinien der ICH.

Die Kommission wünscht Ihrem Forschungsvorhaben gutes Gelingen und geht davon aus, dass Sie nach Abschluss des Vorhabens über die Ergebnisse berichten werden.

Mit freundlichen Grüßen

  
Univ.-Prof. Dr. med. Hans-Werner Bothe M.A.  
Vorsitzender der Ethik-Kommission



### Anhang 1

#### Folgende Unterlagen haben bei der Beschlussfassung vorgelegen:

<b>Eingang</b>	<b>Datierung</b>	<b>Anlage</b>	<b>Version</b>
24.11.2011	22.11.2011	Antragsformular MONOCAD	
24.11.2011	22.11.2011	Curriculum Vitae Univ.-Prof. Dr. med Johannes Waltenberger	
24.11.2011	22.11.2011	Probandenaufklärung und -einwilligung MONOCAD	
24.11.2011	22.11.2011	Studienprotokoll MONOCAD	
13.01.2012	10.01.2012	Antrag MONOCAD	
13.01.2012	10.01.2012	Patienteninformation MONOCAD	
13.01.2012	10.01.2012	Studienprotokoll MONOCAD	

### Anhang 2

#### Folgende Mitglieder der Ethik-Kommission haben an der Beratung und Beschlussfassung in der Sitzung vom 16. Dezember 2011 teilgenommen:

Univ.-Prof. Dr. med. Hans-Werner **Bothe** M.A.  
Klinik und Poliklinik für Neurochirurgie  
Universitätsklinikum Münster  
- *Vorsitz* -

Frau Mechthild **Föcking**  
Landesarbeitsgemeinschaft der Selbsthilfe  
Behinderter e.V.  
Münster

Univ.-Prof. Dr. med. Dr. phil.  
**Peter Hucklenbroich**  
Institut für Ethik, Geschichte und Theorie der  
Medizin  
Universitätsklinikum Münster

Univ.-Prof. Dr. med. Frank U. **Müller**  
Institut für Pharmakologie und Toxikologie  
Universitätsklinikum Münster

Frau Univ.-Prof. Dr. med. Heidi **Pfeiffer**  
Institut für Rechtsmedizin  
Universitätsklinikum Münster

Frau Dr. med. Regine **Rapp-Engels**  
Fachärztin für Allgemeinmedizin  
- Sozialmedizin -  
Münster

Univ.-Prof. theol. Dr. Hans-Richard **Reuter**  
Institut für Ethik und angrenzende  
Sozialwissenschaften  
Westfälische Wilhelms-Universität Münster

Univ.-Prof. Dr. med. Jörg **Ritter**  
Klinik und Poliklinik für Kinder- und  
Jugendmedizin  
- Pädiatrische Hämatologie und Onkologie -  
Universitätsklinikum Münster

Univ.-Prof. Prof. Dr. jur. Ingo **Saenger**  
Institut für Internationales Wirtschaftsrecht (IW3)  
Westfälische Wilhelms-Universität Münster

Frau Univ.-Prof. Dr. med. dent.  
**Petra Scheutzel**  
Poliklinik für Zahnärztliche Prothetik und  
Werkstoffkunde  
Universitätsklinikum Münster

Frau Dr. rer. nat. Dorothea **Voß**  
Apotheke des UKM  
Universitätsklinikum Münster



**Universitätsklinikum  
Jena**

### Ethik-Kommission

Vorsitzende: Prof. Dr. med. Dagmar Barz  
Geschäftsstelle: Dr. phil. Ulrike Skorsetz

Bachstraße 18  
07743 Jena

Telefon 03641 93 37 70  
Telefax 03641 93 37 71

E-Mail: ethikkommission@med.uni-jena.de

Jena, 18. Juli 2014

Universitätsklinikum Jena · Ethik-Kommission · Postfach · 07740 Jena

Prof. Dr. med. Ulrich-Alfons Müller  
Klinik für Innere Medizin III  
FB Endokrinologie/Stoffwechselerkrankungen  
Bachstrasse 18  
07740 Jena

Prof. Dr. Frank-D. Böhmer  
Institut für Molekulare Zellbiologie  
Hans-Knöll-Str. 2  
07745 Jena

#### Bearbeitungsnummer: 4125-06/14

Sehr geehrte Kollegen,

in ihrer Sitzung am 17.07.2014 hat die Ethik-Kommission der Friedrich-Schiller Universität  
Ihren Antrag

*Mechanismen der defekten Migration von Monocyten bei Diabetes mellitus*

beraten und erhebt gegen das Projekt keine ethischen oder berufsrechtlichen Bedenken.

#### Anmerkungen:

- Da es sich um Patienten und nicht um Probanden handelt, sollte das in den  
Unterlagen entsprechend vereinheitlicht werden.
- Bitte ergänzen Sie auf S. 2 der Patienteninformation im letzten Satz des 2. Absatzes  
hinter Universitätsklinikum noch „Jena“.
- Bitte ergänzen Sie in der Information, wie viel Blut abgenommen wird und was mit  
dem Restmaterial passiert.

Geben Sie uns bitte eine überarbeitete Fassung bis zum 22.08.2014 zu den Unterlagen,  
ansonsten verliert diese Stellungnahme ihre Gültigkeit.

Mit freundlichen Grüßen

Prof. Dr. med. U. Brandl  
Stellv. Vorsitzender

Bachstraße 18 · 07743 Jena · Telefon 03641 93 00  
Internet: www.uniklinikum-jena.de  
Gerichtsstand Jena  
UST-IdNr. DE 150545777  
Bankverbindung: Sparkasse Jena · BLZ 830 530 30 · Konto 221  
IBAN: DE97 8305 3030 0000 0002 21  
BIC: HELADEF1JEN

Universitätsklinikum Jena · Körperschaft des öffentlichen Rechts  
als Teilkörperschaft der Friedrich-Schiller-Universität Jena  
Verwaltungsratsvorsitzender: Prof. Dr. Thomas Daufel  
Kaufmännischer Vorstand und Sprecherin  
des Klinikumsvorstandes: Dr. Brunnhilde Seidel-Kwem  
Medizinischer Vorstand: N.N.  
Wissenschaftlicher Vorstand: Prof. Dr. Klaus Berndorf

## 12 Acknowledgement

## 13 Curriculum vitae

